ABSTRACT

IRVIN, SUSAN CARLTON. Functional Domains of Reovirus Protein μ2 that Determine the Interferon Response and Reovirus Replication. (Under the direction of Dr. Barbara Sherry.)

The innate immune system provides a critical first line of protection against invading pathogens. In particular, the type I interferon (IFN) response enables the host to establish an antiviral state upon infection. Reovirus infection in vitro and in vivo provides an opportunity to investigate mechanisms underlying the IFN response as well as its impact on disease. We have focused on viral replication and damage in cardiac cells which together determine myocarditis in a mouse model. A non-myocarditic reovirus can induce myocarditis in mice when the IFN response is ablated either by deletion of genes that are required for induction of IFN or by treatment with anti-IFN antibody. Thus reovirus is an excellent tool for to identifying viral determinants of the IFN response and myocarditis.

Previously, we identified a reovirus strain-specific repressor of IFN signaling: the M1 gene-encoded protein μ2. Here, we demonstrate through the use of recombinant viruses that amino acid 208 of the μ2 protein is both required and sufficient for repression of IFN signaling. A virus encoding a proline at μ2 amino acid 208, such as strain type 1 Lang (T1L), represses IFN signaling while a virus encoding a serine at μ2 amino acid 208, such as type 3 Dearing (T3D), does not repress IFN signaling. Furthermore, in primary cardiac myocyte cultures, μ2 amino acid 208 modulates reovirus induction of IFN, determines reovirus replication, and influences cytopathic effect after multiple cycles of replication. Previously, we found that reovirus induces significantly higher levels of IFN in cardiac myocytes than in cardiac fibroblasts. Accordingly while μ2 amino acid 208 modulates induction of IFN in

cardiac fibroblasts, the impact of IFN on reovirus replication is less dramatic than in cardiac myocytes. Given that the IFN response limits viral spread and cytopathic effect in primary cardiac myocyte cultures, we next investigated the effect of μ2 amino acid 208 on reovirus-induced myocarditis in a mouse model. We determined that the T1L M1 gene is sufficient for reovirus-induced myocarditis and that μ2 amino acid 208 modulates myocarditis, likely through repression of IFN signaling.

Next, we investigated the role of immunoreceptor tyrosine-based activation motifs (ITAMs) in reovirus proteins. ITAMs are signaling domains found in the cytoplasmic tails of receptors that mediate immune cell activation, and in the cytoplasmic tails of surface glycoproteins of some enveloped viruses. Here, ITAMs were identified in three proteins, σ2, μ2, and λ2, which are constituents of the reovirus inner core and outer capsid. These are the first ITAMs identified in a non-enveloped virus. ITAM-mediated cell signaling requires the phosphorylation of two tyrosine residues within the motif. Reverse genetics was used to engineer mutant T3D reoviruses in which the two critical tyrosines in ITAMs of σ2, μ2, and λ2 were replaced with phenylalanine to inhibit ITAM phosphorylation. Although the λ2 mutant virus was not viable, replication kinetics and final yields of the σ2 and μ2 ITAM mutant viruses in L929 cells and in primary cardiac myocyte cultures demonstrated the σ2 and μ2 ITAMs are not required for reovirus replication. Importantly, the μ2 ITAM regulates the activation of NF-κB and influences the induction of interferon-β (IFN-β) in both L929 cells and primary cardiac myocyte cultures. Moreover, the consequences of these μ2 ITAM effects are cell type-specific. In L929 cells, the μ2 ITAM proved to be advantageous for viral fitness. In contrast, in primary cardiac myocyte cultures where the IFN response is critical for antiviral protection and NF-κB is not required for apoptosis, the μ2 ITAM diminishes viral fitness. Results here suggest the μ2 ITAM has a cell type-specific role in viral spread, likely reflecting the cell type-specific roles of NF-κB and IFN-β.

Functional Domains of Reovirus Protein μ2 that Determine the Interferon Response and Reovirus Replication

by
Susan C. Irvin

A dissertation submitted to the Graduate Faculty of
North Carolina State University
in partial fulfillment of the
requirements for the Degree of
Doctor of Philosophy

Comparative Biomedical Sciences

Raleigh, North Carolina

2011

APPROVED BY:

_______________________________ _______________________________

Dr. Barbara Sherry
Committee Chair

Dr. Fred J. Fuller

_______________________________ _______________________________

Dr. Frank Scholle

Dr. Jeffrey A. Yoder

DEDICATION

I dedicate this work to my parents. This work was made possible with your unwavering love and support. I am eternally grateful for your endless encouragement over my many years of school. As two of the most intelligent, honest, and loving people I have ever known, I strive daily to model my own life after yours. I would not be as successful as I am today without both of you.

BIOGRAPHY

Susan is the daughter of Buck and Linda Irvin and the sister of Matthew Irvin. She spent most of her childhood in Oxford, North Carolina, where she was born. When not in school, much of her time was spent outdoors with her family and pets where she began a lifelong love for the environment, animals, and athletics. Her parents, both avid readers, encouraged her love of reading, music and science, while she and her older brother shared a sense of adventure and athleticism as her family enjoyed camping, skiing, and boating. Midway through high school, Susan and her family moved to Greensboro, NC where she graduated in 2001. After graduating from high school, Susan attended North Carolina State University (NCSU) where she continued her passion for science with a major in microbiology. Unwilling to give up her love for reading and the arts, Susan minored in English while at NCSU. Like many students, Susan also worked part time during college at many different jobs. Through these opportunities, her love for animals was deepened through working at the NCSU Equine Education Unit, her palate for good coffee was developed while working at a local coffee shop, and perhaps most importantly, her work in several different laboratories helped guide her career path toward virology. After graduating from NCSU in 2005 with a Bachelors of Science, Susan began her PhD in the laboratory of Dr. Barbara Sherry. Throughout graduate school, Susan has maintained her active lifestyle by remaining an avid runner and by becoming a cyclist. After completing her PhD, Susan plans to continue her love of learning and virology as a post-doctoral scientist.

ACKNOWLEDGMENTS

I would like to thank my graduate advisor, Dr. Barbara Sherry. Her patience, guidance, and support allowed me to successfully complete this work. I especially appreciate the care and compassion that she extends to all members of her lab. To past and current members of the Sherry Lab, I thank all of you for the many helpful discussions about our work, keeping me on my toes, and for your encouragement. To the members of my committee, I thank you for your helpful suggestions. To Jeff Yoder, I extend special thanks for allowing me to be an adjunct member of your lab and especially for free use of your espresso machine! To the faculty, staff, and students of the third floor, I thank all of you for your support and for creating a sense of community here. I would like to thank my undergraduate advisor, Dr. Gerry Luginbuhl, and my agent, TJ Schneeweis, for their guidance and encouragement for me to follow my goal of attending graduate school. I would also like to thank Dr. Terence Dermody and his laboratory members for years of collaboration, helpful discussions, and guidance.

I would especially like to thank Poem Turner and Shengdar Tsai for their invaluable friendship. Thank you for being the best sounding boards and cheerleaders! I would also like to thank Shannon Chiera, Odessa Marks, Laura Ott, Beth Overman, and Radhika Shah for their friendship and for endless laughs! All of you made each day at work even more fun! To my other fun-loving group of friends ("the manatees"), thank you for all of the delicious pot-luck dinners, fun evenings downtown, and wonderful friendships!

To the greater NC State community, I thank you for supplying me with the latest and greatest music on WKNC to keep me going during days and nights of experiments and writing. I would also like to thank The Morning Times for brewing the best coffee in the Triangle which helped me write this dissertation.

Finally, I would like to thank my family. They have endured countless phone calls about science topics that they probably never wished to hear and in turn provided me with endless love, support, and the reminder to not sweat the small stuff.

TABLE OF CONTENTS

LIST OF FIGURES

CHAPTER 1

Literature Review

ORTHOREOVIRUS (REOVIRUS)

Reoviridae is the only family of dsRNA viruses that can infect mammals (154). The prefix reo- is derived from the acronym for **r**espiratory and **e**nteric **o**rphan viruses, since these viruses were first isolated from human respiratory and enteric tracts but were not associated with severe disease (153). *Reoviridae* includes the genus *Orthoreovirus* which is commonly referred to as reovirus. Reovirus serotypes are identified by neutralization and hemagglutination. There are three serotypes of reoviruses which encompass four prototype strains: Lang strain is the type 1 prototype (1), Jones strain for type 2 (146), Dearing (146) and Abney (150) strains for type 3. The dsRNA 23.5 kb genome is encoded by 10 discrete (162) segments. The segments are named according to size classes as seen on a polyacrylamide gel: three large segments (L1, L2, and L3), three medium (M1, M2, and M3), and four small (S1, S2, S3, and S4) (16, 162). The reovirus genome encodes eight structural proteins (λ1, λ2, λ3, μ1, μ2, σ1, σ2, and σ3) and four non-structural proteins (μNS, μNSC, σ1s, and σNS); two of the non-structural proteins, μNSC and σ1s, are products of alternative translation. Reovirus virions are non-enveloped, icosahedral particles that consist of a double layered capsid consisting of the outer capsid and inner core (154). By electron microscopy, fibrous extensions which consist of the viral attachment protein σ1 (68), can be seen projecting from the surface of the spherical virus particles. Reovirus particles are comprised of the eight structural proteins and contain the dsRNA genome as well as short oligonucleotides (15, 131, 161) that are assumed to be products of aborted transcription. Historically, reassortment of reoviruses was used to determine specific role(s) of reovirus genes in viral replication and pathogenesis. The genome segments of reovirus are able to reassort upon coinfection in mice as well as in cell culture (154). More recently, a plasmid-based reverse genetics system was developed for reovirus (93, 96). Through the advent of this system, specific mutations can be engineered in single or multiple reovirus genes. Mutant viruses used in Chapters 2 and 3 of this dissertation were created with the reverse genetics system (Fig. 1.1).

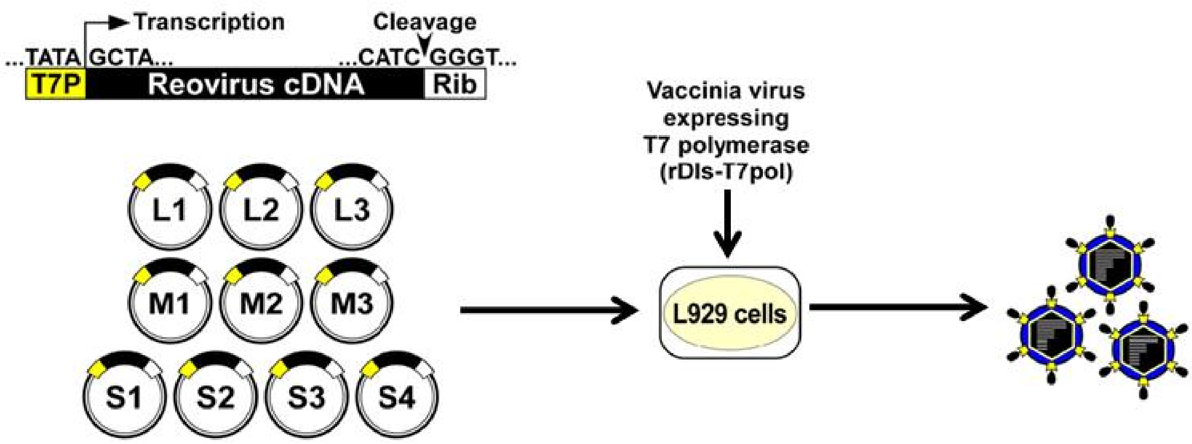

Figure. 1.1. Reovirus reverse genetics system. The 10 reovirus genes can be easily mutated, if desired, when present in plasmid form. The 10 genes are then transfected into L929 cells and live recombinant viruses are recovered.
Figure adapted from T. Kobayashi (93).

Virus Entry

Through the viral attachment protein σ1, encoded by the S1 gene, the reovirus particle first binds to cellular sialic acid with low affinity (10, 27) and then with higher affinity to junctional adhesion molecule-A (JAM-A) (11, 25, 65, 92, 144). The σ1 protein is also the viral hemagglutinin (178). For internalization of the particle, β1-integrin serves as a co-receptor (113, 114) to likely mediate clathrin-dependent endocytosis (20, 61, 152, 172). The L2 encoded λ2 protein contains RGD and KGE motifs (113), which suggests λ2 may interact with β1-integrin. Recently, it has been demonstrated that Src kinase is required for an early step during infection that occurs after attachment and internalization, such as intracellular trafficking to endosomes (115). In the endocytic compartment, cathepsin proteases L, D, and S (60, 72) are responsible for partial disassembly of particles in removing the S4 encoded σ3 protein and cleaving the M2 encoded µ1 protein into the µ1δ fragment, which is myristoylated at the N-terminus, and the Φ fragment. These derivative particles are referred to in the literature as infectious (or intermediate) subviral particles (ISVPs). Further disassembly of ISVPs into another intermediate termed ISVP* results in the release of σ1 from the λ2 pentamer turrets as well as autocatalytic cleavage of µ1δ (130) into myristoylated-µ1N (myr-µ1N) and δ fragments (172). The mechanism of release of reovirus into the cytoplasm is not fully understood; however, the subsequent release of myr-µ1N and Φ fragments likely contributes to exit of viral cores from endosomes into the cytoplasm, the site of viral replication. Studies of virus infection determined both myr-µ1N and Φ fragments, which are released from ISVP*, have a role in pore formation (5, 84). Furthermore, a synthetic peptide corresponding to Φ is capable of pore formation (91). Another fragment released from ISVP* is the δ fragment. While the timing is unclear, it has been established that Hsc70 is associated with the release of the δ fragment from ISPV*s (83) for conversion into transcriptionally active viral cores: this disassociation step occurs before, during or after entry into the cytoplasm (83).

Viral Replication

The core-shell protein λ1, encoded by the L3 gene, has RNA helicase activity (19) and may serve to unwind the dsRNA genome for transcription. The other major component of the core shell is σ2, which is encoded by the S2 gene and is suggested to serve as a stabilizing clamp for λ1 (148). Within the viral core, the precise locations of λ3 and μ2 have not been determined, though it is suggested they are in close proximity to the core spike protein λ2 (90, 185), together forming the replication complex. The RNA-dependent RNA polymerase protein λ3 is encoded by the L1 gene (170). A defined role in replication for μ2 has yet to be determined but studies indicate this protein is the key determinant of replication in MDCK cells (137). The M1 gene, along with the S1 gene, also correlates with the ratio of positive to negative strand synthesis in cardiac myocytes, indicative of the rate of viral RNA synthesis (163). As further evidence for a role in replication, μ2 is able to bind both ssRNA and dsRNA (21). Primary transcription occurs within the core yielding (+)-sense single-stranded RNA (ssRNA). This nascent ssRNA is extruded through λ2 pentameric turrets (9, 58, 148, 185). Primary transcripts are non-polyadenylated but do contain a 5' cap structure that is added as the ssRNA is extruded (69, 148). While core proteins λ1 and μ2 exhibit RTPase and NTPase activity (90, 133, 134), it is suggested the λ2 protein likely mediates the enzymatic reactions of capping through guanylyltransferase (33) and methyltransferase activity (148). The λ2 turrets also appear structurally poised for capping of mRNA (148). The λ1 protein NTPase activity (19, 133) is instead suggested to mediate helicase function. The (+)-sense ssRNA can be translated from mRNA into gene products or the transcripts can serve as templates for (-)-strand synthesis.

As viral synthesis proceeds, there is a parallel decrease in cellular protein synthesis that is attributed to the S4 gene encoded σ3 protein (160) and is at least in part due to the IFN-induced proteins PKR and RNAse L (169). Reovirus infection also leads to cell cycle arrest; the second S1 gene product σ1s is indicated as responsible for arrest at the G2/M phase (142). Reovirus replication and assembly occurs at perinuclear sites (159) termed viral inclusion bodies (VIBs) that are initially formed by the μNS protein (139), but require additional proteins for maturation of the VIB structures (26, 94). Within VIBs, the M3 encoded nonstructural protein μNS, is found to co-localize with all of the structural proteins comprising the viral core (λ1, λ2, λ3, and μ2) along with the S3 encoded non-structural σNS protein (121) as well as with input viral particles (22) and nascent RNA (121). Transcription of the (-)-sense strand of RNA occurs within the newly formed viral cores and remains within the cores as a single copy to form the 10 segments of the dsRNA genome. The mechanism of cellular release of reovirus progeny is likely facilitated by cellular lysis/apoptosis but may be mediated by other events as well.

Reovirus replication, as just described, is measured in Chapter 2 and in Chapter 3. Furthermore, the role of the μ2 protein in replication is particularly important to both chapters.

Apoptosis

Reovirus infection of neonatal mice is used to study viral encephalitis and virus-induced myocarditis. Reovirus provides a highly tractable disease system in which reassortant (154) and recombinant viruses (93, 96) may be utilized. Tissue damage resulting from reovirus infection in this model is not characterized by immune-mediated effects, but rather by virus-induced cellular apoptosis. In genetic studies, the S1 (encodes σ1 protein) and M2 (encodes μ1 protein) genes have been indicated as the determinants of apoptosis (36, 149, 175). Studies suggest reovirus infection stimulates both the extrinsic apoptosis pathway, which utilizes cell surface death receptors (DRs), as well as the intrinsic apoptosis pathway, which is based on the mitochondria. Additionally, reovirus-induced apoptosis is regulated by activation of NF-κB (37, 135). Interestingly, activation of IRF-3 parallels that of NF-κB and maximal reovirus induced apoptosis requires IRF-3 and IPS-1 function (78), demonstrating IRF3 also has a role in cell death. Greater detail of reovirus-induced apoptosis is discussed here, yet reovirus-induced IFN will be reviewed in a subsequent section of this literature review.

Programmed cell death, or apoptosis, is mediated through two different pathways, the intrinsic and extrinsic pathways, which both ultimately result in activation of caspases, as shown in Fig. 1.2. Recently, P. Danthi reviewed these pathways of apoptosis and the mechanisms of virus-induced apoptosis (44). In brief, the focus of the intrinsic pathway involves the mitochondria. When cellular stress occurs, Bcl-2 family members insert in the mitochondrial membrane (44). Upon insertion, cytochrome c and Smac/DIABLO are released from the mitochondria and caspase-9 is activated (44). Cytochrome c, caspase-9 and Apaf-1 form the apoptosome (44). Smack/DIABLO and the apoptosome lead to activation of caspase-3 and caspase-7 which are the end of the signaling pathway for cell death (44). In contrast, the extrinsic pathway is signaled by extracellular ligands, such as TRAIL, which bind transmembrane receptors, e.g. DR4 and DR5 (44). Once the receptors are activated, the death-induced signaling complex (DISC) forms and then activates caspase-8 (44, 97). The activation of caspase-8 leads to activation of caspase-3 and caspase-7, which like the intrinsic pathway are the ultimate signal for cell death (44).

When σ1 binding to cellular JAM-A is inhibited with antibodies, apoptosis is decreased; this suggests the importance of σ1-JAM-A interactions for apoptosis (11). Additionally, it has been indicated that binding of σ1 to the cellular co-receptor sialic acid, results in a higher percentage of apoptosis and enhanced activation of NF-κB (36). However, Danthi et al demonstrated sialic acid and JAM-A interactions with σ1 are not required for apoptosis (46). In this model of JAM-A-independent, Fc-mediated uptake of reovirus, the M2 gene was found to be the primary determinant of apoptosis (46). While the exact step in reovirus replication that leads to apoptosis is unknown, it has been demonstrated that virus particle disassembly is required for apoptosis (36) and that apoptosis is triggered after viral attachment yet before gene transcription (46). Fc-mediated attachment in CHO-B1 cells resulted in apoptosis, yet upon ammonium chloride treatment (which inhibits virus disassembly) apoptosis was inhibited, however ribavirin treatment and UV-inactivation of particles (which preclude transcription) did not affect apoptosis (46). In contrast, ribavirin treatment of reovirus infected HEK293 cells results in inhibition of apoptosis (32), suggesting a cell type-specific event. In vivo studies confirm the importance of the M2 encoded µ1 protein: less tissue damage is seen in the brains of mice infected with a virus encoding a membrane-penetration defective µ1 protein, although viral tropism is unaffected by this mutation (47). As further evidence of the importance of functional µ1 for apoptosis, infection with membrane-penetration defective viruses also results in decreased NF-κB and IRF-3 activation (47). Overexpression of the μ1 protein in vitro results in apoptosis (34). Within cells infected with T1L virus or transfected with the M2 gene, the μ1 protein is found associated with lipid droplets, ER, and mitochondria but not with the Golgi body or lysosomes (34). This location of μ1 suggests it may have a role in apoptosis. The Φ of μ1 is associated with apoptosis: Φ contributes to membrane penetration, in vitro cell apoptosis, NF-κB activation, and in vivo caspase-3 monitored apoptosis and tissue damage in the brain (45). Overexpression of the M2 gene encoding full-length μ1 or overexpression of only the Φ fragment results in cytochrome c release and Smac/DIABLO release (181). Furthermore, a peptide corresponding to Φ is able to permeabilize artificial membranes and cell membranes as well as cause an increase in cytosolic calcium (91). However, the Φ peptide is unable to mediate cytochrome c relase when incubated with purified mitochondria or when microinjected into cells (91). This dichotomy may reflect a requirement for a high concentration of Φ for inducing cytochrome c release. Interestingly, caspases-3, -8- and -9 as well as Bcl-2 family members Bax and Back, which are known to form pores in the mitochondrial membrane for cytochrome c release, are not required for μ1-mediated cytochrome c release (181), suggesting the possibility of a novel mechanism of apoptosis.

Demonstrating use of the extrinsic pathway, reovirus infection of HEK293 cells is able to induce TRAIL release which leads to apoptosis of TRAIL-sensitive HeLa cells (31). Furthermore, reovirus infection results in an increase in protein expression of both TRAIL death receptors DR4 and DR5 (31). This extrinsic pathway of apoptosis can be blocked with anti-TRAIL antibody or with soluble forms of DR4 and DR5 (31). Further downstream of TRAIL ligand-receptor binding, reovirus activates caspase-8 (25-27, 97) which subsequently leads to downstream cleavage of Bid, and downstream to activation of caspase-3 and caspase-7, and to cytochrome c release (97). Bid cleavage also requires activation of NF-κB (77) and this cleavage of Bid is a requirement of reovirus induced-apoptosis (48). In the intrinsic pathway, the induction of cytochrome c by overexpressed μ1 or by reovirus infection is independent of two additional proapoptotic members of the Bcl-2 family, Bax and Bak (181). However, Bax is important for tissue injury and apoptosis in the brain but not in the heart of reovirus infected mice (17), suggesting organ-specific requirements for apoptosis. Furthermore, while Bax is important, it is not required for cytochrome c and Smac/DIABLO release with T3D infection (17). While the aforementioned Bax activation results from a conformational change in Bax protein, reovirus infected cells do not upregulate Bax gene expression (49). Cytochrome c release from the mitochondria in the intrinsic pathway results in cleavage of pro-caspase-9 into active caspase-9 (97), yet this activation is not required for reovirus induced-apoptosis (98). This indicates the mechanism of cytochrome c-to-activation of caspase 9 is not the required event in the reovirus-mediated intrinsic pathway of apoptosis. One study demonstrated that overexpression of Bcl-2 in vitro, inhibits reovirus-induced apoptosis (149). However, this is not known to occur during reovirus infection when endogenous levels of Bcl-2 are present. Smac/DIABLO is also released from the mitochondria (98), and may function in promoting apoptosis by interacting with inhibitor of apoptosis proteins (IAPs). In other systems, Smac/DIABLO can inhibit function of XIAP therefore promoting apoptosis. In parallel, reovirus infection results in decreased protein expression of IAPs survivin and c-IAP1 and cleavage of XIAP (98).

Chapter 3 of this dissertation revisits the cell type-specific role of NF-κB in apoptosis as indicated by cell death.

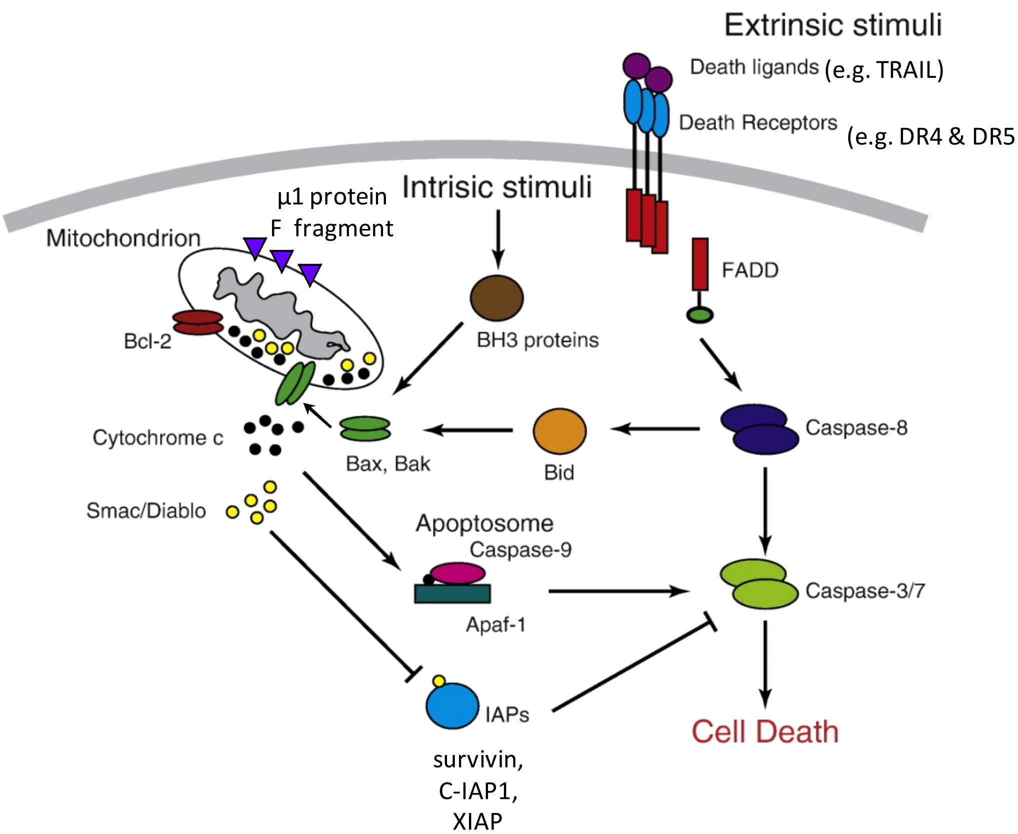

Figure. 1.2. Pathways of reovirus-induced apoptosis. Reovirus infection induces both the intrinsic and extrinsic pathways of cellular apoptosis.
Figure adapted from P. Danthi (44).

M1 GENE-ENCODED μ2 PROTEIN

The reovirus M1 gene, which is 2,304 base pairs in length, encodes the 736 amino acid (139, 179, 183) protein μ2 (Fig. 1.3). Reovirus strains T1L and T3D share approximately 98%

nucleotide sequence homology of the M1 gene and approximately 99% amino acid sequence homology (183, 186), demonstrating a high degree of conservation of this gene between these strains (Fig. 1.3). The T2J strain however has less homology with T1L and T3D; approximately 72% nucleotide and 81% amino acid sequence homology (183). Present as only 12-20 copies per virus particle (39, 57), μ2 proteins are readily detected in infected cells (139). While the crystal structures for the other eight structural proteins of reovirus have been at least partially determined, the μ2 crystal structure remains undetermined. Yin et al suggest the μ2 protein can be divided into four regions based on predicted secondary structure (183). The amino terminal region consists of amino acids 1 through 157 and structurally is predicted to contain 6 α-helices and 3 β-sheets (183). This region is highly conserved across reovirus isolates including laboratory clones and field isolates. The N-terminus of μ2 is capable of functioning as a nuclear localization signal (NLS) (Fig. 1.3) (95). The variable region consists of amino acids 157 through 450 and is predicted to be the most complex region consisting of multiple α-helices and β-strands (183). Amino acids 450 through 606 are part of the predicted highly conserved helix-rich region which is suggested to contain 7 α-helices (183). The least conserved region, amino acids 606 through 736, is the carboxyl-terminus which varies across all three reovirus serotypes (183). The predicted composition of μ2 is 48% α-helix and 14% β-sheet, resulting in classification as an α-β protein (183) with the highest σ-helix content of reovirus capsid proteins (179). While the μ2 protein overall does not appear similar to any other known protein, analysis of the highly conserved regions of μ2 with the FingerPRINTScan program revealed the highest score with SH2 domains (183). In this analysis, four out of five motifs of SH2 matched regions of μ2, though with low significance (183). However, it should be noted that the authors of this study did not specifically identify the SH2 domains in the μ2 sequence. The protein kinases of relevance that also contain SH2 domains are Src family kinases and Syk family kinases. Since the SH2 domain mediates protein-protein interactions, this suggests μ2 may also have this ability. Biochemicially, the μ2 protein has been demonstrated to possess RTPase (90) and NTPase activity (Fig. 1.3) (90, 134); both of these functions are required for production of reovirus progeny (26). As previously mentioned, the μ2 protein is able to bind ssRNA and dsRNA (21) which is likely important during viral replication though the precise role is undefined.

Studies indicate that while a specific role during replication remains elusive, the M1 gene encoded μ2 protein is required for reovirus replication. If the M1 gene is inhibited by siRNA, there is a resulting concomitant inhibition of dsRNA synthesis, protein production, and production of viral progeny (26, 94). In cardiac myocytes, reovirus replication efficiency was mapped to the M1, L1, and L3 genes yet in L929 cells, only the L1 and L3 genes were implicated, thus demonstrating a cell type-specific role for the M1 gene (118). In MDCK cells, reovirus replication efficiency is regulated after primary transcription and translation (137). Furthermore, it was determined that the μ2 protein, specifically amino acid 347 (Fig. 1.3), is the primary determinant of replication in MDCK cells and the λ3 protein can function as a co-regulator of replication but depends on the viral genetic context (137). The M1 gene, along with the S1 gene, also correlates with the ratio of positive to negative strand synthesis in cardiac myocytes (163). Interestingly, reovirus-induced myocarditis correlates with the rate of reovirus RNA synthesis (163), suggesting a link between the M1 gene and myocarditis. Indeed, other studies have found the M1 gene, along with other genes, to be a determinant of myocarditis (164, 165).

During infection, the μ2 protein is abundantly found in viral inclusion bodies (VIBs) (139). The morphology of VIBs, either filamentous or globular, is determined by the M1 gene (119, 139) (Fig. 1.3), specifically amino acid 208 (119, 139), although it can be modulated by amino acid 383 (95). Within VIBs, μ2 associates with μNS, which initiates VIB formation (94, 122), and σNS (122), which binds ssRNA (80). The VIB structure cannot be formed by σNS alone (122), yet it appears μ2 (23, 139) and μNS (23) are both able to form VIB-like structures when overexpressed in the absence of other proteins (23, 139). Studies suggest that formation of mature VIBs requires the μ2 protein because only small globular VIBs are formed when the M1 gene is inhibited by siRNA (26, 94). Small globular VIBs are also formed when σNS is inhibited, suggesting a requirement of σNS for formation of mature VIBs as well (94). When μNS is overexpressed, only globular VIBs are able to form (23), suggesting the requirement of additional proteins to form mature VIBs. The colocalization of μNS and μ2 is independent of strain-specific differences whereas the μNS-μ2 association with microtubules and consequently VIB morphology, is dependent on differences in the μ2 protein (23). T1L μ2 colocalizes with microtubules (139) and according to results indicating hyperacetylation of α-tubulin, appears to stabilize microtubules whereas T3D μ2 does not (139). Overexpression of T1L M3 (μNS) and T1L M1 (μ2) results in formation of thick filamentous structures resembling filamentous VIBs even though overexpression of each of these proteins individually does not result in this structure (23). Together, this suggest T1L μ2 recruits μNS to microtubules to form filamentous VIBs (23).

Conjugated ubiquitin was determined to colocalize with globular VIBs more than filamentous VIBs, however at lower temperature, T3D is able to form filamentous VIBs and has decreased conjugated ubiquitin, possibly due to greater microtubule association, indicating potential temperature sensitive functions of μ2 (123). Furthermore, the μ2 protein is actually ubiquitinated during T3D infection (123). The μ2 protein of strain T3D is resistant to proteasomal degradation whereas μ2 from strain T1L is not; this may be due to aggregation of the T3D μ2 protein (123). Studies utilizing either the overexpression of the T1L M3 gene (μNS) or viral infection along with nocodazole treatment, which depolymerizes microtubules, demonstrated the association with microtubules is required for VIB formation but is not required the maintenance of the structures once they are formed (23, 26, 139).

As mentioned above, the μ2 protein provides an essential role in VIBs. The following information, though not specific to VIBs, is provided to expand VIB knowledge. When either the M3 or S3 genes, which encode μNS or σNS proteins respectively, are inhibited, there is a significant decrease in protein production and synthesis of dsRNA (94), demonstrating the requirement of both of the VIB proteins. While μNSC, a second transcription product of the M3 gene which lacks the N-terminus of μNS, is able to form VIBs, this protein is unable to restore viral replication in an siRNA-complementation assay (94). This lack of restoration with μNSC suggests the N-terminus of μNS is critical for replication. Furthermore, the N-terminus of μNS is required for colocalization with σNS (121, 122) as well as μ2 (23, 121). The first 13 amino acids of μNS are required for σNS recruitment to VIBs (122) whereas amino acids 14-40 are required for μ2 interactions (122). In contrast, amino acids 1-40 of μNS are not required for interactions with λ1, λ2, or σ2 (22, 121). It has been demonstrated, that within VIBs, μNS colocalizes with all of the structural proteins comprising the viral core (λ1, λ2, λ3, and μ2) along with the S3 encoded non-structural σNS protein (121). Studies with using cycloheximide to inhibit protein synthesis determined input viral cores are recruited to VIB-like structures formed by μNS (22). More recently it was determined that amino acids 173-220 of μNS are required for core particle colocalization at VIBs (121). Additionally, nascent RNA colocalizes with μNS in VIBs (121).

As a final point, Zurney et al recently determined that the M1 gene of strain T1L encodes a repressor of IFN signaling (188). This study served as a starting point for Chapter 2 of this dissertation. In Chapter 2, we determined amino acid 208 is responsible for strain-specific differences in repression of interferon-signaling. This study was conducted in primary cardiac myocyte cultures in which the interferon response is critical for antiviral protection, and in primary cardiac fibroblast cultures for comparison. This investigation was then continued the neonatal mouse model to determine if amino acid 208 is a determinant of reovirus-induced myocarditis.

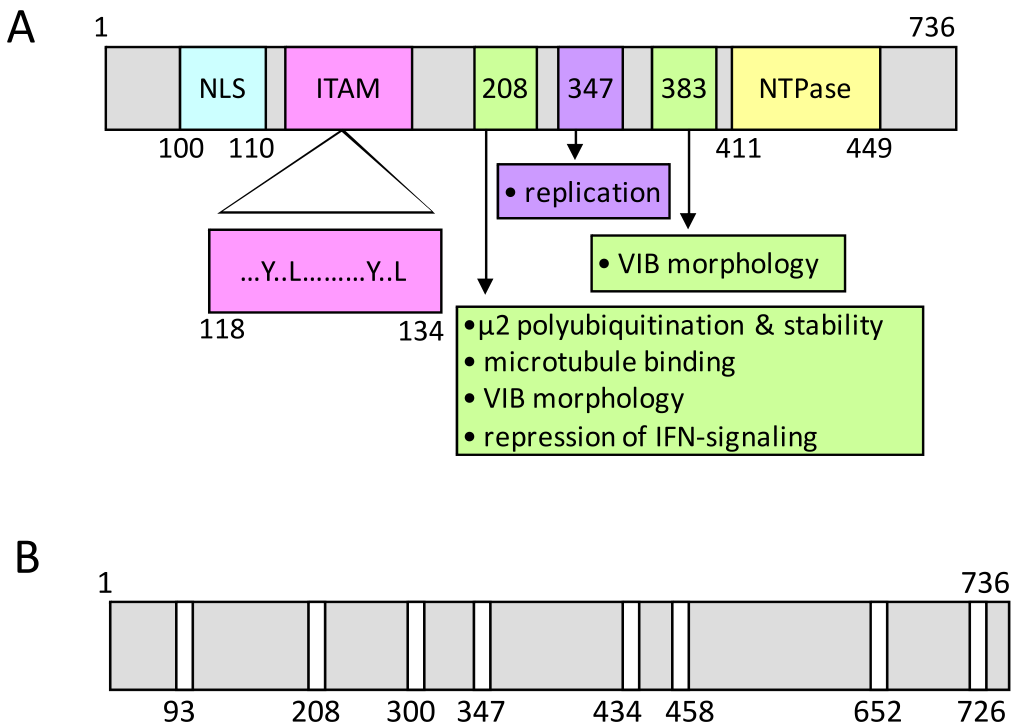

Figure. 1.3. Reovirus M1 gene-encoded μ2 protein. (A) The μ2 protein includes a nuclear localization signal, ITAM, amino acid determinants of viral inclusion body morphology and stability, a repressor of IFN signaling, and an NTPase domain. (B) Eight amino acids differ in the μ2 protein between strains T3D and T1L.

MYOCARDITIS

Myocarditis is clinically defined as inflammation of the heart muscle (64). It is widely believed that viral infection is the leading cause of myocarditis in North American and Europe (64). Clinical diagnosis relies on the Dallas criteria for histopathological samples (64). The criteria require samples to show lymphocyte infiltration and myocyte death or damage for a diagnosis of myocarditis whereas borderline myocarditis may contain less infiltrate and no visible damage (13, 64). Recently the Dallas criteria have been challenged (13) because some patients while negative for histopathological evidence by Dallas criteria are positive for dilated cardiomyopathy and viral infection in cardiac tissue (116, 141).

As reviewed by Feldman and McNamara, most virus families have been implicated in viral myocarditis including, but not limited to adenovirus, coxsackieviruses, hepatitis C virus, herpes simplex virus, human immunodeficiency virus-1, influenza viruses, respiratory syncytial virus (64). However, studies indicate a higher prevalence of enteroviruses, including coxsackievirus B, adenoviruses, and parvovirus B19 are associated with human viral myocarditis cases in the US (40, 64, 99, 101).

While often fatal in infants, viral myocarditis is normally resolved in adults but does have potential to progress to chronic myocarditis or dilated cardiomyopathy and eventually cardiac failure (132). Myocarditis has been indicated as the second leading cause of sudden unexpected death in young adults (56).

Recent work demonstrates less than 50% of cardiac myocytes are replaced during a normal lifespan (18). Until approximately the age of 20, myocytes are renewed at an annual rate of 1%, but later in life there is a decrease to 0.3% cellular turnover (18). Furthermore, as shown in a neonatal mouse model, the mammalian heart has the capacity to regenerate myocytes in response to injury but this potential is lost several days after birth (143). Continued growth of the heart from the point at which myocyte hyperplasia is lost, is mainly due to myocyte hypertrophy and to non-myocyte hyperplasia (108, 138). Since the cellular mechanism for shutting off this potential is unknown and the technology remains out of reach to stimulate massive regeneration of cardiac myocytes in the event of cardiac damage, we can think of cardiac myocytes as virtually non-replenishable and the death of cardiac myocytes as permanent damage to the host.

Cardiac myocyte death can be directly caused by viral cytopathic effect or it can be immune-mediated. In patients positive for adenovirus infection in cardiac tissue, biopsies are often negative for histopathology (116). Enterovirus infection can result in death of cardiac myocytes due to direct virus-induced cytopathic effect (29, 76) and due to inflammatory cell-mediated damage (38). These effects of enterovirus-mediated myocarditis are extensively reviewed by Esfandiarei and McManus along with the possibility of autoimmune-mediated damage of cardiac myocytes during coxsackievirus B3 infection (63). In contrast, Reovirus-induced myocarditis is not immune-mediated, but rather cardiac tissue damage is due to virus-mediated cell death. The use of monoclonal antibodies against reovirus in an immune-competent mouse model was effective at inhibiting myocarditis and transfer of reovirus-immune spleen cells also inhibits myocarditis (166). Thus while immune cells are able to effectively inhibit reovirus-induced myocarditis, this does not normally occur during infection. It has been demonstrated that reovirus induces myocarditis in a nude mouse model, which lacks T cells (167), indicating T cells are not required for reovirus-induced myocarditis. As further evidence of reovirus-induced myocarditis occurring independent of immune cells, reovirus infection in a SCID mouse model, which lacks functional B and T cells, resulted in myocarditis (166). Reovirus myocarditis in vivo correlates with apoptosis of cardiac myocytes in vitro (12, 125). Though the mechanism is unclear, the use of a calpain inhibitor in reovirus infected mice reduces apoptotic cells and myocarditis but does not inhibit reovirus-induced activation of caspases (50). However, when cardiac myocytes were treated with broad caspase inhibitors there was protection against virus-induced apoptosis (51). When these same caspase inhibitors were used in vivo, there was a similar decrease in apoptosis concomitant with a decrease in cardiac damage (51). Since reovirus-induced myocarditis is not immune mediated, but instead is a result of viral apoptosis or other direct viral cytopathic effects, reovirus provides a unique model for studying the cardiac response to viral infection.

Genetic mapping studies found reovirus M1 (164, 165), L1 (164), and L2 (164, 165) genes, which encode viral core proteins, to be determinants of myocarditis. The viral core proteins encoded by these genes form the replication complex, therefore suggesting a role for RNA synthesis in determining myocarditis. Indeed, in cardiac myocytes the rate of RNA synthesis correlates with myocarditis but not with viral yield (163). Of the genes encoding viral core proteins, only the M1 gene is associated with the rate of RNA synthesis (163). However, the S1 gene, which encodes the viral attachment protein, also correlates with RNA synthesis (163). Interestingly, the S1 gene also correlates with the frequency of infection in cardiac myocytes (163). The association of both the M1 and S1 genes with RNA synthesis does not necessarily indicate a common underlying mechanism. Since the S1 gene correlates with RNA synthesis and the frequency of infection, it seems likely that a virus that is able to attach to and infect a large percentage of cells, would be poised for greater synthesis of RNA than a virus that does not infect as many cells. Since the M1 gene determines RNA synthesis and this correlates with myocarditis, though viral yield does not correlate with myocarditis, this suggests another mechanism in determining reovirus myocarditis. During virus infection, RNA is sensed by pathogen recognition receptors to stimulate the antiviral type I interferon response. With this in mind, it seems likely that the rate of RNA synthesis would therefore determine the extent of the antiviral response. In accordance with this hypothesis, Sherry et al. found type I IFN is a determinant of reovirus myocarditis (168). In cardiac myocytes, non-myocarditic reoviruses are strong inducers of IFN-β whereas myocarditic reoviruses induce IFN-β poorly (168). Additionally, non-myocarditic reoviruses are more sensitive to the anti-viral effects of IFN-β than myocarditic viruses (168). The differences in induction of- and sensitivity to-IFN-β are associated with the M1, S2, and L2 genes (168). In a mouse model, infection with a non-myocarditic virus resulted in myocarditic lesions when injected with IFN-α/β antibody to negate the IFN response (168), indicating the importance of the IFN response in protection against reovirus infection in the heart. A larger review of the IFN response to reovirus follows this section in this chapter.

In patients diagnosed with acute myocarditis, treatment normally consists of supportive therapy (100). The use of immunosuppressive drugs, such as prednisone, has been shown to have little to no effect on improving cardiac function or patient survival (117, 140). Consequently immunosuppressive therapy is not recommended for myocarditis (117, 140). In contrast, patients with chronic cardiac dysfunction and chronic viral infection treated with IFN-β, had improvement of cardiac function and elimination of viral infection upon treatment (100). Patients treated with IFN-α showed similar improvement in cardiac function and inhibition of viral replication (41, 124). By better understanding the role of the interferon response to viral infection, development of additional therapeutics may be aided.

TYPE I INTERFERON (IFN)

Issacs and Lindenmann established that when heat-inactivated influenza A virus was exposed to pieces of chorio-allantoic membrane and then the membranes were challenged with live influenza A virus, an interfering agent inhibited the challenging infection (82). They consequently termed this agent “interferon” (82). Currently, three classes of interferon (IFN) have been identified based on sequence and receptor use: type I (IFN-α, -β, -ω, -ε, -κ, -τ, and -ζ), type II (IFN-γ), and type III (IFN-λ_1, -λ_2, and -λ_3). Cellular pathogen recognition receptors (PRRs) are responsible for detection of pathogen-associated molecular patterns (PAMPs) for stimulating the innate immune response, including the induction of IFN. During reovirus infection, the PRRs RIG-I and MDA5 detect viral RNA for the induction of IFN-α/β (110). Furthermore, purified reovirus genomic dsRNA was used to demonstrate RIG-I is able to recognize short segments of dsRNA but MDA5 recognizes longer segments of dsRNA for the induction of IFN-β (87), yet it is unlikely reovirus dsRNA is exposed during replication thus the reovirus triggers for RIG-I and MDA5 continue to remain elusive. When mice are depleted of IFN with anti-IFN-α/β antibody, a non-myocarditic reovirus induces myocarditis (168). Furthermore, reovirus infected IFN-α-receptor-1 (IFN-αR1) knockout mice succumb to infection, have increased viral spread, and tissue damage as compared to wild-type (WT) infected animals (86). Together, these findings demonstrate the requirement of type I IFN for protection against reovirus infection. Though Toll-like receptors (TLRs) are capable of detecting dsRNA, including poly(I:C) and in vitro purified reovirus genomic dsRNA, to stimulate induction of type I IFN (6), studies suggest TLR3 and MyD88, an adaptor for all other TLRs, are not required for protection against lethal reovirus infection (86). Most cell types are capable of expressing IFN, however peroral inoculation of reovirus does not require NK, B, or T cells for intestinal clearance, and in contrast, dendritic cells (DCs) are the primary producers of type I IFN during reovirus infection (86). Although the class of type I IFN encompasses multiple members, studies indicate reovirus infection results in induction of IFN-β and multiple subtypes of IFN-α (109, 171, 187) and consequently, this review will focus on induction and amplification of IFN-α/β.

As well established in the literature, the cytoplasmic sensors RIG-I and MDA5 detect RNA. It has been demonstrated that RIG-I preferentially recognizes RNA containing a 5' triphosphate (5'ppp) (111). However, studies indicate the 5'ppp alone is insufficient for induction of RIG-I signaling; RNA sequence compositions, such as polyuridine motifs, are also important (111). While the 5'ppp is preferentially recognized by RIG-I, RNA cleavage products generated by RNase L containing a 3' monophosphate can also be recognized by RIG-I (111). Of note, reovirus infection does activate RNase L, yet a study by JA Smith et al indicates activated RNase L does not inhibit reovirus replication (169). Additionally, the length of RNA influences detection: RIG-I recognizes short fragments of dsRNA (87), as short as 23 bp (111), whereas MDA5 recognizes longer dsRNA fragments (87). Though RIG-I is able to recognize short RNA fragments, suggesting the possibility of recognizing reovirus short oligos (mostly 2-9 nucleotides) that are contained within packaged virions, these oligos are significantly shorter than reported ligands for RIG-I. In sum, as previously stated the reovirus ligand for RIG-I and MDA5 remains undetermined. Once RNA is detected, activated RIG-I and MDA5 recruit and interact with the adaptor protein IFN-β-promoter stimulator-1 (IPS-1), also known as MAVS, VISA, or Cardif, to mediate antiviral responses that includes induction of IFN-β (89, 120, 157, 182). Downstream of IPS-1, TANK-binding kinase 1 (TBK1) and IKKε mediate activation of transcription factors interferon regulatory factor 3 (IRF3) and when present, IRF7 (158). Additional transcription factors such as NF-κB can also be activated downstream of IPS-1. Once these transcription factors are activated, they translocate to the nucleus to bind DNA and induce gene transcription of chemokines and cytokines including IFN-β. Secreted IFN-β then binds the IFN-α/β-receptor to stimulate amplification of IFN signaling. Engagement of the IFN-α/β-receptor results in phosphorylation of the receptor-associated Janus tyrosine kinases (JAK) members JAK1 and TYK2 which in turn phosphorylate signal transducers and activators of transcription (STAT) members STAT1 and STAT2. Phosphorylated STAT1 and STAT2 heterodimerize and recruit IRF9 to form the trimeric complex interferon stimulated gene factor 3 (ISGF3). The ISGF3 complex translocates to the nucleus to bind interferon-stimulated response elements (ISREs) which are contained in the promoter sequence of interferon-stimulated genes (ISGs). The induction of ISGs, including the essential ISG IRF7 (79), further establishes the antiviral state and amplifies IFN signaling.

While it is well established that reovirus infection results in induction of IFN, the stimulus and mechanism of this signaling pathway remains inconclusive. Studies of reovirus infection determined that empty virus particles (NTC), which lack dsRNA, do not activate IRF3 or induce IFN (78, 104). Reovirus-mediated activation of IRF3 can also be blocked with the endosomal cysteine protease inhibitor E64 (78). Finally, cells infected in the presence of ribavirin activate IRF3, suggesting dsRNA of input virus particles and disassembly of these particles are required for activation of IRF3 yet de novo synthesis of viral RNA is not required for activation of IRF3 (78). As previously mentioned, it seems unlikely that viral dsRNA of input particles is exposed to the cytoplasm for detection by RIG-I and MDA5. Instead the trigger for these sensors may be small oligonucleotides present in virus particles that could be released into the cytoplasm during particle disassembly; this scenario remains to be determined. In terms of the IFN signaling pathway mechanism, one study indicates if either RIG-I or MDA5 is inhibited by shRNA, siRNA, or gene knockout, there is a subsequent decrease in reovirus-mediated IFN signaling that can be detected as decreased IRF3 activation or ISG expression (110). However, when both RIG-I and MDA5 are inhibited, reovirus infection induces only minimal ISG expression (110) and IFN-β secretion (87), demonstrating that both RIG-I and MDA5 are required for IFN signaling. Another study demonstrates reovirus-mediated IFN-β induction is dependent on MDA5 but not RIG-I (87). Yet another study suggests activation of IRF3 by reovirus is dependent on RIG-I but not MDA5 (78). These differences in results may reflect cell-type specific differences. Similarly, when the adaptor protein IPS-1 is inhibited, reovirus infection does not result in IRF3 activation, IRF3 nuclear translocation, or expression of

IRF3-dependent ISGs (78, 110). Interestingly, inhibition of RIG-I and IPS-1 does not affect reovirus-induced activation of NF-κB (78), suggesting an alternative mechanism that is both RIG-I- and IPS-1-independent may be responsible for NF-κB activation. Downstream of IPS-1, the transcription factor IRF3 is activated as early as 2 hours post-infection with reovirus (78). It has been determined that activation of IRF3 is required for induction of IFN-α and IFN-β and is required for limiting viral spread in cell culture (78). Moreover, IRF3 is required for protection against reovirus induced-myocarditis (77), likely due to the role of activated IRF3 in induction of IFN leading to establishment of an anti-viral state. Reovirus infection also leads to expression of the ISG IRF7, but as expected this induction, along with induction of IFN-β, occurs at a slightly later time than activation of IRF3 (78).

As previously mentioned, reovirus infection in a neonatal mouse model can be used to demonstrate virus-induced myocarditis with minimal inflammatory cell infiltrate. Cardiac myocytes, a virtually non-replenishable cell type, are extremely vulnerable to invading pathogens. Thus, it comes as no surprise that cardiac myocytes and the neighboring replenishable cardiac fibroblasts have a unique system of defense which requires IFN-α/β. The induction of IFN-β in cardiac cells requires the transcription factor IRF3 (132). A non-myocarditic reovirus can induce myocarditis when mice are depleted of IFN-α/β with antibody (168). Most likely as a pre-arming mechanism against pathogens, cardiac myocytes have higher basal IFN-β (109, 171, 187) and IFN-α4 (109) than cardiac fibroblasts. Basal levels of ISGs IRF7 and ISG561 are also higher in cardiac myocytes than fibroblasts (171, 187), suggesting basal amplification of IFN occurs in these cells. Though cardiac myocytes secrete IFN at basal levels for protection, basal IFN secreted from cardiac myocytes is insufficient to protect adjacent cardiac fibroblasts from reovirus infection (187), thus secreted IFN offers only autocrine protection. In contrast to cardiac myocytes, cardiac fibroblasts maintain higher basal expression of Jak-STAT signaling components (Jak1, Tyk2, STAT2, and IRF9) (187). Furthermore, a higher percentage of cardiac fibroblasts are positive for basal expression of IFNAR1 and IFNAR2 than cardiac myocytes (187). Collectively, this suggests cardiac fibroblasts are poised to more readily respond to induced IFN during infection. Indeed, when cardiac fibroblasts and cardiac myocytes were treated with increasing doses of exogenous IFN-α/β and monitored for induction of ISG56 and IRF7, cardiac fibroblasts required only 33 U/ml of IFN-α/β to induce the same amount of these ISGs as compared to cardiac myocytes requiring 1,000 U/ml of IFN-α/β (187). Induced IFN also provides greater protection in cardiac fibroblasts than cardiac myocytes as demonstrated by greater reductions in reovirus replication in cardiac fibroblasts treated with IFN-β than in cardiac myocytes treated with IFN-β (171). In response to reovirus infection, more IFN-β (109, 171, 187) and IFN-α1, α2, - α4, - α5, - α8/6 (109) are induced by cardiac myocytes than cardiac fibroblasts, demonstrating cell-type specific differences to reovirus infection. Additionally, in reovirus infected cardiac myocytes, the majority of type I IFN induced is IFN-β and IFN-α4, whereas in fibroblasts there is higher induction of IFN-β along with multiple IFN-α subtypes (109). However, IFN-β provides the greatest protection from reovirus infection in both cardiac myocytes and cardiac fibroblasts (109). The amplification of IFN is indicated to be of more importance for IFN-α4 expression than for IFN-β expression in reovirus infected cardiac myocytes (109). As demonstrated in IFN-α/β-receptor-null mice, cardiac fibroblasts rely less on the amplification of IFN than do cardiac myocytes (109). Interestingly, reovirus-mediated induction of IFN correlates with the myocarditic potential of reoviruses (168). Reovirus sensitivity to IFN also correlates with the myocarditic potential (168). Non-myocarditic reoviruses, such as T3D, induce more IFN-β and are more sensitive to IFN-β whereas myocarditic reoviruses, such as T1L, are poor inducers of IFN-β and are resistant to IFN-β (168). Both induction of IFN and sensitivity to IFN are associated with the reovirus M1, S2, and L2 genes (168). The association of both phenotypes with the same genes is likely explained by interdependence of these events centering on the recent identification of a repressor of IFN signaling. Zurney et al determined the M1 gene (μ2 protein) of T1L encodes a repressor of IFN signaling (188). This finding suggests that myocarditic IFN-resistant reoviruses are poor inducers of IFN-β in part because they repress IFN signaling while non-myocarditic IFN-sensitive reoviruses induce more IFN-β in part because they do not encode for a repressor and induction of IFN is constantly amplified through IFN signaling. This study also determined the repression of IFN signaling is associated with reovirus induced-myocarditis: myocarditic reoviruses encode the repressor whereas non-myocarditic reoviruses do not encode the repressor (188). While the T1L M1 gene encoded μ2 protein is able to inhibit induction of the ISG IRF7, the repressor did not cause degradation of STAT1, STAT2, or IRF9 (188) which is characteristic of some viral inhibitors of IFN signaling (53, 62, 107). Furthermore, the T1L μ2 protein did not inhibit nuclear translocation of STAT1 or STAT2 but interestingly, the T1L μ2 protein is associated with nuclear accumulation of IRF9 (188). According to current literature, only two viruses are reported to be associated with repression of IFN signaling through IRF9-mediated mechanisms: human papillomavirus E7 protein prevents nuclear translocation of IRF9 (7) and adenovirus is associated with a decrease in IRF9 protein (107). Chapter 2 of this dissertation will further explore the role of the reovirus strain-specific repressor of IFN signaling.

Reovirus infection of neonatal mice also results in virus-induced encephalitis. It should be noted that some parallels between the cardiac and brain interferon response have been determined. Furthermore, similarities in approaches exist between these two systems: both use primary cell cultures and both study disease in a mouse-model. Components of IFN signaling are also activated in the brain by reovirus infection (73) and the induction of type I IFN in the brain functions to control viral spread across different regions of the brain and reduces viral replication (55). In primary neuronal cultures and in mice, reovirus infection results in an increase in STAT1 expression and nuclear translocation of phosphorylated STAT1 (73). This activation of STAT1 was demonstrated to be JAK-dependent (73). Although both type I IFN (IFN-α/β) and type II IFN (IFN-γ) signaling pathways utilize JAK-STAT signaling, pretreatment of neuronal cultures with IFN-γ antibody did not affect reovirus induced-phosphorylation of STAT1 (73). In contrast, pretreatment of neuronal cultures with IFN-α/β antibody inhibited reovirus induced-phosphorylation of STAT1, demonstrating STAT1 activation in neuronal cultures is also dependent on IFN-α/β (73). Viral spread across different brain tissues and pathology in reovirus infected STAT1-null mice did not differ from infected WT mice (73), yet mice deficient for the type I IFN receptor have greater spread in various brain regions but do not have significantly more tissue damage than WT mice (55). However, reovirus infected STAT1-null mice succumbed to infection more rapidly than WT mice and reovirus achieved higher titers in the brains of STAT1-null mice, suggesting a role for STAT1 in protection against reovirus infection in the brain (73). Similarly, reovirus infected type I IFN-receptor-null mice succumb to infection significantly sooner than reovirus infected WT mice, suggesting the IFN response is required for protection against reovirus infection in the brain (55) as was demonstrated previously for other organs (77, 86, 168).

NUCLEAR FACTOR-KAPPA B (NF-κB)

Nuclear factor-kappa B (NF-κB) is a family of transcription factors that regulate an array of cellular genes involved in, but not limited to, cellular proliferation, differentiation, and death as well as the innate and adaptive immune responses. The NF-κB family consists of the following subunits: RelA/p65, RelB, c-Rel, p105/NF-κB1, and p100/NF-κB2. These subunits are held in an inactive state in the cytoplasm by the inhibitor of NF-κB (IκB) family. The IκB proteins, which include IκBα, IκBβ, and IκB, are phosphorylated by IκB kinases (IKKs) (54, 184) which then lead to ubiquitination and proteasomal degradation of the IκB proteins. The degradation of IκB allows active NF-κB subunits to then translocate to the nucleus to bind DNA for gene expression (28). There are two pathways of NF-κB signaling which differ according to activation of IKK family members (IKKα, IKKβ, Nemo, or NIK). Please refer to Häcker and Karin for a more in depth review of the IKK family (81). In the classical pathway, IKKβ and Nemo phosphorylate IκBα and p105, resulting in release of the p50 subunit. In the alternative pathway, NIK activates

IKKα, which then phosphorylates p100. Once phosphorylated, the p100 subunit is cleaved to yield the p52 subunit. Recently published, Rahman and McFadden review the current literature of NF-κB signaling with respect to pathogen modulation of NF-κB signaling (145). The following is a review of established reovirus mechanisms of NF-κB activation and the outcomes of this activation. In the literature, the focus of the relationship between reovirus infection and NF-κB consist of two parts: the events leading to activation of NF-κB and an inhibition phase of activation of NF-κB.

In HeLa cells, reovirus T3D induced activation of NF-κB occurs as early as 4 hours post-infection with an increase in activation over time until decreasing by 12 hours post-infection (37). Activated NF-κB subunits p50 and p65 are detected in reovirus-infected cells as well as DNA-binding activity from 2 to 10 hours post-infection, demonstrating activation of the classical pathway of NF-κB activation (37, 75, 135). As anticipated, IκBα also decreases in reovirus T3D infected HeLa cells, and is most likely due to reovirus activated IKK subunits IKKα and Nemo (75). It is suggested that IκBα is regulated by IKKα during reovirus T3D infection, instead of IKKβ-mediated IκBα regulation which normally occurs (75). Reovirus T3D mediated activation of caspase 3/7 requires IKKα and Nemo subunits but does not require IKKβ or NIK (75). Similarly, reovirus induced-apoptosis is inhibited when degradation of IκB is inhibited by overexpression of a dominant negative form of IκBα or IκB which lack sites for phosphorylation (32, 37). Furthermore, inhibition of the proteasome prevents reovirus activation of NF-κB and apoptosis (37). However, in stark contrast, reovirus T3Abney infection of HEK293 cells does not result in IκBα degradation as indicated by Western Blot, but reovirus apoptosis and activation of caspase-3 in HEK293 cells does require IκB degradation (32). This dichotomy of reovirus-mediated IκBα degradation may reflect virus strain-specific or cell type-specific differences. A later phase of NF-κB activation was identified at 16 to 24 hours post-infection in reovirus infected HeLa cells (75). This second phase of activation was identified by decreasing concentrations of the p100 subunit with a parallel increase in the p52 subunit, indicating use of the alternative NF-κB signaling pathway (75).

It has also been demonstrated that a highly apoptotic reovirus, such as T3A or 8B, does not maintain activation of NF-κB at 24 hours post-infection (30, 32). Instead, experiments utilizing NF-κB stimuli such as etoposide and TNF-α in the presence of T3A infection, revealed a phase of NF-κB inhibition at late times post-infection (12 to 24 hours) (30). This inhibition phase is characterized by a block of NF-κB activation as well as a block of IκB degradation, is determined by the reovirus S1 gene, and correlates with apoptosis (30, 32).

It was determined that reovirus strain 8B was able to induce apoptosis in primary cardiac myocytes in the presence of SN50, a peptide that inhibits nuclear translocation of NF-κB, suggesting apoptosis in primary cardiac myocytes, in contrast to HEK293 cells, does not require NF-κB (30). Similarly, it was also demonstrated that infection with reovirus strain T3SA+ of p50-null mice resulted in numerous foci positive for both TUNEL and activated caspase-3 staining in cardiac tissue as compared to only rare positive cells in cardiac sections of WT animals (135). Furthermore, significantly higher viral titers were achieved in the hearts of p50-null mice and the hearts of these animals appears to have myocarditic lesions (135). Collectively, this suggests that in the heart, NF-κB has a protective, rather than destructive, role.

Indeed, in the heart, the induction of IFN-β is dependent on NF-κB, specifically the p50 subunit (135). This anti-viral protection mediated by NF-κB can be recapitulated in reovirus infected p50-null mice treated with exogenous IFN-β to result in decreased viral replication and apoptosis (135). Reovirus infected HeLa cells also result in NF-κB dependent induction of ISGs, including STAT1 and STAT2 (136). While these data suggest NF-κB activation may be a result of PRR signaling, it has been demonstrated that reovirus activation of NF-κB occurs independent of RIG-I and IPS-1 (78). Chapter 3 of this dissertation explores other mechanisms of reovirus NF-κB activation. Interestingly, the role of NF-κB in relation to reovirus-induced apoptosis and disease was found to be organ-specific (135). In the brain of T3SA+ infected p50-null mice, significantly fewer cells were TUNEL-positive and positive for activated caspase-3 despite equivalent viral replication the brains of WT and p50-null mice (135). Apoptosis is also inhibited in immortalized murine fibroblast cell lines deficient in either p50 or p65 (37). This suggests activation of NF-κB, specifically the p50 subunit, is required for efficient apoptosis in HeLa cells and in the brain (135).

IMMUNORECEPTOR TYROSINE-BASED ACTIVATION MOTIFS (ITAMs)

Immunoreceptor tyrosine-based activation motifs (ITAMs) are best known for their function in the adaptive immune system T cell receptor (TCR) and B cell receptor (BCR) (176). In addition to cellular receptors that contain ITAMs, ITAMs are found in adaptor proteins, such as

DAP12 and FcRγ, which associate with cellular receptors (176). Most recently, ITAMs have been reported in viral proteins (8). The canonical sequence of an ITAM consists of two repeats of the sequence YxxI/L, where tyrosine (Y) is separated by any two amino acids (x) from isoleucine (I) or leucine (L) (8). This sequence doublet is separated by a span of any six to twelve amino acids and is abbreviated as YxxI/Lx$_{6-12}$YxxI/L (8). Despite the implication that ITAMs disseminate only an activating signal, they can surprisingly inhibit signaling cascades (8). For example, different IgA isotypes lead to a pro- or anti-inflammatory signal mediated by FcR, which contains an ITAM (8). The outcome of ITAM activation may in part depend on how the ITAM-containing receptor was activated; low level constitutive or "tonic" signaling that is a ligand-independent activation of the ITAM has been reported for the BCR complex (126). In addition to ITAMs, immunoreceptor tyrosine-based inhibition motifs (ITIMs) are often found in immune receptors such as FcγRII and natural killer cell receptors; ITIMs normally function to balance the activating signal from ITAMs through ITIM activation of tyrosine phosphatases such as SHP-1, SHP-2, and SHIP (147). Src and Syk can are also regulated by Cbl which ubqutiniates the kinases for degradation (129). ITIMs are defined by the sequence S/I/V/LxYxxI/V/L, where S is for serine, I is for isoleucine, V is for valine, L is for leucine, Y is tyrosine, and x is any amino acid (147). Due to the sequence composition, ITIMs can actually be found within ITAMs (8). Like ITAMs, ITIM activation can result in inhibitory signals as implied by their name, but can also result in activating signals (8). The tyrosine residues of ITAMs are phosphorylated upon receptor engagement (129). Normally, ITAMs are phosphorylated by Src family kinases and then the phosphorylated ITAM recruits Syk family kinases Syk and/or Zap70 (129). Syk and Zap70 autophosphorylate when bound to an ITAM and then stimulate downstream signaling (129). ITAM-mediated signal transduction results in an array of cellular responses including, but not limited to cell proliferation, cell differentiation, bone development, and cytokine release (3). Triggering receptors expressed by myeloid cells (TREMs) associate with DAP12 and Syk/Zap70 to signal downstream to PI3K and ERK (35). TREMs are suggested to have a role in inflammation in which they induce cytokine expression in response to infection with bacteria or fungi as well as roles in bone development and differentiation of resident cells of the brain (35). Leukocyte rolling on P-selectin requires the tyrosine kinase Syk (2) and likely uses the ITAM containing protein moesin as an adaptor for this association (177) to mediate an immune response. The ITAMs found in adaptor proteins DAP12 and FcRγ are required for integrin signaling (4, 128), though the mechanism of the association between these adaptors and integrins remains unknown (3). It is suggested that ITAM signaling also contributes to the innate immune response. Constitutive or tonic signaling by ITAMs enhance IFN-α and IFN-γ-mediated activation of JAKs and STAT1 (85). The enhancement of signaling is specific for IFN-α mediated STAT1 activation in macrophages that are primed with IFN-γ (174). The ITAM containing adaptors DAP12 and FcRγ are required for this enhancement as well as the protein kinase Syk (174).

Chapter 3 of this dissertation explores the role of a putative ITAM within the reovirus μ2 protein of strain T3D. Reovirus strain T1L also contains an ITAM in the μ2 protein though a role for this ITAM has not been demonstrated. Additionally, ITAMs are found within the σ2 and λ2 proteins of strains T3D and T1L; roles of these ITAMs have not yet been identified. In an effort to determine roles of the reovirus ITAMs, it is important to consider the role of known viral

ITAMs and the mechanisms by which they function. The remainder of this section will focus on these known viral ITAMs.

There are only two viruses with reported ITAMs that are not oncogenic. The first reviewed here is the Bunyaviridae family member hantavirus. This enveloped, negative-sense RNA virus is well characterized for the two diseases it causes in infected humans: hemorrhagic fever with renal syndrome (HFRS) and hantavirus pulmonary syndrome (HPS). The ITAM of hantavirus is found in the cytoplasmic tail of the G1 protein (71) which is encoded by the M gene segment. Interestingly, the ITAM is highly conserved in HPS-causing hantaviruses but not in HFRS or nonpathogenic strains. Studies in endothelial and immune cells suggest that the G1 protein ITAM likely functions to disrupt normal responses of these cells to aid viral pathogenesis (71). The G1 protein binds Src family member Lyn as well as Syk family members Syk and Zap70, however when the tyrosine residues of the ITAM are mutated to phenylalanine, these associations are lost (71). The G1 ITAM is also responsible for ubiquitination and degradation of the G1 protein, as demonstrated by an inhibition of ubiquitination and of degradation when the tyrosine residues of the ITAM are mutated to phenylalanine residues (70). The lentivirus simian immunodeficiency virus (SIV) also encodes an ITAM that contributes to pathogenesis. SIV strains encoding an ITAM in the Nef protein cause substantial disease in infected macaques, often requiring euthanasia, and these macaques have significantly fewer lymphocytes circulating in their blood than animals infected with SIV strains that do not encode functional ITAMs (52). Pathologically, the ITAM encoding SIV strains also cause changes in the intestinal structures such as blunting and fusion of villi as well as cellular infiltration of the intestinal tissue, whereas SIV strains that do not contain tyrosine residues in the ITAM do not cause these alterations in the intestine (52). Furthermore, the ITAM-encoding SIV strains induce more cellular proliferation of unstimulated PBMCs in culture (52). Interestingly, all of these differences between ITAM-encoding SIV strains and SIV strains that do not encode tyrosine residues in the ITAM do not lead to differences in viral replication in infected macaques (52). In terms of mechanism, the SIV Nef protein ITAM can be phosphorylated by Src and associates with Src in 3T3 cells (59). In Jurkat cells, a T cell line, phosphorylated Nef binds Zap70 whereas un-phosphorylated Nef is unable to bind Zap70 (112). Since Src is expressed at low levels in T cells, it seems unlikely that Src is responsible for Nef phosphorylation in these cells. Instead, it has been demonstrated that Lck, which is highly expressed in T cells, is required for Nef ITAM signaling in T cells (112). Furthermore, the Nef protein ITAM is able to induce NFAT activation whereas Nef that does not encode tyrosine residues in the ITAM is unable to cause this activation (112). Thus the ITAMs found in the G1 protein of hantavirus and the Nef protein of SIV contribute to pathogenesis.

The *Gammaherpesviridae* family member Epstein-Barr virus (EBV) is associated with a number of diseases in humans. Burkitt's lymphoma, Hodgkin's lymphoma, nasopharyngeal carcinoma (NPC), and HIV-associated oral hairy leukoplakia (OHL) are just some of the diseases associated with EBV. Viral latency is established in B cells; selective viral gene expression occurs during latency. One of the genes often expressed during latency is latent membrane protein 2 (LMP2) which forms LMP2A and LMP2B proteins depending on the promoter used. The amino terminus of LMP2A consists of eight tyrosine residues including one ITAM. Studies indicate

LMP2A contributes to the establishment of viral latency. Through studies using LMP2A-expressing cells to demonstrate tumor formation in mice and other characteristics of transformed cells, LMP2A is indicated to be oncogenic (155). The ITAM of LMP2A is suggested to be the main site of phosphorylation on this protein despite an abundance of tyrosine residues (156). Furthermore, though activation of the LMP2A does not appear to result from ligand-receptor-binding, the phosphorylation of LMP2A is suggested to be regulated by cell adhesion (156). LMP2A association with tyrosine kinases is suggested to be cell-type specific. In epithelial cells, phosphorylation of LMP2A appears to be independent of Src family kinases and instead phosphorylation can be mediated by Csk (156). However studies in BJAB cells, a B cell line, indicate LMP2A can associate with Src family kinase members Lyn, Lck, and Fyn but has a preference to associate with Lyn and Fyn as demonstrated by immunoprecipitation (24). Additionally, though it is not part of the LMP2A ITAM, tyrosine residue 112 is required for the LMP2A association with Lyn in BJAB cells (67). Importantly, the ITAM of LMP2A is required for activation of Syk (66, 67). Activation of B cells, through the BCR ITAM, normally results in activation of Syk which then leads to downstream signaling which includes activation of phospholipase Cγ (PLCγ), release of intracellular calcium, and activation of MAPKs. The LMP2A-mediated inhibition of B cell receptor (BCR) signaling requires the ITAM (66). This was demonstrated by making tyrosine-to-phenylalanine mutations in the LMP2A ITAM which alleviate inhibition of BCR-mediated calcium release, tyrosine phosphorylation, and activation of BZLF1 (66). By constructing CD8-LMP2A chimeras, it has been demonstrated that upon anti-CD8 antibody crosslinking, the LMP2A can function to increase release of intracellular calcium and induce IL-2 production in B cells (14). In both B cells and epithelial cells, the LMP2A-mediated activation of Akt requires the ITAM of LMP2A (127, 173). It seems the ITAM of LMP2A functions in concert with the other domains of LMP2A to mimic BCR signaling. Activation of Akt and ITAM-mediated PI3K determine β-catenin expression (127). However, it is another motif of LMP2A, the PY domain, that is required for β-catenin stabilization though both the PY and ITAM contribute to nuclear translocation of β-catenin in epithelial cells (127). It was also determined that the PY motif of LMP2A mediates inhibition of epithelial cell differentiation and the ITAM has only minimal impact (127). The ITAM of LMP2A is associated with kinase activity in epithelial cells and is the major site of phosphorylation of LMP2A (156), however data suggests tyrosine residue 112 is required for phosphorylation in lymphoblastoid cell lines(67), again indicating cell-type specific differences.

Two oncogenic retroviruses are currently reported to contain ITAMs: mouse mammary tumor virus (MMTV) and bovine leukemia virus (BLV). Part of the betaretrovirus family, MMTV is often used as a model for breast cancer due to its ability to induce mammary tumors in mice. In MMTV, the envelop protein (Env) consists of two subunits; there is a cell surface (SU) domain and a transmembrane (TM) domain. The ITAM of Env is found within the SU domain. When mice are infected with wild-type (WT) virus, which encodes the Env ITAM, and an ITAM-mutated virus, which contains tyrosine-to-phenylalanine mutations in the ITAM, the latter is delayed in tumor formation (151). The animals infected with WT virus have increased expression wnt1 and fgf3 (151), suggesting the ITAM-mediated tumor formation may be through pathways including these proteins. Overexpression of the Env protein causes depolarization of mammary epithelial cells but can be inhibited with the Syk inhibitor piceatannol and the Src inhibitor PP2 (88). Overexpressed Env is associated with Syk as demonstrated by immunoprecipitation (88). Other markers of mammary cell transformation displayed by WT Env-expressing cells include downregulated Keratin-18 and E-cadherin as well as sensitivity to TRAIL and TNF-α (88), which are all markers of cell transformation. When the ITAM is mutated from tyrosine to phenylalanine residues, this effect is diminished (88). BLV, another retrovirus, causes persistent B cell expansion in cattle but can also infect sheep where it leads to leukemia and death. The gp30 protein of BLV contains three YXXL motifs that make two highly conserved ITAMs (180) as well as two ITIMs. One study demonstrated all ITAMs and ITIMs appear un-phosphorylated in mononuclear cells extracted from BLV infected cows, infected cell lines of fetal lamb kidney cells and bat lung cells, and in DT40 cells that overexpressed a CD8 chimeric protein (74), however this negative data for ITAM phosphorylation may simply indicate further experiments are needed to determine when the ITAM is phosphorylated. In sheep infected with WT BLV and mutated BLV that contain tyrosine-to-aspartic acid substitutions in the ITAM, it was demonstrated the second YXXL motif, part of the first ITAM, is required for infection and viral persistence (180). When the extracellular and transmembrane portions of CD8 are fused to the cytoplasmic domain of gp30, which contains the ITAM, antibody crosslinking of this chimeric protein leads to IL-2 production (14). For this function, only the tyrosine residues of the first ITAM are required (14). Upon anti-CD8 antibody crosslinking, the CD8/gp30 chimeric protein can also induce release of intracellular calcium, which is an early cellular activation signal (14).

Two herpesviruses, Kaposi's sarcoma-associated herpesvirus (KSHV) and rhesus monkey rhadinovirus (RRV), contain ITAMs that contribute to the oncogenic nature of these viruses. KSHV is mainly associated with Kaposi's sarcoma and Castleman's disease. Unlike other ITAM-linked oncogenic viruses, KS is suggested to result from hyperplastic growth instead of clonal expansion. The KSHV protein K1 is a transmembrane protein: the cytoplasmic tail of K1 contains an ITAM (106) and the extracellular domain of K1 is responsible for constitutive activation of the K1 ITAM (103). The K1 ITAM may have a role in KSHV lytic replication in B cells (102). While KSHV is normally found in a latent state in KS tumors, it is believed that lytic replication also plays a role in KS development. Though the Src family member Lyn has been shown to interact with the ITAM of K1, it appears Lyn may function to inhibit K1 signaling (105). This was demonstrated by using cells deficient for specific tyrosine kinases, including Syk and Lyn, and examining NFAT activation in response to overexpressed K1 constructs (105). Lyn-null cells had higher background levels of NFAT activation than Syk-null cells but perhaps more importantly, overexpression of Lyn in Lyn-null cells resulted in a decrease in K1-mediated activation of NFAT whereas overexpression of Syk rescued K1-mediated activation of NFAT in Syk-null cells (105). The ITAM of K1 associations with Syk and with PLCγ2 are required for K1-mediated NFAT activation (105). Moreover, activation of transcription factors NFAT and AP-1 (102) and the release of intracellular calcium require K1 ITAM-mediated Syk activation as well as K1 ITAM-mediated PI3K activation (105). In BJAB cells, a B cell line, it has been demonstrated that the K1 ITAM induces cytokine production which may have a role in disease (105). As mentioned previously, KSHV replicates in both latent and lytic cycles of replication.

Interestingly, high sustained levels of K1 which occur during overexpression appear to inhibit normal K1-mediated lytic reactivation albeit to a lower degree of inhibition than a K1 ITAM mutant (103). In this study, the authors propose the reduction in lytic reactivation resulting from K1 overexpression may be due to desensitization of K1 ITAM signaling pathways (103). This demonstrates the virus has evolved to produce the K1 protein at a very precise concentration as to prevent overwhelming the infected cell (102). This same effect was also observed with the closely related virus RRV (42). The RRV R1 protein contains five well conserved YXXL sites which comprise two putative ITAMs (43). As demonstrated in rat fibroblast cells, the R1 protein can cause cellular transformation (43). Furthermore, nude mice injected with Rat-1 cells expressing the R1 protein develop large tumors whereas control mice injected with Rat-1 cells do not develop tumors (43). Thus, similar to the KSHV K1 protein, the RRV R1 protein can be oncogenic (43). Though overexpressed R1 can be phosphorylated by Syk and Src kinases in COS-1 cells, only Syk associates with R1 as determined by coimmunoprecipitation, and Syk, but not Src, is able to phosphorylate R1 in an in vitro kinase assay (42). For signaling, when CD8-R1 chimeric proteins containing the R1 ITAM, are crosslinked with anti-CD8 antibody, intracellular calcium is released (42). As expected, ITAM deletion mutants as well as SH2 deletion mutants are unable to induce calcium release (42), demonstrating the importance of these domains for signaling. Similar to the KSHV K1 protein, overexpression of the R1 protein as well as antibody crosslinked CD8-R1 chimeric proteins can activate NFAT whereas ITAM deletion mutants do not activate NFAT (42).

REFERENCES

1. 1955. ENTERIC cytopathogenic human orphan (ECHO) viruses. Science **122:**1187-1188.

2. **Abbal, C., M. Lambelet, D. Bertaggia, C. Gerbex, M. Martinez, A. Arcaro, M. Schapira, and O. Spertini.** 2006. Lipid raft adhesion receptors and Syk regulate selectin-dependent rolling under flow conditions. Blood **108:**3352-3359.

3. **Abram, C. L., and C. A. Lowell.** 2007. The expanding role for ITAM-based signaling pathways in immune cells. Sci STKE **2007:**re2.

4. **Abtahian, F., N. Bezman, R. Clemens, E. Sebzda, L. Cheng, S. J. Shattil, M. L. Kahn, and G. A. Koretzky.** 2006. Evidence for the requirement of ITAM domains but not SLP-76/Gads interaction for integrin signaling in hematopoietic cells. Mol Cell Biol **26:**6936-6949.

5. **Agosto, M. A., T. Ivanovic, and M. L. Nibert.** 2006. Mammalian reovirus, a nonfusogenic nonenveloped virus, forms size-selective pores in a model membrane. Proc Natl Acad Sci U S A **103:**16496-16501.

6. **Alexopoulou, L., A. C. Holt, R. Medzhitov, and R. A. Flavell.** 2001. Recognition of double-stranded RNA and activation of NF-kappaB by Toll-like receptor 3. Nature **413:**732-738.

7. **Barnard, P., and N. A. McMillan.** 1999. The human papillomavirus E7 oncoprotein abrogates signaling mediated by interferon-alpha. Virology **259:**305-313.

8. **Barrow, A. D., and J. Trowsdale.** 2006. You say ITAM and I say ITIM, let's call the whole thing off: the ambiguity of immunoreceptor signalling. Eur J Immunol **36:**1646-1653.

9. **Bartlett, N. M., S. C. Gillies, S. Bullivant, and A. R. Bellamy.** 1974. Electron microscopy study of reovirus reaction cores. J Virol **14:**315-326.

10. **Barton, E. S., J. L. Connolly, J. C. Forrest, J. D. Chappell, and T. S. Dermody.** 2001. Utilization of sialic acid as a coreceptor enhances reovirus attachment by multistep adhesion strengthening. J Biol Chem **276:**2200-2211.

11. **Barton, E. S., J. C. Forrest, J. L. Connolly, J. D. Chappell, Y. Liu, F. J. Schnell, A. Nusrat, C. A. Parkos, and T. S. Dermody.** 2001. Junction adhesion molecule is a receptor for reovirus. Cell **104:**441-451.

12. **Baty, C. J., and B. Sherry.** 1993. Cytopathogenic effect in cardiac myocytes but not in cardiac fibroblasts is correlated with reovirus-induced acute myocarditis. J Virol **67:**6295-6298.

13. **Baughman, K. L.** 2006. Diagnosis of myocarditis: death of Dallas criteria. Circulation **113:**593-595.

14. **Beaufils, P., D. Choquet, R. Z. Mamoun, and B. Malissen.** 1993. The (YXXL/I)2 signalling motif found in the cytoplasmic segments of the bovine leukaemia virus envelope protein and Epstein-Barr virus latent membrane protein 2A can elicit early and late lymphocyte activation events. EMBO J **12:**5105-5112.

15. **Bellamy, A. R., and W. K. Joklik.** 1967. Studies on the A-rich RNA of reovirus. Proc Natl Acad Sci U S A **58:**1389-1395.

16. **Bellamy, A. R., L. Shapiro, J. T. August, and W. K. Joklik.** 1967. Studies on reovirus RNA. I. Characterization of reovirus genome RNA. J Mol Biol **29:**1-17.

17. **Berens, H. M., and K. L. Tyler.** 2011. The pro-apoptotic Bcl-2 protein Bax plays an important role in the pathogenesis of reovirus encephalitis. J Virol.

18. **Bergmann, O., R. D. Bhardwaj, S. Bernard, S. Zdunek, F. Barnabé-Heider, S. Walsh, J. Zupicich, K. Alkass, B. A. Buchholz, H. Druid, S. Jovinge, and J. Frisén.** 2009. Evidence for cardiomyocyte renewal in humans. Science **324:**98-102.

19. **Bisaillon, M., J. Bergeron, and G. Lemay.** 1997. Characterization of the nucleoside triphosphate phosphohydrolase and helicase activities of the reovirus lambda1 protein. J Biol Chem **272:**18298-18303.

20. **Borsa, J., B. D. Morash, M. D. Sargent, T. P. Copps, P. A. Lievaart, and J. G. Szekely.** 1979. Two modes of entry of reovirus particles into L cells. J Gen Virol **45:**161-170.

21. **Brentano, L., D. L. Noah, E. G. Brown, and B. Sherry.** 1998. The reovirus protein mu2, encoded by the M1 gene, is an RNA-binding protein. J Virol **72:**8354-8357.

22. **Broering, T. J., J. Kim, C. L. Miller, C. D. Piggott, J. B. Dinoso, M. L. Nibert, and J. S. Parker.** 2004. Reovirus nonstructural protein mu NS recruits viral core surface proteins and entering core particles to factory-like inclusions. J Virol **78:**1882-1892.

23. **Broering, T. J., J. S. Parker, P. L. Joyce, J. Kim, and M. L. Nibert.** 2002. Mammalian reovirus nonstructural protein microNS forms large inclusions and colocalizes with reovirus microtubule-associated protein micro2 in transfected cells. J Virol **76:**8285-8297.

24. **Burkhardt, A. L., J. B. Bolen, E. Kieff, and R. Longnecker.** 1992. An Epstein-Barr virus transformation-associated membrane protein interacts with src family tyrosine kinases. J Virol **66:**5161-5167.

25. **Campbell, J. A., P. Schelling, J. D. Wetzel, E. M. Johnson, J. C. Forrest, G. A. Wilson, M. Aurrand-Lions, B. A. Imhof, T. Stehle, and T. S. Dermody.** 2005. Junctional adhesion molecule a serves as a receptor for prototype and field-isolate strains of mammalian reovirus. J Virol **79:**7967-7978.

26. **Carvalho, J., M. M. Arnold, and M. L. Nibert.** 2007. Silencing and complementation of reovirus core protein mu2: functional correlations with mu2-microtubule association and differences between virus- and plasmid-derived mu2. Virology **364:**301-316.

27. **Chappell, J. D., J. L. Duong, B. W. Wright, and T. S. Dermody.** 2000. Identification of carbohydrate-binding domains in the attachment proteins of type 1 and type 3 reoviruses. J Virol **74:**8472-8479.

28. **Chen, F. E., D. B. Huang, Y. Q. Chen, and G. Ghosh.** 1998. Crystal structure of p50/p65 heterodimer of transcription factor NF-kappaB bound to DNA. Nature **391:**410-413.

29. **Chow, L. H., K. W. Beisel, and B. M. McManus.** 1992. Enteroviral infection of mice with severe combined immunodeficiency. Evidence for direct viral pathogenesis of myocardial injury. Lab Invest **66:**24-31.

30. **Clarke, P., R. L. Debiasi, S. M. Meintzer, B. A. Robinson, and K. L. Tyler.** 2005. Inhibition of NF-kappa B activity and cFLIP expression contribute to viral-induced apoptosis. Apoptosis **10:**513-524.

31. **Clarke, P., S. M. Meintzer, S. Gibson, C. Widmann, T. P. Garrington, G. L. Johnson, and K. L. Tyler.** 2000. Reovirus-induced apoptosis is mediated by TRAIL. J Virol **74:**8135-8139.

32. **Clarke, P., S. M. Meintzer, L. A. Moffitt, and K. L. Tyler.** 2003. Two distinct phases of virus-induced nuclear factor kappa B regulation enhance tumor necrosis factor-related apoptosis-inducing ligand-mediated apoptosis in virus-infected cells. J Biol Chem **278:**18092-18100.

33. **Cleveland, D. R., H. Zarbl, and S. Millward.** 1986. Reovirus guanylyltransferase is L2 gene product lambda 2. J Virol **60:**307-311.

34. **Coffey, C. M., A. Sheh, I. S. Kim, K. Chandran, M. L. Nibert, and J. S. Parker.** 2006. Reovirus outer capsid protein micro1 induces apoptosis and associates with lipid droplets, endoplasmic reticulum, and mitochondria. J Virol **80:**8422-8438.

35. **Colonna, M.** 2003. TREMs in the immune system and beyond. Nat Rev Immunol **3:**445-453.

36. **Connolly, J. L., E. S. Barton, and T. S. Dermody.** 2001. Reovirus binding to cell surface sialic acid potentiates virus-induced apoptosis. J Virol **75:**4029-4039.

37. **Connolly, J. L., S. E. Rodgers, P. Clarke, D. W. Ballard, L. D. Kerr, K. L. Tyler, and T. S. Dermody.** 2000. Reovirus-induced apoptosis requires activation of transcription factor NF-kappaB. J Virol **74:**2981-2989.

38. **Cook, D. N., M. A. Beck, T. M. Coffman, S. L. Kirby, J. F. Sheridan, I. B. Pragnell, and O. Smithies.** 1995. Requirement of MIP-1 alpha for an inflammatory response to viral infection. Science **269:**1583-1585.

39. **Coombs, K. M.** 1998. Stoichiometry of reovirus structural proteins in virus, ISVP, and core particles. Virology **243:**218-228.

40. **Cooper, L. T.** 2009. Myocarditis. N Engl J Med **360:**1526-1538.

41. **Daliento, L., F. Calabrese, F. Tona, A. L. Caforio, G. Tarsia, A. Angelini, and G. Thiene.** 2003. Successful treatment of enterovirus-induced myocarditis with interferon-alpha. J Heart Lung Transplant **22:**214-217.

42. **Damania, B., M. DeMaria, J. U. Jung, and R. C. Desrosiers.** 2000. Activation of lymphocyte signaling by the R1 protein of rhesus monkey rhadinovirus. J Virol **74:**2721-2730.

43. **Damania, B., M. Li, J. K. Choi, L. Alexander, J. U. Jung, and R. C. Desrosiers.** 1999. Identification of the R1 oncogene and its protein product from the rhadinovirus of rhesus monkeys. J Virol **73:**5123-5131.

44. **Danthi, P.** 2011. Enter the kill zone: initiation of death signaling during virus entry. Virology **411:**316-324.

45. **Danthi, P., C. M. Coffey, J. S. Parker, T. W. Abel, and T. S. Dermody.** 2008. Independent regulation of reovirus membrane penetration and apoptosis by the mu1 phi domain. PLoS Pathog **4:**e1000248.

46. **Danthi, P., M. W. Hansberger, J. A. Campbell, J. C. Forrest, and T. S. Dermody.** 2006. JAM-A-independent, antibody-mediated uptake of reovirus into cells leads to apoptosis. J Virol **80:**1261-1270.

47. **Danthi, P., T. Kobayashi, G. H. Holm, M. W. Hansberger, T. W. Abel, and T. S. Dermody.** 2008. Reovirus apoptosis and virulence are regulated by host cell membrane penetration efficiency. J Virol **82:**161-172.

48. **Danthi, P., A. J. Pruijssers, A. K. Berger, G. H. Holm, S. S. Zinkel, and T. S. Dermody.** 2010. Bid regulates the pathogenesis of neurotropic reovirus. PLoS Pathog **6:**e1000980.

49. **DeBiasi, R. L., P. Clarke, S. Meintzer, R. Jotte, B. K. Kleinschmidt-Demasters, G. L. Johnson, and K. L. Tyler.** 2003. Reovirus-induced alteration in expression of apoptosis and DNA repair genes with potential roles in viral pathogenesis. J Virol **77:**8934-8947.

50. **DeBiasi, R. L., C. L. Edelstein, B. Sherry, and K. L. Tyler.** 2001. Calpain inhibition protects against virus-induced apoptotic myocardial injury. J Virol **75:**351-361.

51. **DeBiasi, R. L., B. A. Robinson, B. Sherry, R. Bouchard, R. D. Brown, M. Rizeq, C. Long, and K. L. Tyler.** 2004. Caspase inhibition protects against reovirus-induced myocardial injury in vitro and in vivo. J Virol **78:**11040-11050.

52. **Dehghani, H., C. R. Brown, R. Plishka, A. Buckler-White, and V. M. Hirsch.** 2002. The ITAM in Nef influences acute pathogenesis of AIDS-inducing simian immunodeficiency viruses SIVsm and SIVagm without altering kinetics or extent of viremia. J Virol **76:**4379-4389.

53. **Didcock, L., D. F. Young, S. Goodbourn, and R. E. Randall.** 1999. The V protein of simian virus 5 inhibits interferon signalling by targeting STAT1 for proteasome-mediated degradation. J Virol **73:**9928-9933.

54. **DiDonato, J. A., M. Hayakawa, D. M. Rothwarf, E. Zandi, and M. Karin.** 1997. A cytokine-responsive IkappaB kinase that activates the transcription factor NF-kappaB. Nature **388:**548-554.

55. **Dionne, K. R., J. M. Galvin, S. A. Schittone, P. Clarke, and K. L. Tyler.** 2011. Type I interferon signaling limits reoviral tropism within the brain and prevents lethal systemic infection. J Neurovirol.

56. **Drory, Y., Y. Turetz, Y. Hiss, B. Lev, E. Z. Fisman, A. Pines, and M. R. Kramer.** 1991. Sudden unexpected death in persons less than 40 years of age. Am J Cardiol **68:**1388-1392.

57. **Dryden, K. A., D. L. Farsetta, G. Wang, J. M. Keegan, B. N. Fields, T. S. Baker, and M. L. Nibert.** 1998. Internal/structures containing transcriptase-related proteins in top component particles of mammalian orthoreovirus. Virology **245:**33-46.

58. **Dryden, K. A., G. Wang, M. Yeager, M. L. Nibert, K. M. Coombs, D. B. Furlong, B. N. Fields, and T. S. Baker.** 1993. Early steps in reovirus infection are associated with dramatic changes in supramolecular structure and protein conformation: analysis of virions and subviral particles by cryoelectron microscopy and image reconstruction. J Cell Biol **122:**1023-1041.

59. **Du, Z., S. M. Lang, V. G. Sasseville, A. A. Lackner, P. O. Ilyinskii, M. D. Daniel, J. U. Jung, and R. C. Desrosiers.** 1995. Identification of a nef allele that causes lymphocyte activation and acute disease in macaque monkeys. Cell **82:**665-674.

60. **Ebert, D. H., J. Deussing, C. Peters, and T. S. Dermody.** 2002. Cathepsin L and cathepsin B mediate reovirus disassembly in murine fibroblast cells. J Biol Chem **277:**24609-24617.

61. **Ehrlich, M., W. Boll, A. Van Oijen, R. Hariharan, K. Chandran, M. L. Nibert, and T. Kirchhausen.** 2004. Endocytosis by random initiation and stabilization of clathrin-coated pits. Cell **118:**591-605.

62. **Elliott, J., O. T. Lynch, Y. Suessmuth, P. Qian, C. R. Boyd, J. F. Burrows, R. Buick, N. J. Stevenson, O. Touzelet, M. Gadina, U. F. Power, and J. A. Johnston.** 2007. Respiratory syncytial virus NS1 protein degrades STAT2 by using the Elongin-Cullin E3 ligase. J Virol **81:**3428-3436.

63. **Esfandiarei, M., and B. M. McManus.** 2008. Molecular biology and pathogenesis of viral myocarditis. Annu Rev Pathol **3:**127-155.

64. **Feldman, A. M., and D. McNamara.** 2000. Myocarditis. N Engl J Med **343:**1388-1398.

65. **Forrest, J. C., J. A. Campbell, P. Schelling, T. Stehle, and T. S. Dermody.** 2003. Structure-function analysis of reovirus binding to junctional adhesion molecule 1. Implications for the mechanism of reovirus attachment. J Biol Chem **278:**48434-48444.

66. **Fruehling, S., and R. Longnecker.** 1997. The immunoreceptor tyrosine-based activation motif of Epstein-Barr virus LMP2A is essential for blocking BCR-mediated signal transduction. Virology **235:**241-251.

67. **Fruehling, S., R. Swart, K. M. Dolwick, E. Kremmer, and R. Longnecker.** 1998. Tyrosine 112 of latent membrane protein 2A is essential for protein tyrosine kinase loading and regulation of Epstein-Barr virus latency. J Virol **72:**7796-7806.

68. **Furlong, D. B., M. L. Nibert, and B. N. Fields.** 1988. Sigma 1 protein of mammalian reoviruses extends from the surfaces of viral particles. J Virol **62:**246-256.

69. **Furuichi, Y., M. Morgan, S. Muthukrishnan, and A. J. Shatkin.** 1975. Reovirus messenger RNA contains a methylated, blocked 5'-terminal structure: m-7G(5')ppp(5')G-MpCp-. Proc Natl Acad Sci U S A **72:**362-366.

70. **Geimonen, E., I. Fernandez, I. N. Gavrilovskaya, and E. R. Mackow.** 2003. Tyrosine residues direct the ubiquitination and degradation of the NY-1 hantavirus G1 cytoplasmic tail. J Virol **77:**10760-10868.

71. **Geimonen, E., R. LaMonica, K. Springer, Y. Farooqui, I. N. Gavrilovskaya, and E. R. Mackow.** 2003. Hantavirus pulmonary syndrome-associated hantaviruses contain conserved and functional ITAM signaling elements. J Virol **77:**1638-1643.

72. **Golden, J. W., J. A. Bahe, W. T. Lucas, M. L. Nibert, and L. A. Schiff.** 2004. Cathepsin S supports acid-independent infection by some reoviruses. J Biol Chem **279:**8547-8557.

73. **Goody, R. J., J. D. Beckham, K. Rubtsova, and K. L. Tyler.** 2007. JAK-STAT signaling pathways are activated in the brain following reovirus infection. J Neurovirol **13:**373-383.

74. **Hamilton, V. T., D. M. Stone, S. M. Pritchard, and G. H. Cantor.** 2002. Bovine leukemia virus gp30 transmembrane (TM) protein is not tyrosine phosphorylated: examining potential interactions with host tyrosine-mediated signaling. Virus Res **90:**155-169.

75. **Hansberger, M. W., J. A. Campbell, P. Danthi, P. Arrate, K. N. Pennington, K. B. Marcu, D. W. Ballard, and T. S. Dermody.** 2007. IkappaB kinase subunits alpha and gamma are required for activation of NF-kappaB and induction of apoptosis by mammalian reovirus. J Virol **81:**1360-1371.

76. **Herzum, M., V. Ruppert, B. Kuytz, H. Jomaa, I. Nakamura, and B. Maisch.** 1994. Coxsackievirus B3 infection leads to cell death of cardiac myocytes, p. 907-913, J Mol Cell Cardiol, vol. 26, England.

77. **Holm, G. H., A. J. Pruijssers, L. Li, P. Danthi, B. Sherry, and T. S. Dermody.** 2010. Interferon regulatory factor 3 attenuates reovirus myocarditis and contributes to viral clearance. J Virol **84:**6900-6908.

78. **Holm, G. H., J. Zurney, V. Tumilasci, S. Leveille, P. Danthi, J. Hiscott, B. Sherry, and T. S. Dermody.** 2007. Retinoic acid-inducible gene-I and interferon-beta promoter stimulator-1 augment proapoptotic responses following mammalian reovirus infection via interferon regulatory factor-3. J Biol Chem **282:**21953-21961.

79. **Honda, K., H. Yanai, H. Negishi, M. Asagiri, M. Sato, T. Mizutani, N. Shimada, Y. Ohba, A. Takaoka, N. Yoshida, and T. Taniguchi.** 2005. IRF-7 is the master regulator of type-I interferon-dependent immune responses. Nature **434:**772-777.

80. **Huismans, H., and W. K. Joklik.** 1976. Reovirus-coded polypeptides in infected cells: isolation of two native monomeric polypeptides with affinity for single-stranded and double-stranded RNA, respectively. Virology **70:**411-424.

81. **Häcker, H., and M. Karin.** 2006. Regulation and function of IKK and IKK-related kinases. Sci STKE **2006:**re13.

82. **Isaacs, A., and J. Lindenmann.** 1957. Virus interference. I. The interferon. Proc R Soc Lond B Biol Sci **147:**258-267.

83. **Ivanovic, T., M. A. Agosto, K. Chandran, and M. L. Nibert.** 2007. A role for molecular chaperone Hsc70 in reovirus outer capsid disassembly. J Biol Chem **282:**12210-12219.

84. **Ivanovic, T., M. A. Agosto, L. Zhang, K. Chandran, S. C. Harrison, and M. L. Nibert.** 2008. Peptides released from reovirus outer capsid form membrane pores that recruit virus particles. EMBO J **27:**1289-1298.

85. **Ivashkiv, L. B.** 2008. A signal-switch hypothesis for cross-regulation of cytokine and TLR signalling pathways. Nat Rev Immunol **8:**816-822.

86. **Johansson, C., J. D. Wetzel, J. He, C. Mikacenic, T. S. Dermody, and B. L. Kelsall.** 2007. Type I interferons produced by hematopoietic cells protect mice against lethal infection by mammalian reovirus. J Exp Med **204:**1349-1358.

87. **Kato, H., O. Takeuchi, E. Mikamo-Satoh, R. Hirai, T. Kawai, K. Matsushita, A. Hiiragi, T. S. Dermody, T. Fujita, and S. Akira.** 2008. Length-dependent recognition of double-stranded ribonucleic acids by retinoic acid-inducible gene-I and melanoma differentiation-associated gene 5. J Exp Med **205:**1601-1610.

88. **Katz, E., M. H. Lareef, J. C. Rassa, S. M. Grande, L. B. King, J. Russo, S. R. Ross, and J. G. Monroe.** 2005. MMTV Env encodes an ITAM responsible for transformation of mammary epithelial cells in three-dimensional culture. J Exp Med **201:**431-439.

89. **Kawai, T., K. Takahashi, S. Sato, C. Coban, H. Kumar, H. Kato, K. J. Ishii, O. Takeuchi, and S. Akira.** 2005. IPS-1, an adaptor triggering RIG-I- and Mda5-mediated type I interferon induction. Nat Immunol **6:**981-988.

90. **Kim, J., J. S. Parker, K. E. Murray, and M. L. Nibert.** 2004. Nucleoside and RNA triphosphatase activities of orthoreovirus transcriptase cofactor mu2. J Biol Chem **279:**4394-4403.

91. **Kim, J. W., S. M. Lyi, C. R. Parrish, and J. S. Parker.** 2011. A proapoptotic peptide derived from reovirus outer capsid protein {micro}1 has membrane-destabilizing activity. J Virol **85:**1507-1516.

92. **Kirchner, E., K. M. Guglielmi, H. M. Strauss, T. S. Dermody, and T. Stehle.** 2008. Structure of reovirus sigma1 in complex with its receptor junctional adhesion molecule-A. PLoS Pathog **4:**e1000235.

93. **Kobayashi, T., A. A. Antar, K. W. Boehme, P. Danthi, E. A. Eby, K. M. Guglielmi, G. H. Holm, E. M. Johnson, M. S. Maginnis, S. Naik, W. B. Skelton, J. D. Wetzel, G. J. Wilson, J. D. Chappell, and T. S. Dermody.** 2007. A plasmid-based reverse genetics system for animal double-stranded RNA viruses. Cell Host Microbe **1:**147-157.

94. **Kobayashi, T., J. D. Chappell, P. Danthi, and T. S. Dermody.** 2006. Gene-specific inhibition of reovirus replication by RNA interference. J Virol **80:**9053-9063.

95. **Kobayashi, T., L. S. Ooms, J. D. Chappell, and T. S. Dermody.** 2009. Identification of functional domains in reovirus replication proteins muNS and mu2. J Virol **83:**2892-2906.

96. **Kobayashi, T., L. S. Ooms, M. Ikizler, J. D. Chappell, and T. S. Dermody.** 2010. An improved reverse genetics system for mammalian orthoreoviruses. Virology **398:**194-200.

97. **Kominsky, D. J., R. J. Bickel, and K. L. Tyler.** 2002. Reovirus-induced apoptosis requires both death receptor- and mitochondrial-mediated caspase-dependent pathways of cell death. Cell Death Differ **9:**926-933.

98. **Kominsky, D. J., R. J. Bickel, and K. L. Tyler.** 2002. Reovirus-induced apoptosis requires mitochondrial release of Smac/DIABLO and involves reduction of cellular inhibitor of apoptosis protein levels. J Virol **76:**11414-11424.

99. **Kühl, U., M. Pauschinger, M. Noutsias, B. Seeberg, T. Bock, D. Lassner, W. Poller, R. Kandolf, and H. P. Schultheiss.** 2005. High prevalence of viral genomes and multiple viral infections in the myocardium of adults with "idiopathic" left ventricular dysfunction. Circulation **111:**887-893.

100. **Kühl, U., M. Pauschinger, P. L. Schwimmbeck, B. Seeberg, C. Lober, M. Noutsias, W. Poller, and H. P. Schultheiss.** 2003. Interferon-beta treatment eliminates cardiotropic

viruses and improves left ventricular function in patients with myocardial persistence of viral genomes and left ventricular dysfunction. Circulation **107:**2793-2798.

101. **Kühl, U., M. Pauschinger, B. Seeberg, D. Lassner, M. Noutsias, W. Poller, and H. P. Schultheiss.** 2005. Viral persistence in the myocardium is associated with progressive cardiac dysfunction. Circulation **112:**1965-1970.

102. **Lagunoff, M., D. M. Lukac, and D. Ganem.** 2001. Immunoreceptor tyrosine-based activation motif-dependent signaling by Kaposi's sarcoma-associated herpesvirus K1 protein: effects on lytic viral replication. J Virol **75:**5891-5898.

103. **Lagunoff, M., R. Majeti, A. Weiss, and D. Ganem.** 1999. Deregulated signal transduction by the K1 gene product of Kaposi's sarcoma-associated herpesvirus. Proc Natl Acad Sci U S A **96:**5704-5709.

104. **Lai, M. H., and W. K. Joklik.** 1973. The induction of interferon by temperature-sensitive mutants of reovirus, UV-irradiated reovirus, and subviral reovirus particles. Virology **51:**191-204.

105. **Lee, B. S., S. H. Lee, P. Feng, H. Chang, N. H. Cho, and J. U. Jung.** 2005. Characterization of the Kaposi's sarcoma-associated herpesvirus K1 signalosome. J Virol **79:**12173-12184.

106. **Lee, H., J. Guo, M. Li, J. K. Choi, M. DeMaria, M. Rosenzweig, and J. U. Jung.** 1998. Identification of an immunoreceptor tyrosine-based activation motif of K1 transforming protein of Kaposi's sarcoma-associated herpesvirus. Mol Cell Biol **18:**5219-5228.

107. **Leonard, G. T., and G. C. Sen.** 1996. Effects of adenovirus E1A protein on interferon-signaling. Virology **224:**25-33.

108. **Li, F., X. Wang, J. M. Capasso, and A. M. Gerdes.** 1996. Rapid transition of cardiac myocytes from hyperplasia to hypertrophy during postnatal development. J Mol Cell Cardiol **28:**1737-1746.

109. **Li, L., and B. Sherry.** 2010. IFN-alpha expression and antiviral effects are subtype and cell type specific in the cardiac response to viral infection. Virology **396:**59-68.

110. **Loo, Y. M., J. Fornek, N. Crochet, G. Bajwa, O. Perwitasari, L. Martinez-Sobrido, S. Akira, M. A. Gill, A. García-Sastre, M. G. Katze, and M. Gale.** 2008. Distinct RIG-I and MDA5 signaling by RNA viruses in innate immunity. J Virol **82:**335-345.

111. **Loo, Y. M., and M. Gale.** 2011. Immune Signaling by RIG-I-like Receptors. Immunity **34:**680-692.

112. **Luo, W., and B. M. Peterlin.** 1997. Activation of the T-cell receptor signaling pathway by Nef from an aggressive strain of simian immunodeficiency virus. J Virol **71:**9531-9537.

113. **Maginnis, M. S., J. C. Forrest, S. A. Kopecky-Bromberg, S. K. Dickeson, S. A. Santoro, M. M. Zutter, G. R. Nemerow, J. M. Bergelson, and T. S. Dermody.** 2006. Beta1 integrin mediates internalization of mammalian reovirus. J Virol **80:**2760-2770.

114. **Maginnis, M. S., B. A. Mainou, A. Derdowski, E. M. Johnson, R. Zent, and T. S. Dermody.** 2008. NPXY motifs in the beta1 integrin cytoplasmic tail are required for functional reovirus entry. J Virol **82:**3181-3191.

115. **Mainou, B. A., and T. S. Dermody.** 2011. Src Kinase Mediates Productive Endocytic Sorting of Reovirus during Cell Entry. J Virol **85:**3203-3213.

116. **Martin, A. B., S. Webber, F. J. Fricker, R. Jaffe, G. Demmler, D. Kearney, Y. H. Zhang, J. Bodurtha, B. Gelb, and J. Ni.** 1994. Acute myocarditis. Rapid diagnosis by PCR in children. Circulation **90:**330-339.

117. **Mason, J. W., J. B. O'Connell, A. Herskowitz, N. R. Rose, B. M. McManus, M. E. Billingham, and T. E. Moon.** 1995. A clinical trial of immunosuppressive therapy for myocarditis. The Myocarditis Treatment Trial Investigators. N Engl J Med **333:**269-275.

118. **Matoba, Y., B. Sherry, B. N. Fields, and T. W. Smith.** 1991. Identification of the viral genes responsible for growth of strains of reovirus in cultured mouse heart cells. J Clin Invest **87:**1628-1633.

119. **Mbisa, J. L., M. M. Becker, S. Zou, T. S. Dermody, and E. G. Brown.** 2000. Reovirus mu2 protein determines strain-specific differences in the rate of viral inclusion formation in L929 cells. Virology **272:**16-26.

120. **Meylan, E., J. Curran, K. Hofmann, D. Moradpour, M. Binder, R. Bartenschlager, and J. Tschopp.** 2005. Cardif is an adaptor protein in the RIG-I antiviral pathway and is targeted by hepatitis C virus. Nature **437:**1167-1172.

121. **Miller, C. L., M. M. Arnold, T. J. Broering, C. E. Hastings, and M. L. Nibert.** 2010. Localization of mammalian orthoreovirus proteins to cytoplasmic factory-like structures via nonoverlapping regions of microNS. J Virol **84:**867-882.

122. **Miller, C. L., T. J. Broering, J. S. Parker, M. M. Arnold, and M. L. Nibert.** 2003. Reovirus sigma NS protein localizes to inclusions through an association requiring the mu NS amino terminus. J Virol **77:**4566-4576.

123. **Miller, C. L., J. S. Parker, J. B. Dinoso, C. D. Piggott, M. J. Perron, and M. L. Nibert.** 2004. Increased ubiquitination and other covariant phenotypes attributed to a strain- and temperature-dependent defect of reovirus core protein mu2. J Virol **78:**10291-10302.

124. **Mirić, M., J. Vasiljević, M. Bojić, Z. Popović, N. Keserović, and M. Pesić.** 1996. Long-term follow up of patients with dilated heart muscle disease treated with human leucocytic interferon alpha or thymic hormones initial results. Heart **75:**596-601.

125. **Miyamoto, S. D., R. D. Brown, B. A. Robinson, K. L. Tyler, C. S. Long, and R. L. Debiasi.** 2009. Cardiac cell-specific apoptotic and cytokine responses to reovirus infection: determinants of myocarditic phenotype. J Card Fail **15:**529-539.

126. **Monroe, J. G.** 2006. ITAM-mediated tonic signalling through pre-BCR and BCR complexes. Nat Rev Immunol **6:**283-294.

127. **Morrison, J. A., and N. Raab-Traub.** 2005. Roles of the ITAM and PY motifs of Epstein-Barr virus latent membrane protein 2A in the inhibition of epithelial cell differentiation and activation of {beta}-catenin signaling. J Virol **79:**2375-2382.

128. **Mócsai, A., C. L. Abram, Z. Jakus, Y. Hu, L. L. Lanier, and C. A. Lowell.** 2006. Integrin signaling in neutrophils and macrophages uses adaptors containing immunoreceptor tyrosine-based activation motifs. Nat Immunol **7:**1326-1333.

129. **Mócsai, A., J. Ruland, and V. L. Tybulewicz.** 2010. The SYK tyrosine kinase: a crucial player in diverse biological functions. Nat Rev Immunol **10:**387-402.

130. **Nibert, M. L., A. L. Odegard, M. A. Agosto, K. Chandran, and L. A. Schiff.** 2005. Putative autocleavage of reovirus mu1 protein in concert with outer-capsid disassembly and activation for membrane permeabilization. J Mol Biol **345:**461-474.

131. **Nichols, J. L., A. R. Bellamy, and W. K. Joklik.** 1972. Identification of the nucleotide sequences of the oligonucleotides present in reovirions. Virology **49:**562-572.

132. **Noah, D. L., M. A. Blum, and B. Sherry.** 1999. Interferon regulatory factor 3 is required for viral induction of beta interferon in primary cardiac myocyte cultures. J Virol **73:**10208-10213.

133. **Noble, S., and M. L. Nibert.** 1997. Characterization of an ATPase activity in reovirus cores and its genetic association with core-shell protein lambda1. J Virol **71:**2182-2191.

134. **Noble, S., and M. L. Nibert.** 1997. Core protein mu2 is a second determinant of nucleoside triphosphatase activities by reovirus cores. J Virol **71:**7728-7735.

135. **O'Donnell, S. M., M. W. Hansberger, J. L. Connolly, J. D. Chappell, M. J. Watson, J. M. Pierce, J. D. Wetzel, W. Han, E. S. Barton, J. C. Forrest, T. Valyi-Nagy, F. E. Yull, T. S. Blackwell, J. N. Rottman, B. Sherry, and T. S. Dermody.** 2005. Organ-specific roles for transcription factor NF-kappaB in reovirus-induced apoptosis and disease. J Clin Invest **115:**2341-2350.

136. **O'Donnell, S. M., G. H. Holm, J. M. Pierce, B. Tian, M. J. Watson, R. S. Chari, D. W. Ballard, A. R. Brasier, and T. S. Dermody.** 2006. Identification of an NF-kappaB-dependent gene network in cells infected by mammalian reovirus. J Virol **80:**1077-1086.

137. **Ooms, L. S., T. Kobayashi, T. S. Dermody, and J. D. Chappell.** 2010. A post-entry step in the mammalian orthoreovirus replication cycle is a determinant of cell tropism. J Biol Chem **285:**41604-41613.

138. **Oparil, S., S. P. Bishop, and F. J. Clubb.** 1984. Myocardial cell hypertrophy or hyperplasia. Hypertension **6:**III38-43.

139. **Parker, J. S., T. J. Broering, J. Kim, D. E. Higgins, and M. L. Nibert.** 2002. Reovirus core protein mu2 determines the filamentous morphology of viral inclusion bodies by interacting with and stabilizing microtubules. J Virol **76:**4483-4496.

140. **Parrillo, J. E., R. E. Cunnion, S. E. Epstein, M. M. Parker, A. F. Suffredini, M. Brenner, G. L. Schaer, S. T. Palmeri, R. O. Cannon, and D. Alling.** 1989. A prospective, randomized, controlled trial of prednisone for dilated cardiomyopathy. N Engl J Med **321:**1061-1068.

141. **Pauschinger, M., N. E. Bowles, F. J. Fuentes-Garcia, V. Pham, U. Kühl, P. L. Schwimmbeck, H. P. Schultheiss, and J. A. Towbin.** 1999. Detection of adenoviral genome in the myocardium of adult patients with idiopathic left ventricular dysfunction. Circulation **99:**1348-1354.

142. **Poggioli, G. J., C. Keefer, J. L. Connolly, T. S. Dermody, and K. L. Tyler.** 2000. Reovirus-induced G(2)/M cell cycle arrest requires sigma1s and occurs in the absence of apoptosis. J Virol **74:**9562-9570.

143. **Porrello, E. R., A. I. Mahmoud, E. Simpson, J. A. Hill, J. A. Richardson, E. N. Olson, and H. A. Sadek.** 2011. Transient regenerative potential of the neonatal mouse heart. Science **331:**1078-1080.

144. **Prota, A. E., J. A. Campbell, P. Schelling, J. C. Forrest, M. J. Watson, T. R. Peters, M. Aurrand-Lions, B. A. Imhof, T. S. Dermody, and T. Stehle.** 2003. Crystal structure of human junctional adhesion molecule 1: implications for reovirus binding. Proc Natl Acad Sci U S A **100:**5366-5371.

145. **Rahman, M. M., and G. McFadden.** 2011. Modulation of NF-κB signalling by microbial pathogens. Nat Rev Microbiol **9:**291-306.

146. **Ramos-Alvarez, M., and A. B. Sabin.** 1958. Enteropathogenic viruses and bacteria; role in summer diarrheal diseases of infancy and early childhood. J Am Med Assoc **167:**147-156.

147. **Ravetch, J. V., and L. L. Lanier.** 2000. Immune inhibitory receptors. Science **290:**84-89.

148. **Reinisch, K. M., M. L. Nibert, and S. C. Harrison.** 2000. Structure of the reovirus core at 3.6 A resolution. Nature **404:**960-967.

149. **Rodgers, S. E., E. S. Barton, S. M. Oberhaus, B. Pike, C. A. Gibson, K. L. Tyler, and T. S. Dermody.** 1997. Reovirus-induced apoptosis of MDCK cells is not linked to viral yield and is blocked by Bcl-2. J Virol **71:**2540-2546.

150. **Rosen, L., J. F. Hovis, F. M. Mastrota, J. A. Bell, and R. J. Huebner.** 1960. Observations on a newly recognized virus (Abney) of the reovirus family. Am J Hyg **71:**258-265.

151. **Ross, S. R., J. W. Schmidt, E. Katz, L. Cappelli, S. Hultine, P. Gimotty, and J. G. Monroe.** 2006. An immunoreceptor tyrosine activation motif in the mouse mammary tumor virus envelope protein plays a role in virus-induced mammary tumors. J Virol **80:**9000-9008.

152. **Rubin, D. H., D. B. Weiner, C. Dworkin, M. I. Greene, G. G. Maul, and W. V. Williams.** 1992. Receptor utilization by reovirus type 3: distinct binding sites on thymoma and fibroblast cell lines result in differential compartmentalization of virions. Microb Pathog **12:**351-365.

153. **Sabin, A. B.** 1959. Reoviruses. A new group of respiratory and enteric viruses formerly classified as ECHO type 10 is described. Science **130:**1387-1389.

154. **Schiff, L. A., M. L. Nibert, and K. L. Tyler.** 2007. Orthoreoviruses and Their Replication, p. 1854-1915. *In* D. M. Knipe and P. M. Howley (ed.), Fields' virology, 5th ed, vol. 2. Wolters Kluwer Health/Lippincott Williams & Wilkins, Philadelphia.

155. **Scholle, F., K. M. Bendt, and N. Raab-Traub.** 2000. Epstein-Barr virus LMP2A transforms epithelial cells, inhibits cell differentiation, and activates Akt. J Virol **74:**10681-10689.

156. **Scholle, F., R. Longnecker, and N. Raab-Traub.** 1999. Epithelial cell adhesion to extracellular matrix proteins induces tyrosine phosphorylation of the Epstein-Barr virus latent membrane protein 2: a role for C-terminal Src kinase. J Virol **73:**4767-4775.

157. **Seth, R. B., L. Sun, C. K. Ea, and Z. J. Chen.** 2005. Identification and characterization of MAVS, a mitochondrial antiviral signaling protein that activates NF-kappaB and IRF 3. Cell **122:**669-682.

158. **Sharma, S., B. R. tenOever, N. Grandvaux, G. P. Zhou, R. Lin, and J. Hiscott.** 2003. Triggering the interferon antiviral response through an IKK-related pathway. Science **300:**1148-1151.

159. **Sharpe, A. H., L. B. Chen, and B. N. Fields.** 1982. The interaction of mammalian reoviruses with the cytoskeleton of monkey kidney CV-1 cells. Virology **120:**399-411.

160. **Sharpe, A. H., and B. N. Fields.** 1982. Reovirus inhibition of cellular RNA and protein synthesis: role of the S4 gene. Virology **122:**381-391.

161. **Shatkin, A. J., and J. D. Sipe.** 1968. Single-stranded, adenine-rich RNA from purified reoviruses. Proc Natl Acad Sci U S A **59:**246-253.

162. **Shatkin, A. J., J. D. Sipe, and P. Loh.** 1968. Separation of ten reovirus genome segments by polyacrylamide gel electrophoresis. J Virol **2:**986-991.

163. **Sherry, B., C. J. Baty, and M. A. Blum.** 1996. Reovirus-induced acute myocarditis in mice correlates with viral RNA synthesis rather than generation of infectious virus in cardiac myocytes. J Virol **70:**6709-6715.

164. **Sherry, B., and M. A. Blum.** 1994. Multiple viral core proteins are determinants of reovirus-induced acute myocarditis. J Virol **68:**8461-8465.

165. **Sherry, B., and B. N. Fields.** 1989. The reovirus M1 gene, encoding a viral core protein, is associated with the myocarditic phenotype of a reovirus variant. J Virol **63:**4850-4856.

166. **Sherry, B., X. Y. Li, K. L. Tyler, J. M. Cullen, and H. W. Virgin.** 1993. Lymphocytes protect against and are not required for reovirus-induced myocarditis. J Virol **67:**6119-6124.

167. **Sherry, B., F. J. Schoen, E. Wenske, and B. N. Fields.** 1989. Derivation and characterization of an efficiently myocarditic reovirus variant. J Virol **63:**4840-4849.

168. **Sherry, B., J. Torres, and M. A. Blum.** 1998. Reovirus induction of and sensitivity to beta interferon in cardiac myocyte cultures correlate with induction of myocarditis and are determined by viral core proteins. J Virol **72:**1314-1323.

169. **Smith, J. A., S. C. Schmechel, B. R. Williams, R. H. Silverman, and L. A. Schiff.** 2005. Involvement of the interferon-regulated antiviral proteins PKR and RNase L in reovirus-induced shutoff of cellular translation. J Virol **79:**2240-2250.

170. **Starnes, M. C., and W. K. Joklik.** 1993. Reovirus protein lambda 3 is a poly(C)-dependent poly(G) polymerase. Virology **193:**356-366.

171. **Stewart, M. J., K. Smoak, M. A. Blum, and B. Sherry.** 2005. Basal and reovirus-induced beta interferon (IFN-beta) and IFN-beta-stimulated gene expression are cell type specific in the cardiac protective response. J Virol **79:**2979-2987.

172. **Sturzenbecker, L. J., M. Nibert, D. Furlong, and B. N. Fields.** 1987. Intracellular digestion of reovirus particles requires a low pH and is an essential step in the viral infectious cycle. J Virol **61:**2351-2361.

173. **Swart, R., I. K. Ruf, J. Sample, and R. Longnecker.** 2000. Latent membrane protein 2A-mediated effects on the phosphatidylinositol 3-Kinase/Akt pathway. J Virol **74:**10838-10845.

174. **Tassiulas, I., X. Hu, H. Ho, Y. Kashyap, P. Paik, Y. Hu, C. A. Lowell, and L. B. Ivashkiv.** 2004. Amplification of IFN-alpha-induced STAT1 activation and inflammatory function by Syk and ITAM-containing adaptors. Nat Immunol **5:**1181-1189.

175. **Tyler, K. L., M. K. Squier, S. E. Rodgers, B. E. Schneider, S. M. Oberhaus, T. A. Grdina, J. J. Cohen, and T. S. Dermody.** 1995. Differences in the capacity of reovirus strains to induce apoptosis are determined by the viral attachment protein sigma 1. J Virol **69:**6972-6979.

176. **Underhill, D. M., and H. S. Goodridge.** 2007. The many faces of ITAMs. Trends Immunol **28:**66-73.

177. **Urzainqui, A., J. M. Serrador, F. Viedma, M. Yáñez-Mó, A. Rodríguez, A. L. Corbí, J. L. Alonso-Lebrero, A. Luque, M. Deckert, J. Vázquez, and F. Sánchez-Madrid.** 2002. ITAM-based interaction of ERM proteins with Syk mediates signaling by the leukocyte adhesion receptor PSGL-1. Immunity **17:**401-412.

178. **Weiner, H. L., R. F. Ramig, T. A. Mustoe, and B. N. Fields.** 1978. Identification of the gene coding for the hemagglutinin of reovirus. Virology **86:**581-584.

179. **Wiener, J. R., J. A. Bartlett, and W. K. Joklik.** 1989. The sequences of reovirus serotype 3 genome segments M1 and M3 encoding the minor protein mu 2 and the major nonstructural protein mu NS, respectively. Virology **169:**293-304.

180. **Willems, L., J. S. Gatot, M. Mammerickx, D. Portetelle, A. Burny, P. Kerkhofs, and R. Kettmann.** 1995. The YXXL signalling motifs of the bovine leukemia virus transmembrane protein are required for in vivo infection and maintenance of high viral loads. J Virol **69:**4137-4141.

181. **Wisniewski, M. L., B. G. Werner, L. G. Hom, L. J. Anguish, C. M. Coffey, and J. S. Parker.** 2011. Reovirus infection or ectopic expression of outer capsid protein micro1 induces apoptosis independently of the cellular proapoptotic proteins Bax and Bak. J Virol **85:**296-304.

182. **Xu, L. G., Y. Y. Wang, K. J. Han, L. Y. Li, Z. Zhai, and H. B. Shu.** 2005. VISA is an adapter protein required for virus-triggered IFN-beta signaling. Mol Cell **19:**727-740.

183. **Yin, P., N. D. Keirstead, T. J. Broering, M. M. Arnold, J. S. Parker, M. L. Nibert, and K. M. Coombs.** 2004. Comparisons of the M1 genome segments and encoded mu2 proteins of different reovirus isolates. Virol J **1:**6.

184. **Zandi, E., D. M. Rothwarf, M. Delhase, M. Hayakawa, and M. Karin.** 1997. The IkappaB kinase complex (IKK) contains two kinase subunits, IKKalpha and IKKbeta, necessary for IkappaB phosphorylation and NF-kappaB activation. Cell **91:**243-252.

185. **Zhang, X., S. B. Walker, P. R. Chipman, M. L. Nibert, and T. S. Baker.** 2003. Reovirus polymerase lambda 3 localized by cryo-electron microscopy of virions at a resolution of 7.6 A. Nat Struct Biol **10:**1011-1018.

186. **Zou, S., and E. G. Brown.** 1992. Nucleotide sequence comparison of the M1 genome segment of reovirus type 1 Lang and type 3 Dearing. Virus Res **22:**159-164.

187. **Zurney, J., K. E. Howard, and B. Sherry.** 2007. Basal expression levels of IFNAR and Jak-STAT components are determinants of cell-type-specific differences in cardiac antiviral responses. J Virol **81:**13668-13680.

188. **Zurney, J., T. Kobayashi, G. H. Holm, T. S. Dermody, and B. Sherry.** 2009. Reovirus mu2 protein inhibits interferon signaling through a novel mechanism involving nuclear accumulation of interferon regulatory factor 9. J Virol **83:**2178-2187.

CHAPTER 2

A Single Amino Acid Polymorphism in Reovirus Protein μ2 Determines Repression of Interferon Signaling and Modulates Myocarditis

Susan C. Irvin[1], Jennifer Zurney[1†], Laura S. Ooms[2,4], James D. Chappell[2,3,4], Terence S. Dermody[2,3,4], and Barbara Sherry[1]

[1] Department of Molecular Biomedical Sciences, North Carolina State University, Raleigh NC 27607 and Departments of [2]Pathology, Microbiology, and Immunology and [3]Pediatrics and [4]Elizabeth B. Lamb Center for Pediatric Research, Vanderbilt University School of Medicine, Nashville, TN 37232, USA

† Present address: Burleson Research Technologies, Morrisville, NC 27560

Manuscript submitted

ABSTRACT

Myocarditis is indicated as the second leading cause of sudden death in young adults. Reovirus induces myocarditis in neonatal mice, providing an outstanding model system for investigation of this important human disease. Interferon-α/β (IFN-α/β) treatment improves cardiac function and inhibits viral replication in patients with chronic myocarditis, and the host IFN-α/β response is a determinant of reovirus strain-specific differences in induction of myocarditis. Virus-induced IFN-β stimulates a signaling cascade that establishes an antiviral state and further induces IFN-α/β through an amplification loop. Reovirus strain-specific differences in induction of and sensitivity to IFN-α/β are associated with the viral M1, L2, and S2 genes. The reovirus M1 gene-encoded μ2 protein is a strain-specific repressor of IFN-β signaling, providing one possible mechanism for the variation in resistance to IFN and induction of myocarditis between different reovirus strains. Here, we report that μ2 amino acid 208 determines repression of IFN-β signaling and modulates reovirus induction of IFN-β in cardiac myocytes. Moreover, μ2 amino acid 208 determines reovirus replication, both in initially infected cardiac myocytes and after spread, by regulating the IFN-β response. Amino acid 208 of μ2 also influences cytopathic effect in cardiac myocytes after spread. Finally, μ2 amino acid 208 modulates myocarditis in neonatal mice. Thus, repression of IFN-β signaling mediated by reovirus μ2 amino acid 208 is a determinant of the IFN-β response, viral replication and damage in cardiac myocytes, and myocarditis. Results here demonstrate that a single amino acid

difference between viruses can dictate virus strain-specific differences in suppression of the host IFN-β response and, consequently, damage to the heart.

INTRODUCTION

Viral infection is the leading cause of myocarditis in North America and Europe (12). This disease can be fatal in infants and, although usually resolved in adults, can lead to dilated cardiomyopathy and cardiac failure. Importantly, myocarditis is indicated as the second leading cause of sudden death in young adults (10). Most virus families are implicated in myocarditis in humans (12), with enteroviruses, such as coxsackievirus B (8, 12), adenoviruses (8, 12), and more recently parvovirus B19 (8, 21, 23) as the most frequently identified. While enterovirus-induced myocarditis in mice is predominantly immune-mediated, cardiac damage is also due to direct viral cytopathic effects (CPE). Indeed, immunosuppressive therapy is only minimally beneficial in affected humans (29, 38). Furthermore, adenovirus-positive cardiac sections from patients with myocarditis often lack inflammatory cell infiltrates (28). Therefore, the importance of immune-mediated damage in myocarditis is unclear. Reovirus induction of cardiac lesions in newborn mice reflects direct viral CPE in cardiac myocytes (2, 45) and is virus strain-specific (44). Thus, reovirus infection in mice provides a tractable experimental system to study the direct effects of viral infection on the heart.

The interferon (IFN) response is critical for protection of cardiac cells against reovirus infection in vitro. Accordingly, non-myocarditic reoviruses induce myocarditis in mice depleted of IFN-α/β (46) or lacking a transcription factor critical for induction of IFN (14). Reoviruses that are either strong inducers of IFN or are most sensitive to IFN-mediated antiviral effects, such as strain type 3 Dearing (T3D), do not induce myocarditis (46). Conversely, reoviruses that are weak inducers of IFN or are highly resistant to its effects, such as strain type 1 Lang (T1L), induce myocarditis (46). Given that cardiac myocytes are essentially non-replenishable (4) and thus vulnerable to systemic viral infections, the IFN response provides a critical first-line of protection for these cells. Indeed, cardiac myocytes are pre-armed with higher basal expression of IFN-β than neighboring cardiac fibroblasts (52). Moreover, IFN-α (9, 31) and IFN-β (22) treatment has improved cardiac function and inhibited viral replication in patients with chronic myocarditis.

Viral nucleic acids can be recognized by pattern-recognition receptors (PRRs), including RIG-I-like receptors (RLRs), to stimulate intracellular signaling cascades that result in the induction and secretion of IFN-α/β (50). Through autocrine and paracrine signaling, IFN-α/β induces expression of IFN-stimulated genes (ISGs) including those with antiviral activity (35) and the transcription factor, IRF7, which further amplifies IFN expression (16, 40). Viruses have evolved mechanisms to inhibit the induction of IFN, IFN signaling, and ISG protein function (5, 13, 49). Reovirus subverts IFN signaling by a novel mechanism associated with nuclear accumulation of IRF9 (53). Reovirus strain-specific differences in this subversion are determined by the M1 gene-encoded protein μ2 (53). While strain-specific differences in reovirus repression of IFN signaling correlate with induction of myocarditis (53), the role of this repression in disease is not known.

The M1 gene is the primary determinant of reovirus strain-specific differences in murine myocarditis (43, 44). Reovirus strain-specific differences in induction of and sensitivity to IFN are also determined by the M1 gene in concert with the L2 and S2 genes (46). In this study, we investigated μ2 determinants of IFN induction, repression of IFN signaling, viral replication and cytopathic effects in cardiac myocytes, and reovirus-induced myocarditis in mice. We found that μ2 amino acid 208 is a determinant of IFN responses, viral spread, and damage in cardiac cells and that this amino acid modulates myocarditis.

MATERIALS and METHODS

Cells and mice. Mouse L929 cells were maintained in minimal essential medium (MEM) (SAFC Biosciences) supplemented to contain 5% fetal calf serum (FCS) (Atlanta Biologicals) and 2 mM L-glutamine (Mediatech, Inc). L929 cells were plated at 5 x 10^5 cells per well in 24-well clusters and allowed to adhere 2 hours prior to infection.

Timed-pregnant Cr:NIH(S) mice from the National Cancer Institute were maintained as a colony in a facility that is accredited by the Association for Assessment and Accreditation of Laboratory Animal Care. All animal procedures were approved by the North Carolina State University institutional animal care and use committee.

Primary cardiac myocyte and fibroblast cultures were generated from 1-day-old neonatal or term fetal Cr:NIH(S) mice resulting from timed pregnancies. Neonatal or term fetal mice were euthanized and the apical two-thirds of hearts were excised and trypsinized (2).

Cardiac myocytes were separated from cardiac fibroblasts by differential adherence to culture wells and resuspended in Dulbecco's modified Eagle's medium (DMEM) (Gibco) supplemented to contain 7% FCS (Atlanta Biologicals) and 10 µg per ml of gentamicin (Sigma-Aldrich Corp.). Myocyte culture medium also contained 0.06% thymidine (Sigma-Aldrich, Corp.). Myocyte cultures contain ≤ 5% fibroblasts, and fibroblast cultures contain < 1% myocytes (52). Myocyte cultures were plated at 1.5 x 10^5 cells per well in 96-well clusters or at 5 x 10^5 cells per well in 48-well clusters. Fibroblast cultures were plated at one half those densities in 96-well or 48-well clusters, were confluent by the day of infection, and were assumed to double from the initial plating density. Cells were incubated for 2 days prior to infection. Myocyte and fibroblast cultures were not passaged before use.

Two day-old mice from timed litters were injected in the left hindlimb with 20 µl of gel saline (44) containing 10^6 PFU of various virus strains or gel saline as mock-infection. At 7 days post-injection, mice were euthanized and hearts were removed, fixed in 10% buffered formalin, and sectioned for hematoxylin and eosin staining. Sections were photographed with a Nikon AZ100 zoom microscope at 75x magnification. A minimum of 8 hearts (minimum 15 sections per heart) were scored as blinded cardiac sections for each virus. Mice were considered "positive" if more than a single lesion was detected in the ≥ 15 sections examined. Lesions in adjacent sections were not scored as independent lesions.

Viruses. All viruses were generated from plasmids by reverse genetics as described (19, 36). The recombinant viruses were plaque purified, amplified using L929 cells, purified using CsCl gradients (47), and stored as diluted aliquots at -80°C.

Virus replication. Primary cardiac myocyte and cardiac fibroblast cultures were plated in 96-well clusters. Cells were infected at a multiplicity of infection (MOI) of 3 PFU per cell for single-cycle assays and 0.1 PFU per cell for multi-cycle assays. After 1 h incubation at 37°C, additional supplemented medium was added to each well. For some experiments, this overlay also contained 640 neutralizing units per ml (final concentration) of anti-IFN-β antibody (Cat. # 32400-1, PBL, Inc., Piscataway, NJ) and, at two days post-infection, these cells were again treated with anti-IFN-β antibody (320 neutralizing units per ml). Cells were incubated for various times before freezing at -80°C. Plates of cells were frozen and thawed twice more, and cells were lysed in 0.5% Nonidet P-40. For plaque assays, serial dilutions of the lysates were used to infect monolayers of L929 cells, which were subsequently overlaid with agar and stained with neutral red as described (42). In each experiment, duplicate or triplicate wells of cardiac cells were each assessed for viral replication by duplicate plaque assay wells. Averages and standard deviations of results from duplicate or triplicate wells of cardiac cells were determined.

Cytopathic effect. Primary cardiac myocyte and cardiac fibroblast cultures were plated in 96-well clusters. Cells were infected at an MOI of 10 PFU per cell (single-cycle assays) or 0.1 PFU per cell (multi-cycle assays) in 5 replicate wells. After 1 h incubation at 37°C, additional supplemented medium was added to each well. At 2 days (single-cycle assays) or 5 days (multi-cycle assays) post-infection, an MTT assay was performed to quantify cell viability (46). An automated microplate reader (TECAN Sunrise Microplate Reader) was used to determine the optical density (OD) at 570 nm and 650 nm. The absorbance was determined by subtracting OD at 650 nm from OD at 570 nm, and replicate wells were averaged and standard error of the mean (SEM) determined.

Quantitative (real-time) reverse transcription-PCR (qRT-PCR). Duplicate wells were plated in 24-well (L929 cells) or 48-well (primary cardiac cell cultures) clusters. Cells were infected at an MOI of 25 PFU per cell (L929 cells) or 10 PFU per cell (primary cardiac cell cultures). After 1 h incubation at 37°C, additional supplemented medium was added to each well. L929 cells were incubated for 20 h, treated with 100 or 1,000 U/ml of IFN-β (Cat. # 12400-1; PBL, Inc.), and incubated for an additional 5 h. Primary cardiac myocyte and cardiac fibroblast cultures were incubated for 8 and 12 h post-infection. All cells were lysed with an RNeasy kit (Qiagen, Inc.), and total RNA was harvested and treated with RNase-free DNase I (Qiagen, Inc.). From each harvested well, one-third of the total RNA was used to generate cDNA by reverse transcription in a 100 µl reaction containing 5 µM oligo(dT) (Invitrogen Corp.), 1X Taq buffer (Promega Corp.), 7.5 mM $MgCl_2$ (Promega Corp.), 1 mM dithiothreitol (Promega Corp.), 1 mM each deoxynucleoside triphosphate (Roche), 0.67 U/µl RNasin (Promega Corp.), and 0.20 U/µl AMV reverse transcriptase (Promega Corp.). Five percent of the reverse transcription product was amplified on an iCycler iQ fluorescence thermocycler (Bio-Rad Laboratories) in 96-well plates. Each duplicate 25 µl reactions contained 1X Quantitech SYBR Green master mix (Qiagen, Inc.), 10 mM fluorescein, and 0.3 µM of each forward and reverse primer. Primer sequences were as previously published (48). Relative abundance of IRF7, IFN-β, and GAPDH mRNA was determined by comparison to a standard curve generated from serial dilutions of a DNA standard; IRF7 and IFN-β expression and IRF7 fold repression were normalized to GAPDH expression.

Statistical analysis. A Student's two-sample *t* test (pooled variance; Systat 9.0) or a Chi-square test was applied. Results were considered significant if the *P* value was < 0.05.

RESULTS

Amino acid (aa) 208 in reovirus protein μ2 determines reovirus repression of IFN signaling. The M1 gene product, μ2, of reovirus strain T1L but not that of strain T3D represses IFN signaling in L929 cells (53). To identify the μ2 amino acids responsible for repression of IFN signaling, viruses containing mutations in the M1 gene or viruses containing T1L-T3D chimeric M1 genes (Fig. 1A) were tested for the capacity to repress IFN signaling in L929 cells (Fig. 1B). A recombinant virus containing 9 genes from T3D and a chimeric M1 gene expressing the N-terminal 126 μ2 amino acids from T3D and remaining amino acids from T1L (Ch1) was as effective as T1L at repressing IFN induction of IRF7. In contrast, viruses containing a chimeric M1 gene expressing the N-terminal 208 μ2 amino acids (Ch2) or more (Ch3 and Ch4) from T3D failed to repress IFN signaling. Strains T1L and T3D differ at only aa 208 in the μ2 region spanning aa 127 through aa 208. Remarkably, a T3D virus mutated at only μ2 residue 208 (T3D-S208P), changing it from the T3D serine (S) to a T1L proline (P), repressed IFN signaling as effectively as T1L. Conversely, a virus containing 9 T3D genes and the T1L M1 gene mutated to T3D serine at μ2 residue 208 (T3D-T1LM1-P208S) failed to repress IFN signaling. Together, the data demonstrate that T1L μ2 aa 208 is both required and sufficient for reovirus repression of IFN signaling.

μ2 aa 208 modulates reovirus induction of IFN-β in cardiac cells. As anticipated from previous reports (46, 52), in cardiac myocytes, T3D induced IFN-β well and T1L induced IFN-β poorly (Fig. 2A). Differences in T3D and T1L induction of IFN in cardiac myocytes segregate with the M1, L2, and S2 genes (46). Reovirus infection stimulates PRRs to induce IFN-β (15, 17, 25). While strain-specific differences in induction of IFN could reflect differences in this stimulation, they also could reflect differences in repression of IFN signaling since reovirus-mediated induction of IFN involves the positive feedback loop in cardiac myocytes (48, 53). T3D-T1LM1 induced markedly less IFN-β than T3D (Fig. 2A), consistent with the association of the T1L M1 gene with poor induction of IFN (46). T1L-T3DM1 also induced minimal IFN-β, consistent with the association of the T1L L2 and S2 genes with poor IFN induction (46).

To determine directly the effect of μ2 aa 208 on reovirus induction of IFN, viruses with single aa substitutions at that site were tested. At 8 h post-infection in cardiac myocytes (Fig. 2A), viral induction of IFN-β was decreased almost 3-fold by changing T3D μ2 aa 208 to that of T1L (T3D-S208P), indicating that μ2 aa 208 modulates reovirus induction of IFN-β at this early time. However, by 24 h post-infection, T3D and T3D-S208P induction of IFN-β (Fig. 2A) and IRF7 (Fig. 2B) were similar, indicating that repression of IFN signaling is not the primary determinant of strain-specific differences in reovirus induction of IFN-β. The similar induction of IRF7 by T3D and T3D-S208P (Fig. 2B) contrasts with T3D-S208P repression of exogenous IFN induction of IRF7 (Fig. 1B), likely reflecting the difference between induction of IRF7 concomitant with (Fig.

2B) or after (Fig. 1B) the majority of μ2 expression. Interestingly, other sequences in the T1L M1 gene also affected induction of IFN-β.Specifically, in contrast to the minimal effect of changing T3D μ2 aa 208 to that of T1L (T3D-S208P), induction of IFN-β and IRF7 was significantly increased by changing T1L μ2 aa 208 of T3D-T1LM1 to that of T3D (T3D-T1LM1-P208S, Figs. 2A and 2B).Additionally, the substantial increase in the induction of IFN-β at 24 h by T3D-T1LM1-P208S relative to T3D (Fig. 2A) suggests effects of T1L M1 sequences other than aa 208. Results for cardiac fibroblasts (Figs. 2B and 2C) were similar to those for cardiac myocytes, with the notable and expected difference (52) that reovirus induction of IFN-β is much higher in cardiac myocytes than in cardiac fibroblasts (compare scales between Figs. 2A and 2C), but the opposite is true for reovirus induction of ISGs (Fig. 2B). Thus, reovirus T1L μ2 aa 208 modulates induction of IFN-β in both cardiac myocytes and cardiac fibroblasts, but predominantly when expressed in the context of the entire T1L M1 gene.

μ2 aa 208 determines reovirus single-cycle and multi-cycle replication in cardiac myocytes. As expected (46, 48), T1L achieved higher titers in cardiac myocytes than did T3D after single or multiple cycles of replication (Figs. 3A and 3B; $P < 0.005$ for both cases). Differences between T1L and T3D could reflect IFN-dependent, IFN-independent, or both mechanisms. After single or multiple cycles of replication, T1L-T3DM1 titers were as low as those for T3D, while T3D-T1LM1 titers were as high as those for T1L, demonstrating that the T1L M1 gene is both required and sufficient for reovirus to replicate maximally in cardiac myocytes. After single (Fig. 3A) or multiple (Fig. 3B) cycles of replication, titers for T3D-T1LM1-P208S decreased to those of T3D, demonstrating that T1L μ2 aa 208 is required for production of high titers in cardiac myocytes. Conversely, after single or multiple rounds of replication, titers for T3D-S208P were as high as those for T1L, demonstrating that T1L μ2 aa 208 is sufficient for high titers in cardiac myocytes.

To determine whether T1L μ2 aa 208 regulates replication in cardiac myocytes solely by regulating the IFN response, titers were compared after multiple cycles of replication in the absence or presence of anti-IFN-β antibody (Fig. 3C). As anticipated (46), elimination of the IFN response in cardiac myocytes increased T3D replication 11.5-fold, consistent with evidence that the IFN response dictates the replication efficiency of this strain in these cells. Furthermore, elimination of the IFN response increased replication of all viruses tested to the level of T1L, demonstrating that μ2 aa 208 regulates reovirus multi-cycle replication in cardiac myocytes by regulating the IFN response.

μ2 aa 208 influences reovirus single-cycle and multi-cycle replication in cardiac fibroblasts. In contrast to results obtained in experiments using cardiac myocytes, differences in yields of T1L and T3D were apparent in cardiac fibroblasts only after multiple cycles of replication, suggesting that the IFN response has little effect on initial infection in cardiac fibroblasts (Figs. 4A and 4B). This finding is consistent with the dramatically lower induction of IFN by reovirus in cardiac fibroblasts (Fig. 2C) than in cardiac myocytes (Fig. 2A). Indeed, in contrast to cardiac myocytes, the T1L M1 gene did not contribute to a higher yield of T3D (T3D-T1LM1) after a single cycle of replication in cardiac fibroblasts (Fig. 4A). Replication of T3D-T1LM1-P208S was markedly reduced relative to the parent T3D-T1LM1 virus, most likely reflecting the effect of the single aa 208 substitution on induction of IFN (Fig. 2C) and suggesting that the IFN response can modulate reovirus replication in cardiac fibroblasts if the IFN response is sufficiently strong. After multiple cycles of replication in cardiac fibroblasts, T3D replicated less well than T1L, a property determined by the M1 gene (Fig. 4B). T3D-T1LM1-P208S produced the lowest titers of the viruses tested, consistent with its dramatically higher induction of IFN (Fig. 2C).

To directly test the role of IFN in μ2 aa 208 effects on reovirus replication in cardiac fibroblasts, virus titers in the presence and absence of anti-IFN-β antibody were compared (Fig. 4C). In comparison to results using cardiac myocytes, all viruses achieved only slightly higher titers when IFN was eliminated, consistent with the low level of IFN induced in cardiac fibroblasts relative to cardiac myocytes (Fig. 2).

μ2 aa 208 determines reovirus CPE in cardiac myocytes only after spread. Results thus far suggested that T1L μ2 aa 208 influences the IFN response to reovirus in both cardiac myocytes and cardiac fibroblasts, but that the effect on viral replication is greater in cardiac myocytes than in cardiac fibroblasts. To determine the contribution of μ2 aa 208 to viral CPE, cardiac cells were infected at a high MOI (10 PFU per cell) and cell viability was quantified after a single cycle of replication (2 days) or were infected at a low MOI (0.1 PFU per cell) and cell viability was quantified after multiple cycles of replication (5 days). PFU are quantified using L929 cells and virus is less infectious in cardiac cells than in L929 cells (data not shown); therefore, even at an MOI of 10 PFU per cell, not all cardiac cells are infected (42). In cardiac fibroblasts, none of the viruses were cytopathic after a single cycle of replication, and CPE increased only minimally after multiple cycles (data not shown). As expected (46), T1L and T3D were similarly cytopathic in cardiac myocytes after a single cycle of replication (Fig. 5). However, after multiple cycles of replication, the panel of viruses clearly differed in induction of CPE (Fig. 5). The overall trend was equivalent to the trend for viral replication in cardiac myocytes (Figs. 3A and 3B), demonstrating that T1L μ2 aa 208 determines CPE after viral spread, likely through repression of IFN signaling that is required for the positive feedback loop of induction of IFN-β.

μ2 aa 208 modulates myocarditis. To determine the effect of μ2 aa 208 on viral myocarditis, mice were inoculated with the panel of recombinant viruses, and cardiac lesions were quantified. As expected when injecting a high dose of reovirus (43), T1L induced cardiac lesions in all mice, while T3D induced few lesions (Fig. 6). Reovirus strain-specific differences in the capacity to induce myocarditis segregate with the M1, L1, and L2 genes (43, 44), but the role of the M1 gene alone has not been previously determined. A virus containing the T1L M1 gene in the T3D genetic background (T3D-T1LM1) induced a higher frequency of myocarditis than did T3D ($P < 0.05$), demonstrating that the T1L M1 gene when introduced into the genetic background of T3D is sufficient to cause myocarditis. The T3D M1 gene in the T1L genetic background (T1L-T3DM1) induced a lower frequency of myocarditis than did T1L ($P < 0.05$), confirming the importance of the T1L M1 gene in this phenotype. Furthermore, although not statistically significant, T1L-T3DM1 appeared to induce myocarditis more efficiently than did T3D, providing evidence to support previous conclusions that genes in T1L in addition to M1 contribute to myocarditis (43, 44). Finally, changing T3D μ2 aa 208 to that of T1L (T3D-S208P) dramatically increased the frequency of myocarditis ($P < 0.05$) compared to that caused by T3D

($P < 0.05$), suggesting that repression of IFN signaling alone can modulate this disease. T3D-T1LM1-P208S appeared to be less myocarditic than the parental T3D-T1LM1 virus but more myocarditic than T3D (not statistically significant), supporting the importance of repression of IFN signaling but indicating that other T1L M1 functions are also determinants of myocarditis. Collectively, these results demonstrate that μ2 aa 208 modulates myocarditis, suggesting that repression of IFN signaling is a determinant of reovirus-induced cardiac disease.

DISCUSSION

The IFN-α/β response is essential for protection against reovirus infection of cardiac cells in vitro and reovirus-induced myocarditis in mice (46). Virus-strain specific differences in the IFN-α/β response segregate with the reovirus M1, L2, and S2 genes (46), and the M1 gene-encoded μ2 protein represses IFN-β signaling (53). Here, we demonstrate that sequence polymorphisms at μ2 aa 208 are both required and sufficient for strain-specific differences in reovirus repression of IFN-β signaling. Furthermore, μ2 aa 208 modulation of IFN expression and signaling determines viral replication and spread in cardiac myocytes and modulates myocarditis in mice.

Viruses are recognized by PRRs that in turn trigger activation of transcription factors NF-κB and IRF3 for induction of IFN-β gene expression (13). Secreted IFN-β binds to the common IFN-α/β-receptor, stimulating JAKs to phosphorylate and activate STAT1 and STAT2, which then associate with IRF9 to form the heterotrimeric transcription factor complex, ISGF3. ISGF3 translocates to the nucleus and induces expression of hundreds of ISGs, which include those that mediate antiviral activity as well as the transcription factor IRF7. Activation of IRF7 results in further induction of IFN-β expression in a positive amplification loop. Viral repression of IFN signaling could therefore have two major effects on the protective IFN response of the host: it could 1) limit IFN expression to those that are initiated by PRRs and 2) suppress IFN-induced expression of antiviral genes.

Viruses have evolved many mechanisms to antagonize IFN signaling, including inactivation of JAKs, degradation or sequestration of STATs, and inhibition of karyopherins required for ISGF3 nuclear translocation (39). Only two viruses are known to repress IFN signaling through IRF9: human papillomavirus type 16 sequesters IRF9 to inhibit its nuclear translocation (1) and adenovirus infection leads to a decrease in IRF9 levels (24). The μ2 protein from reovirus strain T1L but not strain T3D represses IFN-β signaling and this repression is associated with nuclear accumulation of IRF9 (53). However, it is not known whether alterations in IRF9 mediate repression or are merely a consequence of that event. In the present study, we found that sequence polymorphisms in μ2 aa 208 determines these reovirus strain-specific differences in repression of IFN-β signaling (Fig. 1).

Strain-specific differences in reovirus induction of IFN-α/β genetically segregate with the reovirus M1, L2, and S2 genes (46). While T3D induces IFN well and T1L induces IFN poorly (46), it is unclear whether this polymorphism reflects differences in PRR-stimulated induction, IRF7-mediated amplification, or both effects. The roles of the L2-encoded λ2 and S2-encoded σ2 proteins in these processes have not been reported, but one possible role for the M1-

encoded μ2 protein could be to suppress IFN induction of IRF7 thereby inhibiting further induction of IFN. Indeed, substitution of only μ2 aa 208 in T3D to provide a repressor of IFN signaling (T3D-S208P), significantly reduced reovirus induction of IFN in both cardiac myocytes and cardiac fibroblasts at 8 h post-infection (Fig. 2). Interestingly, the converse substitution, in which only μ2 aa 208 in T3D-T1LM1 is replaced to remove the repressor of IFN signaling (T3D-T1LM1-P208S), had a much more substantial effect on reovirus induction of IFN in both cell types (Fig. 2). Specifically, T3D-T1LM1-P208S induced 10-fold more IFN-β than did T3D-T1LM1 at 8 h, and a remarkable 150-fold more at 24 h (Fig. 2A) with a concomitant increase in induction of IRF7 (Fig. 2B). Therefore, in the context of the T1L M1 gene, T1L μ2 aa 208 repression of IFN signaling dramatically affected reovirus induction of IRF7 and consequently IFN-β. Importantly, viruses with a T1L M1 gene display enhanced kinetics of viral RNA synthesis in cardiac myocytes in comparison to those with a T3D M1 gene (42). Thus, T1L μ2 should be synthesized earlier than T3D μ2, offering T3D-T1LM1 greater opportunity than T3D-S208P to repress induction of IRF7. The substantial increase in the induction of IFN-β at 24 h by T3D-T1LM1-P208S relative to T3D (Fig. 2A) is consistent with both the absence of the T1L μ2 aa 208 repressor of IFN signaling and the T1L M1-associated rapid RNA synthesis phenotype facilitating RNA-stimulated activation of IRF7 (42). Together, these data indicate that reovirus induction of IFN in cardiac cells involves a positive amplification loop and that repression of IFN signaling reduces reovirus induction of IFN-β.

The reovirus M1-, L2-, and S2-encoded proteins also could modulate reovirus activation of PRRs. Depending on the cell type, reovirus activates the PRRs RIG-I, MDA5, or both molecules to induce IFN (15, 17, 25), although the specific nucleic acid stimulus remains unclear. While reovirus particles contain genomic dsRNA, virions are not thought to fully uncoat during viral replication (41), and thus genomic dsRNA should be protected from PRRs. Instead, reovirus cores synthesize ssRNA, which is extruded and then complexed into new subviral particles for RNA second-strand synthesis (41). The μ2 protein is found at the icosahedral vertices of viral cores as part of a probable RNA-synthesizing complex (18, 51), has both NTPase (18, 33) and RNA-binding activity (6, 18, 33), and determines the rate of viral RNA synthesis in cardiac myocytes (42). However, reoviruses with a T1L M1 gene synthesize RNA more rapidly than those with a T3D M1 gene (42), the opposite of what would be predicted if μ2-stimulated viral RNA synthesis solely determined the level of IFN induction. It is possible that the location of both μ2 and λ2 at the icosahedral vertices (7, 11) influences particle stability. Virions contain not only genomic dsRNA, a potential RIG-I and MDA5 ligand, but also short oligonucleotides with free 5' triphosphates (3, 32, 41), an additional potential RIG-I ligand although shorter than other RIG-I agonists (26, 27). Therefore, T3D particles may aberrantly disassemble more readily than T1L particles, resulting in commensurately greater PRR activation and induction of IFN. We found that T3D induction of IFN in cardiac cells was reduced when its M1 gene was replaced with that of T1L (T3D-T1LM1, Figs. 2A and 2C). However, the striking increase in induction of IFN when the T1LM1 repressor of IFN signaling was removed (T3D-T1LM1-P208S) suggests that the main function of μ2 in the IFN response is to repress IFN signaling (as in T1L) rather than to shield PRR ligands from the innate immune surveillance machinery.

In previous work, we demonstrated that infection with reoviruses containing a T1L M1 gene or transfection of T1L M1 alone represses IFN signaling (53). While this repression is associated with an unusual nuclear accumulation of IRF9, the mechanism for repression is unclear (53). Here, we determined that aa 208 of μ2 is both required and sufficient for repression of IFN signaling. Interestingly, μ2 aa 208 governs several differences displayed by strains T1L and T3D. Reovirus replicates and assembles in viral inclusion bodies (VIBs). While T3D induces formation of globular VIBs, T1L induces formation of filamentous VIBs, reflecting T1L μ2-stimulated hyperacetylation and stabilization of microtubules (37). These T1L μ2-stimulated events are disrupted when the T1L proline at aa 208 is substituted with the T3D serine (37). However, the T1L proline at aa 208 is not the sole determinant of VIB morphology, as substitutions at aa 383 can prevent formation of filamentous VIBs even when μ2 contains T1L proline aa 208 (20). Importantly, aa 208 also mediates greater ubiquitination and aggregation of T3D μ2 than T1L μ2, suggesting that the capacity of T1L μ2 to stabilize microtubules and induce filamentous VIBs may be a consequence of virus strain-specific post-translational μ2 modifications (30). Results presented here identify T1L μ2 aa 208 as both required and sufficient for reovirus repression of IFN signaling and suggest two possible models: 1) repression of IFN signaling requires the cytoskeletal changes that accompany formation of filamentous VIBs or 2) ubiquitinated and aggregated μ2 cannot function to repress IFN signaling. Future studies are planned to discriminate between these possibilities.

The protective effects of secreted IFN should be greater in cells that have not been infected, i.e., as a paracrine signal, than in cells already infected, i.e., as an autocrine signal, since the former have more time to induce antiviral proteins. In addition, IFN-mediated reductions in viral yield should result in fewer secondary infections. Therefore, the effect of the IFN response on viral yield should be amplified following viral spread. The IFN response determines reovirus yields in primary cardiac myocyte cultures and, as expected, the effect is increased following viral spread (46). We found that μ2 aa 208 determines strain-specific differences in viral replication in cardiac myocytes even after a single cycle of replication (Fig. 3A), suggesting that IFN can reduce viral replication in these cells even after infection is initiated. As expected, the effect was enhanced after multiple cycles (Fig. 3B). When IFN was removed, viruses containing the T3D-encoded serine at aa 208 achieved titers equivalent to those containing the T1L-encoded proline at aa 208 (Fig. 3C), demonstrating that aa 208 regulation of the IFN response determines reovirus replication and spread between cardiac myocytes.

Virus strain-specific differences in induction of myocarditis correlate with differences in CPE in primary cardiac myocyte cultures only after viral spread (2, 46), consistent with the IFN response regulating viral spread in vitro and in vivo (14, 34, 46). Many investigations have used IFN-deficient mice or viruses that are defective in repressing the IFN response to demonstrate the importance of the IFN response in protection against virus-induced disease, but few have pinpointed the populations of differentiated cells in which IFN critically acts to limit progression of viral infection. Here, we found that a serine-proline polymorphism at aa 208 in the reovirus μ2 protein influences CPE after multiple cycles of replication in cardiac myocytes (Fig. 5) and modulates myocarditis (Fig. 6), providing evidence that viral repression of IFN signaling in a target differentiated cell can determine disease outcome.

ACKNOWLEDGEMENTS

We thank Lianna Li and Ray Pickles for insightful discussions and Lance Johnson for excellent technical assistance.

This research was supported by Public Health Service awards R01 AI32539 (T.S.D.), R37 AI38296 (T.S.D.), and R01 A1083333 (B.S.) and the Elizabeth B. Lamb Center for Pediatric Research. Additional support was provided by Public Health Service awards CA68485 for the Vanderbilt-Ingram Cancer Center and DK20593 for the Vanderbilt Diabetes Research and Training Center.

REFERENCES

1. **Barnard, P., and N. A. McMillan.** 1999. The human papillomavirus E7 oncoprotein abrogates signaling mediated by interferon-alpha. Virology **259:**305-313.

2. **Baty, C. J., and B. Sherry.** 1993. Cytopathogenic effect in cardiac myocytes but not in cardiac fibroblasts is correlated with reovirus-induced acute myocarditis. J Virol **67:**6295-6298.

3. **Bellamy, A. R., and W. K. Joklik.** 1967. Studies on the A-rich RNA of reovirus. Proc Natl Acad Sci U S A **58:**1389-1395.

4. **Bergmann, O., R. D. Bhardwaj, S. Bernard, S. Zdunek, F. Barnabé-Heider, S. Walsh, J. Zupicich, K. Alkass, B. A. Buchholz, H. Druid, S. Jovinge, and J. Frisén.** 2009. Evidence for cardiomyocyte renewal in humans. Science **324:**98-102.

5. **Bowie, A. G., and L. Unterholzner.** 2008. Viral evasion and subversion of pattern-recognition receptor signalling. Nat Rev Immunol **8:**911-922.

6. **Brentano, L., D. L. Noah, E. G. Brown, and B. Sherry.** 1998. The reovirus protein mu2, encoded by the M1 gene, is an RNA-binding protein. J Virol **72:**8354-8357.

7. **Coombs, K. M.** 1998. Stoichiometry of reovirus structural proteins in virus, ISVP, and core particles. Virology **243:**218-228.

8. **Cooper, L. T.** 2009. Myocarditis. N Engl J Med **360:**1526-1538.

9. **Daliento, L., F. Calabrese, F. Tona, A. L. Caforio, G. Tarsia, A. Angelini, and G. Thiene.** 2003. Successful treatment of enterovirus-induced myocarditis with interferon-alpha. J Heart Lung Transplant **22:**214-217.

10. **Drory, Y., Y. Turetz, Y. Hiss, B. Lev, E. Z. Fisman, A. Pines, and M. R. Kramer.** 1991. Sudden unexpected death in persons less than 40 years of age. Am J Cardiol **68:**1388-1392.

11. **Dryden, K. A., D. L. Farsetta, G. Wang, J. M. Keegan, B. N. Fields, T. S. Baker, and M. L. Nibert.** 1998. Internal/structures containing transcriptase-related proteins in top component particles of mammalian orthoreovirus. Virology **245:**33-46.

12. **Feldman, A. M., and D. McNamara.** 2000. Myocarditis. N Engl J Med **343:**1388-1398.

13. **Fensterl, V., and G. C. Sen.** 2009. Interferons and viral infections. Biofactors **35:**14-20.

14. **Holm, G. H., A. J. Pruijssers, L. Li, P. Danthi, B. Sherry, and T. S. Dermody.** 2010. Interferon regulatory factor 3 attenuates reovirus myocarditis and contributes to viral clearance. J Virol **84:**6900-6908.

15. **Holm, G. H., J. Zurney, V. Tumilasci, S. Leveille, P. Danthi, J. Hiscott, B. Sherry, and T. S. Dermody.** 2007. Retinoic acid-inducible gene-I and interferon-beta promoter stimulator-1 augment proapoptotic responses following mammalian reovirus infection via interferon regulatory factor-3. J Biol Chem **282:**21953-21961.

16. **Honda, K., H. Yanai, H. Negishi, M. Asagiri, M. Sato, T. Mizutani, N. Shimada, Y. Ohba, A. Takaoka, N. Yoshida, and T. Taniguchi.** 2005. IRF-7 is the master regulator of type-I interferon-dependent immune responses. Nature **434:**772-777.

17. **Kato, H., O. Takeuchi, E. Mikamo-Satoh, R. Hirai, T. Kawai, K. Matsushita, A. Hiiragi, T. S. Dermody, T. Fujita, and S. Akira.** 2008. Length-dependent recognition of double-

stranded ribonucleic acids by retinoic acid-inducible gene-I and melanoma differentiation-associated gene 5. J Exp Med **205:**1601-1610.

18. **Kim, J., J. S. Parker, K. E. Murray, and M. L. Nibert.** 2004. Nucleoside and RNA triphosphatase activities of orthoreovirus transcriptase cofactor mu2. J Biol Chem **279:**4394-4403.

19. **Kobayashi, T., A. A. Antar, K. W. Boehme, P. Danthi, E. A. Eby, K. M. Guglielmi, G. H. Holm, E. M. Johnson, M. S. Maginnis, S. Naik, W. B. Skelton, J. D. Wetzel, G. J. Wilson, J. D. Chappell, and T. S. Dermody.** 2007. A plasmid-based reverse genetics system for animal double-stranded RNA viruses. Cell Host Microbe **1:**147-157.

20. **Kobayashi, T., L. S. Ooms, J. D. Chappell, and T. S. Dermody.** 2009. Identification of functional domains in reovirus replication proteins muNS and mu2. J Virol **83:**2892-2906.

21. **Kühl, U., M. Pauschinger, M. Noutsias, B. Seeberg, T. Bock, D. Lassner, W. Poller, R. Kandolf, and H. P. Schultheiss.** 2005. High prevalence of viral genomes and multiple viral infections in the myocardium of adults with "idiopathic" left ventricular dysfunction. Circulation **111:**887-893.

22. **Kühl, U., M. Pauschinger, P. L. Schwimmbeck, B. Seeberg, C. Lober, M. Noutsias, W. Poller, and H. P. Schultheiss.** 2003. Interferon-beta treatment eliminates cardiotropic viruses and improves left ventricular function in patients with myocardial persistence of viral genomes and left ventricular dysfunction. Circulation **107:**2793-2798.

23. **Kühl, U., M. Pauschinger, B. Seeberg, D. Lassner, M. Noutsias, W. Poller, and H. P. Schultheiss.** 2005. Viral persistence in the myocardium is associated with progressive cardiac dysfunction. Circulation **112:**1965-1970.

24. **Leonard, G. T., and G. C. Sen.** 1996. Effects of adenovirus E1A protein on interferon-signaling. Virology **224:**25-33.

25. **Loo, Y. M., J. Fornek, N. Crochet, G. Bajwa, O. Perwitasari, L. Martinez-Sobrido, S. Akira, M. A. Gill, A. García-Sastre, M. G. Katze, and M. Gale.** 2008. Distinct RIG-I and MDA5 signaling by RNA viruses in innate immunity. J Virol **82:**335-345.

26. **Loo, Y. M., and M. Gale.** 2011. Immune Signaling by RIG-I-like Receptors. Immunity **34:**680-692.

27. **Marques, J. T., T. Devosse, D. Wang, M. Zamanian-Daryoush, P. Serbinowski, R. Hartmann, T. Fujita, M. A. Behlke, and B. R. Williams.** 2006. A structural basis for

discriminating between self and nonself double-stranded RNAs in mammalian cells. Nat Biotechnol **24:**559-565.

28. **Martin, A. B., S. Webber, F. J. Fricker, R. Jaffe, G. Demmler, D. Kearney, Y. H. Zhang, J. Bodurtha, B. Gelb, and J. Ni.** 1994. Acute myocarditis. Rapid diagnosis by PCR in children. Circulation **90:**330-339.

29. **Mason, J. W., J. B. O'Connell, A. Herskowitz, N. R. Rose, B. M. McManus, M. E. Billingham, and T. E. Moon.** 1995. A clinical trial of immunosuppressive therapy for myocarditis. The Myocarditis Treatment Trial Investigators. N Engl J Med **333:**269-275.

30. **Miller, C. L., J. S. Parker, J. B. Dinoso, C. D. Piggott, M. J. Perron, and M. L. Nibert.** 2004. Increased ubiquitination and other covariant phenotypes attributed to a strain- and temperature-dependent defect of reovirus core protein mu2. J Virol **78:**10291-10302.

31. **Mirić, M., J. Vasiljević, M. Bojić, Z. Popović, N. Keserović, and M. Pesić.** 1996. Long-term follow up of patients with dilated heart muscle disease treated with human leucocytic interferon alpha or thymic hormones initial results. Heart **75:**596-601.

32. **Nichols, J. L., A. R. Bellamy, and W. K. Joklik.** 1972. Identification of the nucleotide sequences of the oligonucleotides present in reovirions. Virology **49:**562-572.

33. **Noble, S., and M. L. Nibert.** 1997. Core protein mu2 is a second determinant of nucleoside triphosphatase activities by reovirus cores. J Virol **71:**7728-7735.

34. **O'Donnell, S. M., M. W. Hansberger, J. L. Connolly, J. D. Chappell, M. J. Watson, J. M. Pierce, J. D. Wetzel, W. Han, E. S. Barton, J. C. Forrest, T. Valyi-Nagy, F. E. Yull, T. S. Blackwell, J. N. Rottman, B. Sherry, and T. S. Dermody.** 2005. Organ-specific roles for transcription factor NF-kappaB in reovirus-induced apoptosis and disease. J Clin Invest **115:**2341-2350.

35. **O'Neill, L. A., and A. G. Bowie.** 2010. Sensing and signaling in antiviral innate immunity. Curr Biol **20:**R328-333.

36. **Ooms, L. S., T. Kobayashi, T. S. Dermody, and J. D. Chappell.** 2010. A post-entry step in the mammalian orthoreovirus replication cycle is a determinant of cell tropism. J Biol Chem **285:**41604-41613.

37. **Parker, J. S., T. J. Broering, J. Kim, D. E. Higgins, and M. L. Nibert.** 2002. Reovirus core protein mu2 determines the filamentous morphology of viral inclusion bodies by interacting with and stabilizing microtubules. J Virol **76:**4483-4496.

38. **Parrillo, J. E., R. E. Cunnion, S. E. Epstein, M. M. Parker, A. F. Suffredini, M. Brenner, G. L. Schaer, S. T. Palmeri, R. O. Cannon, and D. Alling.** 1989. A prospective, randomized, controlled trial of prednisone for dilated cardiomyopathy. N Engl J Med **321:**1061-1068.

39. **Randall, R. E., and S. Goodbourn.** 2008. Interferons and viruses: an interplay between induction, signalling, antiviral responses and virus countermeasures. J Gen Virol **89:**1-47.

40. **Sato, M., N. Hata, M. Asagiri, T. Nakaya, T. Taniguchi, and N. Tanaka.** 1998. Positive feedback regulation of type I IFN genes by the IFN-inducible transcription factor IRF-7. FEBS Lett **441:**106-110.

41. **Schiff, L. A., M. L. Nibert, and K. L. Tyler.** 2007. Orthoreoviruses and Their Replication, p. 1854-1915. *In* D. M. Knipe and P. M. Howley (ed.), Fields' virology, 5th ed, vol. 2. Wolters Kluwer Health/Lippincott Williams & Wilkins, Philadelphia.

42. **Sherry, B., C. J. Baty, and M. A. Blum.** 1996. Reovirus-induced acute myocarditis in mice correlates with viral RNA synthesis rather than generation of infectious virus in cardiac myocytes. J Virol **70:**6709-6715.

43. **Sherry, B., and M. A. Blum.** 1994. Multiple viral core proteins are determinants of reovirus-induced acute myocarditis. J Virol **68:**8461-8465.

44. **Sherry, B., and B. N. Fields.** 1989. The reovirus M1 gene, encoding a viral core protein, is associated with the myocarditic phenotype of a reovirus variant. J Virol **63:**4850-4856.

45. **Sherry, B., X. Y. Li, K. L. Tyler, J. M. Cullen, and H. W. Virgin.** 1993. Lymphocytes protect against and are not required for reovirus-induced myocarditis. J Virol **67:**6119-6124.

46. **Sherry, B., J. Torres, and M. A. Blum.** 1998. Reovirus induction of and sensitivity to beta interferon in cardiac myocyte cultures correlate with induction of myocarditis and are determined by viral core proteins. J Virol **72:**1314-1323.

47. **Smith, R. E., H. J. Zweerink, and W. K. Joklik.** 1969. Polypeptide components of virions, top component and cores of reovirus type 3. Virology **39:**791-810.

48. **Stewart, M. J., K. Smoak, M. A. Blum, and B. Sherry.** 2005. Basal and reovirus-induced beta interferon (IFN-beta) and IFN-beta-stimulated gene expression are cell type specific in the cardiac protective response. J Virol **79:**2979-2987.

49. **Takeuchi, O., and S. Akira.** 2009. Innate immunity to virus infection. Immunol Rev **227:**75-86.

50. **Wilkins, C., and M. Gale.** 2010. Recognition of viruses by cytoplasmic sensors. Curr Opin Immunol **22:**41-47.

51. **Zhang, X., S. B. Walker, P. R. Chipman, M. L. Nibert, and T. S. Baker.** 2003. Reovirus polymerase lambda 3 localized by cryo-electron microscopy of virions at a resolution of 7.6 A. Nat Struct Biol **10:**1011-1018.

52. **Zurney, J., K. E. Howard, and B. Sherry.** 2007. Basal expression levels of IFNAR and Jak-STAT components are determinants of cell-type-specific differences in cardiac antiviral responses. J Virol **81:**13668-13680.

53. **Zurney, J., T. Kobayashi, G. H. Holm, T. S. Dermody, and B. Sherry.** 2009. Reovirus mu2 protein inhibits interferon signaling through a novel mechanism involving nuclear accumulation of interferon regulatory factor 9. J Virol **83:**2178-2187.

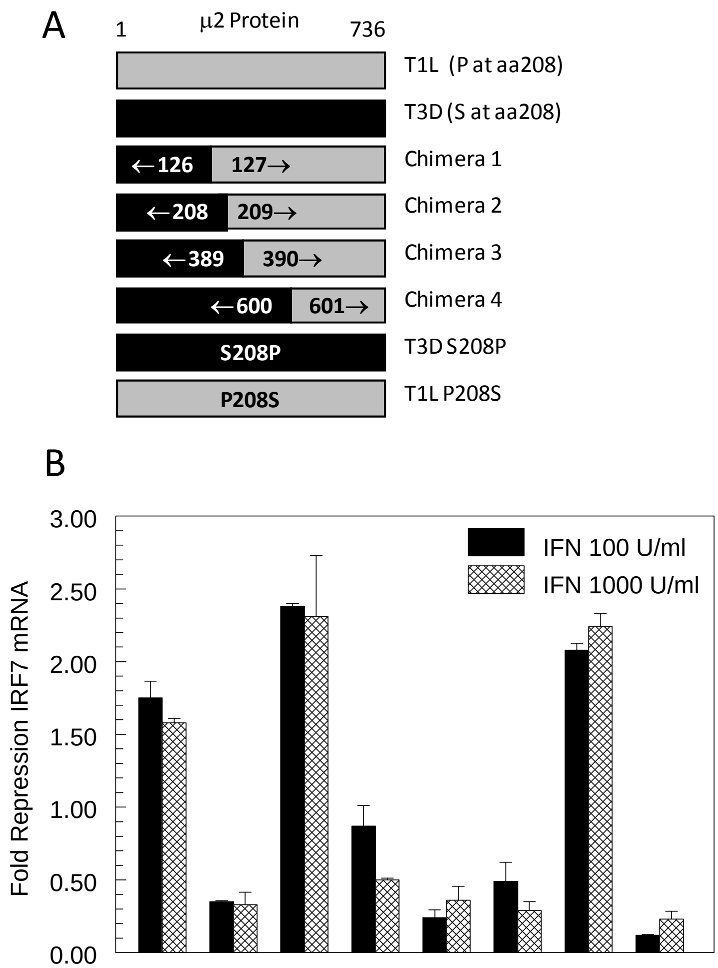

Virus Name	T1L	T3D	Ch 1	Ch 2	Ch 3	Ch 4	T3D-S208P	T3D-T1LM1-P208S
9 Genes	T1L	T3D	T3D	T3D	T3D	T3D	T3D	T3D
Substitute M1 Gene	–	–	Ch 1	Ch 2	Ch 3	Ch 4	–	T1L
T1L μ2 Amino Acids	–	–	127 - 736	209 - 736	390 - 736	601 - 736	208	all except 208

Figure 2.1. μ2 aa 208 determines reovirus repression of IFN signaling. (A) Viruses with a chimeric M1 gene or viruses with a mutated aa at position 208 of μ2 were generated by reverse genetics (107, 152). (B) L929 cells were infected with the indicated viruses, cells were treated with IFN, and mRNA was harvested for qRT-PCR. Fold repression was calculated as ([copies IRF7 / GAPDH in IFN-treated mock-infected cells] / [copies IRF7 / GAPDH in IFN-treated virus-infected cells]). Viruses that induce high levels of IFN resulted in values < 1, but relative repression between viruses was the same (211). Results are mean ± SD (representative of four experiments).

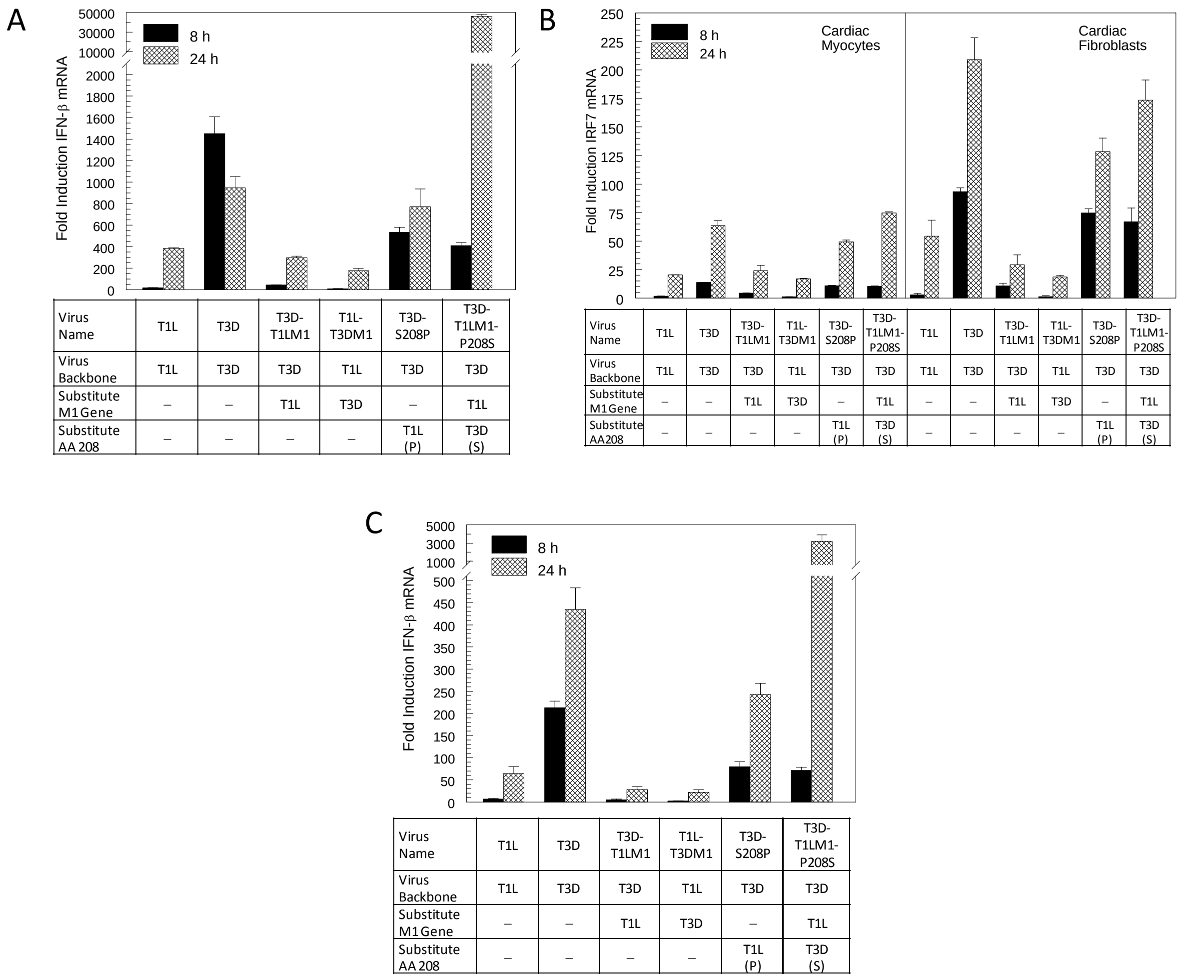

A

Virus Name	T1L	T3D	T3D-T1LM1	T1L-T3DM1	T3D-S208P	T3D-T1LM1-P208S
Virus Backbone	T1L	T3D	T3D	T1L	T3D	T3D
Substitute M1 Gene	–	–	T1L	T3D	–	T1L
Substitute AA 208	–	–	–	–	T1L (P)	T3D (S)

B

Virus Name	T1L	T3D	T3D-T1LM1	T1L-T3DM1	T3D-S208P	T3D-T1LM1-P208S	T1L	T3D	T3D-T1LM1	T1L-T3DM1	T3D-S208P	T3D-T1LM1-P208S
Virus Backbone	T1L	T3D	T3D	T1L	T3D	T3D	T1L	T3D	T3D	T1L	T3D	T3D
Substitute M1 Gene	–	–	T1L	T3D	–	T1L	–	–	T1L	T3D	–	T1L
Substitute AA208	–	–	–	–	T1L (P)	T3D (S)	–	–	–	–	T1L (P)	T3D (S)

C

Virus Name	T1L	T3D	T3D-T1LM1	T1L-T3DM1	T3D-S208P	T3D-T1LM1-P208S
Virus Backbone	T1L	T3D	T3D	T1L	T3D	T3D
Substitute M1 Gene	–	–	T1L	T3D	–	T1L
Substitute AA 208	–	–	–	–	T1L (P)	T3D (S)

Figure 2.2. μ2 aa 208 modulates reovirus induction of IFN in cardiac cells. Primary cardiac myocyte (A, B) or fibroblast (B, C) cultures were infected with the indicated viruses, and mRNA was harvested for qRT-PCR using primers specific for IFN-β (A, C) or IRF7 (B) and GAPDH. Fold induction was calculated as copies IFN-β or IRF7 / GAPDH in infected cultures relative to uninfected cultures. (A, C) Results are mean ± SEM (average of two experiments); (B) results are mean ± SD (representative of two experiments).

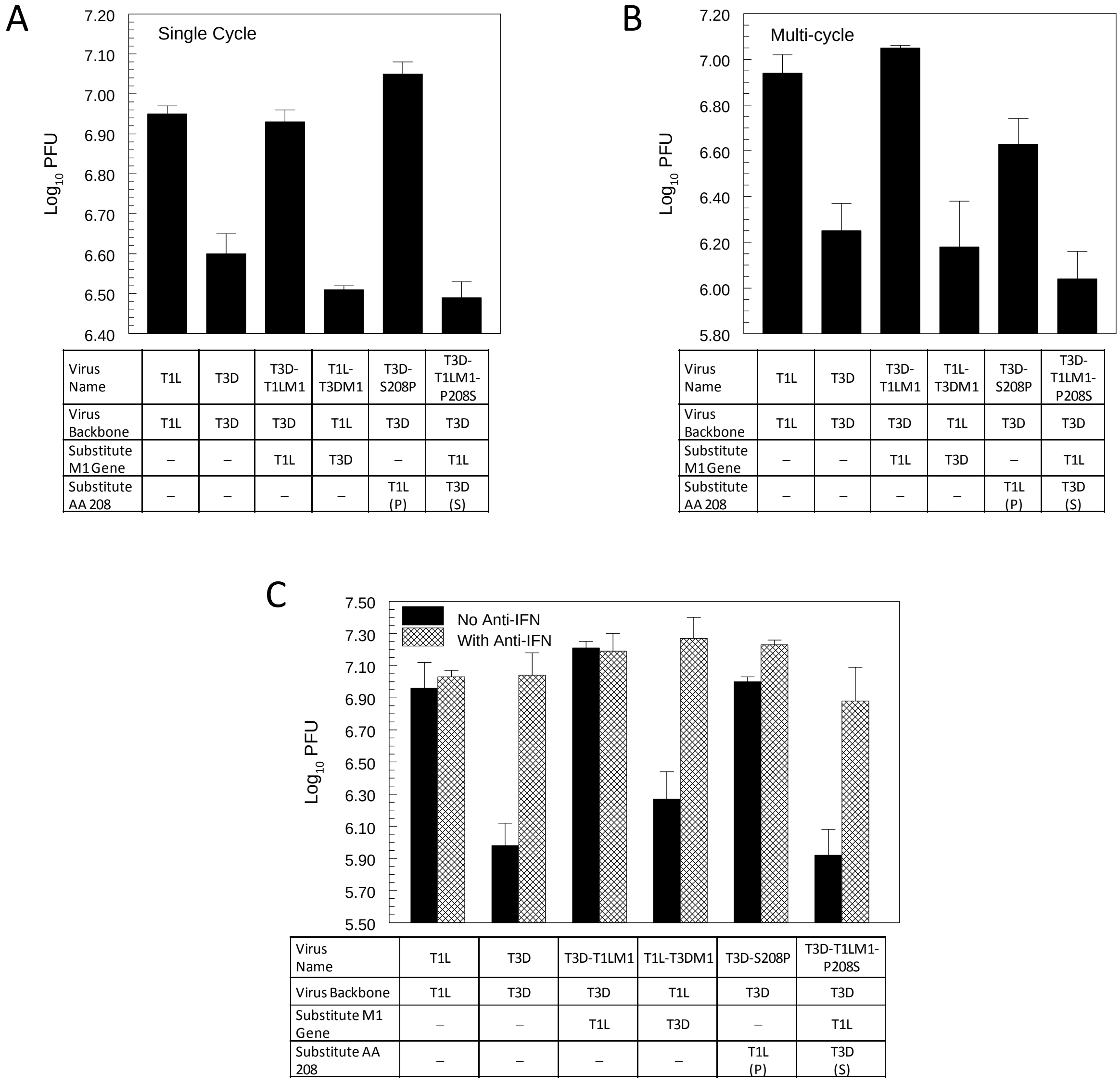

Figure 2.3. μ2 aa 208 determines reovirus single-cycle and multi-cycle replication in cardiac myocytes. Primary cardiac myocyte cultures were infected with the indicated viruses at an MOI of 3 PFU per cell and incubated for 24 h (A) or at an MOI of 0.1 PFU per cell and incubated for 5 days (B) and harvested for plaque assay. (C) Primary cardiac myocyte cultures were infected as in (B), treated with anti-IFN-β antibody where indicated, and harvested for plaque assay. Results are mean ± SD (representative of two experiments).

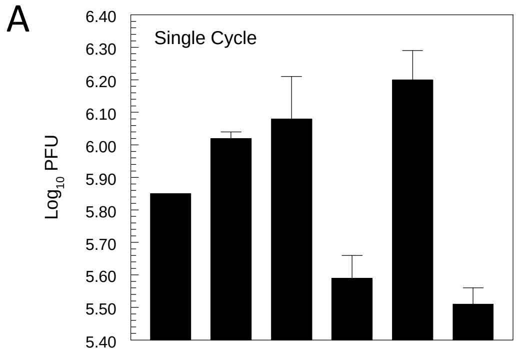

Virus Name	T1L	T3D	T3D-T1LM1	T1L-T3DM1	T3D-S208P	T3D-T1LM1-P208S
Virus Backbone	T1L	T3D	T3D	T1L	T3D	T3D
Substitute M1 Gene	–	–	T1L	T3D	–	T1L
Substitute AA 208	–	–	–	–	T1L (P)	T3D (S)

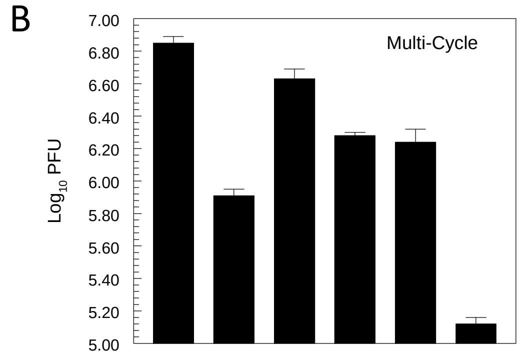

Virus Name	T1L	T3D	T3D-T1LM1	T1L-T3DM1	T3D-S208P	T3D-T1LM1-P208S
Virus Backbone	T1L	T3D	T3D	T1L	T3D	T3D
Substitute M1 Gene	–	–	T1L	T3D	–	T1L
Substitute AA 208	–	–	–	–	T1L (P)	T3D (S)

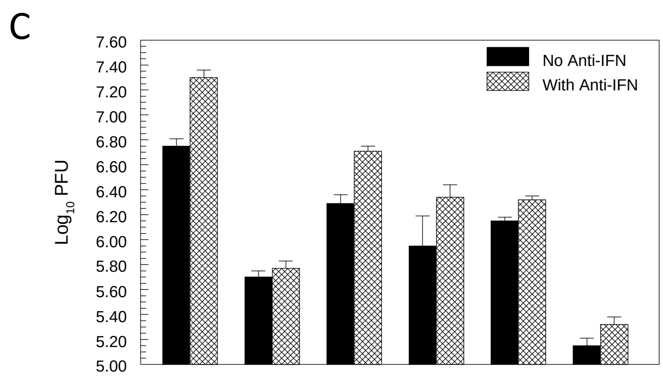

Virus Name	T1L	T3D	T3D-T1LM1	T1L-T3DM1	T3D-S208P	T3D-T1LM1-P208S
Virus Backbone	T1L	T3D	T3D	T1L	T3D	T3D
Substitute M1 Gene	–	–	T1L	T3D	–	T1L
Substitute AA 208	–	–	–	–	T1L (P)	T3D (S)

Figure 2.4. μ2 aa 208 influences reovirus single-cycle and multi-cycle replication in cardiac fibroblasts. Primary cardiac fibroblast cultures were infected with the indicated viruses at an MOI of 3 PFU per cell and incubated for 24 h (A) or at an MOI of 0.1 PFU per cell and incubated for 5 days (B) and harvested for plaque assay. (C) Primary cardiac fibroblast cultures were infected as in (B), treated with anti-IFN-β where indicated, and harvested for plaque assay. Results are mean ± SD (representative of two experiments).

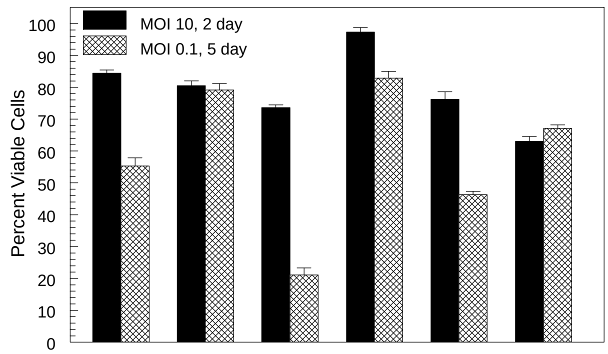

Virus Name	T1L	T3D	T3D-T1LM1	T1L-T3DM1	T3D-S208P	T3D-T1LM1-P208S
Virus Backbone	T1L	T3D	T3D	T1L	T3D	T3D
Substitute M1 Gene	–	–	T1L	T3D	–	T1L
Substitute AA 208	–	–	–	–	T1L (P)	T3D (S)

Figure 2.5. μ2 aa 208 determines reovirus CPE in cardiac myocytes only after spread. Primary cardiac myocyte cultures were infected with the indicated viruses at an MOI of 10 PFU per cell and incubated for 2 days (single cycle) or at an MOI 0.1 PFU per cell and incubated for 5 days (multi-cycle) and harvested for MTT assay. Percent viable cells was calculated relative to mock-infected cells. Results are mean ± SEM (average of two experiments).

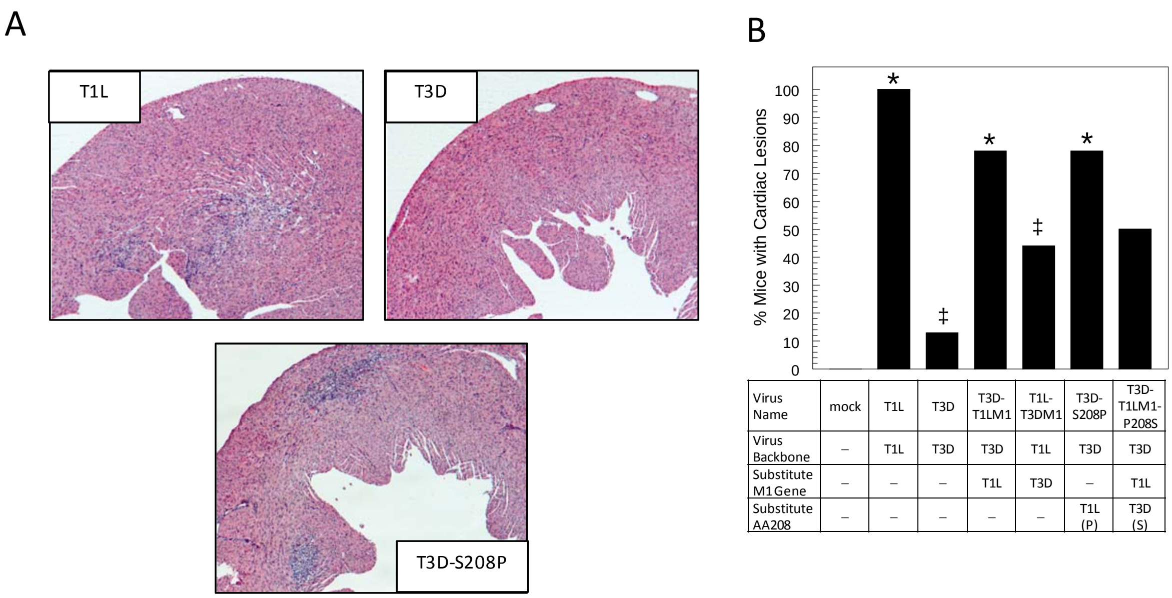

Virus Name	mock	T1L	T3D	T3D-T1LM1	T1L-T3DM1	T3D-S208P	T3D-T1LM1-P208S
Virus Backbone	–	T1L	T3D	T3D	T1L	T3D	T3D
Substitute M1 Gene	–	–	–	T1L	T3D	–	T1L
Substitute AA208	–	–	–	–	–	T1L (P)	T3D (S)

Figure 2.6. μ2 aa 208 modulates myocarditis. Neonatal mice were inoculated with the indicated viruses and euthanized seven days post-injection. Hematoxylin- and eosin-stained cardiac sections were scored for lesions. (A) Representative sections. (B) A minimum of 8 hearts (minimum 15 sections per heart) were scored for each virus. Lesions in adjacent sections were not scored as independent lesions. Hearts were considered "positive" if more than a single lesion was detected in the ≥ 15 sections examined. Asterisks (*) indicate significantly different from T3D (Chi Square, $P < 0.05$); daggers (‡) indicate significantly different from T1L (Chi Square, $P < 0.05$). Results are representative of two independent experiments.

CHAPTER 3

An ITAM in Reovirus Regulates Activation of NF-κB, Induction of Interferon-β, and Viral Spread

Susan C. Irvin[1], Karl W. Boehme[2,4], Mine Ikizler[2,4], Jeffrey A. Yoder[1], Terence S. Dermody[2,3,4], and Barbara Sherry[1]

[1] Department of Molecular Biomedical Sciences and Center for Comparative Medicine and Translational Research, North Carolina State University, Raleigh NC 27607

[2] Departments of Pediatrics and [3]Pathology, Microbiology, and Immunology and [4] Elizabeth B. Lamb Center for Pediatric Research, Vanderbilt University School of Medicine, Nashville, TN 37232, USA

Manuscript submitted

ABSTRACT

Immunoreceptor tyrosine-based activation motifs (ITAMs) are signaling domains present in the cytoplasmic tails of many receptors that mediate immune cell activation. ITAMs also have been identified in the cytoplasmic tails of some enveloped virus glycoproteins. Here, ITAMs were identified in three mammalian reovirus proteins, σ2, μ2, and λ2, which are viral outer capsid and core constituents. These are the first ITAMs identified in a nonenveloped virus. ITAM-mediated cell signaling requires the phosphorylation of two tyrosine residues within the motif. To determine the role of ITAMs in reovirus replication and pathogenesis, reverse genetics was used to engineer mutant reoviruses in which the two critical tyrosine residues in each ITAM were replaced with phenylalanine to prevent ITAM phosphorylation. Although the λ2 mutant virus was not viable, replication kinetics and progeny yields of the remaining two ITAM mutant viruses in L929 cells and in primary cardiac myocyte cultures demonstrated the σ2 and μ2 ITAMs are not required for viral replication. Importantly, the μ2 ITAM regulates the activation of NF-κB and also influences the induction of interferon-β (IFN-β) in both L929 cells and primary cardiac myocyte cultures. Moreover, the consequences of these μ2 ITAM effects are cell type-specific. In L929 cells, the μ2 ITAM enhances viral fitness. In contrast, in primary cardiac myocyte cultures where the IFN-β response is critical for antiviral protection and NF-κB is not required for apoptosis, the μ2 ITAM diminishes viral fitness. These results suggest

the μ2 ITAM has a cell type-specific role in viral spread, likely reflecting the cell type-specific functions of NF-κB and IFN-β.

INTRODUCTION

Immunoreceptor tyrosine-based activation motifs (ITAMs) consist of YxxI/LX$_{6-12}$YxxI/L sequences and are found in the cytoplasmic tails of certain transmembrane proteins, particularly those associated with immune cell activation. Examples include B-cell and T-cell receptors as well as receptor-associated adaptor proteins such as DAP12 (56). Upon ligand-receptor binding, the ITAM-containing protein recruits Src family kinases for phosphorylation of the ITAM tyrosine residues (4, 56). Phosphorylated ITAMs then recruit Syk family kinases, which autophosphorylate and stimulate downstream signaling (41, 46). Cellular ITAMs signal through intermediates, including MAPKs, NFAT, and NF-κB, to stimulate an array of responses, such as cellular differentiation, cytokine release, and cell death (1, 20, 23, 41, 56).

ITAMs also have been identified in enveloped viruses, where they utilize the same signaling intermediates as cellular ITAMs and participate in pathogenesis and oncogenesis (32). For example, hantavirus strains that cause hantavirus pulmonary syndrome contain an ITAM in the cytoplasmic tail of the G1 envelope protein, while non-pathogenic hantavirus strains lack this motif (19). Similarly, studies implicate an ITAM in the Nef protein of simian immunodeficiency virus (SIV) as an important virulence determinant (13). All other known viral ITAMs are associated with oncogenic viruses in the *Herpesviridae* (3, 34) and *Retroviridae* (3, 25) families. To date, ITAMs have not been reported in nonenveloped viruses.

Mammalian orthoreoviruses (reoviruses), members of the *Reoviridae* family, are nonenveloped dsRNA viruses that exhibit strain-specific differences in tropism and virulence in newborn mice (47). Reoviruses cause a spectrum of disease in these animals, including myocarditis, encephalitis, hepatitis, and hydrocephalus. Reovirus strain-specific differences in the capacity to induce myocarditis (cardiac tissue damage and inflammation) in mice correlate with virus strain-specific differences in induction of and sensitivity to the antiviral cytokine, interferon-β (IFN-β), in cardiac myocytes (53). Concordantly, non-myocarditic reovirus strains induce cardiac lesions when the IFN response is disrupted (21, 43, 53). The reovirus M1 gene, which encodes the μ2 protein, is the primary determinant of reovirus myocarditic potential (51, 52). Differences in induction of and sensitivity to IFN-β also segregate with the reovirus M1 gene as well as the S2 and L2 genes, which encode the σ2 and λ2 proteins, respectively (53). While the M1 gene of reovirus strains that display resistance to IFN-β encodes a repressor of IFN signaling (61), other reovirus effectors that modulate the IFN response are unclear.

Reoviruses induce IFN by activating pathogen recognition receptors (PRRs) RIG-I and/or MDA5 (22, 24, 35). Viral RNA synthesis occurs within the infecting particle and in newly formed cores from which nascent single-stranded RNA is extruded (47). However, the reovirus RNA species that triggers RIG-I and/or MDA5 is undefined. IFN transcription factors

IRF3 and NF-κB are activated upon reovirus infection and activation of IRF3 is dependent on RIG-I and the adaptor protein IPS-1. However, activation of NF-κB requires neither of these signaling intermediaries (22). The activation of NF-κB during reovirus infection also plays a role in apoptosis that is cell type-specific (43). Importantly, apoptosis induced by reovirus requires NF-κB in many cell types (10, 11) but not in cardiac myocytes (9, 43).

In this study, we identified ITAMs in the reovirus σ2, μ2, and λ2 proteins. We found that the M1 gene-encoded μ2 ITAM in reovirus strain type 3 Dearing (T3D) regulates the activation of NF-κB and the induction of IFN-β in both L929 cells and primary cardiac myocyte cultures. In L929 cells, the μ2 ITAM enhances viral fitness. In contrast, in primary cardiac myocyte cultures where the IFN response is critical for antiviral protection and NF-κB is not required for apoptosis (9, 43), the μ2 ITAM limits viral fitness. These results suggest the μ2 ITAM has a cell type-specific role in viral spread, likely reflecting the cell type-specific roles of NF-κB and IFN-β.

MATERIALS and METHODS

Cell lines. Mouse L929 cells were maintained in minimal essential medium (MEM, SAFC Biosciences) supplemented with 5% fetal calf serum (FCS) (Atlanta Biologicals) and 2 mM L-glutamine (Mediatech). L929 cells were plated at 1.25 x 10^4 cells per well in 96-well clusters or at 5 x 10^5 cells per well in 24-well clusters. AD-293 cells (Agilent Technologies, no. 240085), a derivative of HEK-293 cells with improved adherence, and HEK-293 cells were maintained in Dulbecco's MEM (DMEM, Gibco) supplemented with 10% FCS, and 110 mg/L sodium pyruvate (Mediatech). AD-293 cells were plated at 1.875 x 10^4 cells per well in 96-well clusters.. HEK-293 cells were plated at 3.5 x 10^4 cells per well in 96-well clusters or at 4 x 10^5 cells per well in 6-well clusters. All cell lines were allowed to adhere 3 hours (h) prior to infection or transfection.

Primary cardiac myocyte cultures. Timed-pregnant Cr:NIH(S) mice from the National Cancer Institute were maintained as a colony in a facility accredited by the Association for Assessment and Accreditation of Laboratory Animal Care. All animal procedures were approved by the North Carolina State University Institutional Animal Care and Use Committee. Primary cardiac myocyte cultures were generated from 1-day-old neonatal or term fetal Cr:NIH(S) mice resulting from timed pregnancies. Neonatal or term fetal mice were euthanized, and the apical two-thirds of hearts were excised and trypsinized (2). To separate cardiac myocytes from rapidly adherent cardiac fibroblasts, cells were plated at 1.25 x 10^5 cells per well in 6-well clusters and incubated for 2 h at 37°C. Cardiac myocytes were resuspended in DMEM (Gibco) supplemented with 7% FCS (Atlanta Biologicals), 0.06% thymidine (Sigma-Aldrich), and 10 µg per ml of gentamicin (Sigma-Aldrich). Myocyte cultures contained ≤ 5% contamination with fibroblasts (60) and were never passaged prior to use. Myocyte cultures were plated at 1.5 x 10^5 cells per well in 96-well clusters or 5 x 10^5 cells per well in 48-well clusters. Cells were incubated for 2 days prior to infection.

Viruses. Wild-type reovirus strain T3D and mutant recombinant viruses were generated using plasmid-based reverse genetics (28). Tyrosine-to-phenylalanine mutations in the ITAMs were introduced into plasmids containing the T3D S2, M1, or L2 genes (28, 61) using the QuikChange Site-Directed Mutagenesis Kit (Agilent Technologies) according to the manufacturer's instructions with the following primers: σ2 Y130F forward 5'-GTACGACTGCGATGATTTTCCATTTCTAGCGCGTG-3' and reverse 5'-CACGCGCTAGAAATGGAAAATCATCGCAGTCGTAC-3'; σ2 Y144F forward 5'-GATTCAAACATCGGGTGTTTCAGCAATTGAGTGCTGTAAC-3' and reverse 5'-GTTACAGCACTCAATTGCTGAAACACCCGATGTTTGAATC-3'; μ2 Y118F forward 5'-CTCAGGAAAGATGATGAATTCAATCAGCTAGCGCGTGC-3' and reverse 5'-GCACGCGCTAGCTGATTGAATTCATCATCTTTCCTGAG-3'; μ2 Y131F forward 5'-CAAGATATCGGATGTCTTCGCACCTCTCATCTCATCC-3' and reverse 5'-GGATGAGATGAGAGGTGCGAAGACATCCGATATCTTG-3'; λ2 Y671F forward 5'-CTTGGACATCTGGAGTGTTCTTCTTCTTGGTGGACC -3' and reverse 5'-GGTCCACCAAGAAGAAGAACACTCCAGATGTCCAAG -3'; λ2 Y681F forward 5'-GGTGGACCATTTTTATCGTTTTGAGACTTTATCTACGATCTCACG -3' and reverse 5'-CGTGAGATCGTAGATAAAGTCTCAAAACGATAAAAATGGTCCACC -3'. Monolayers of BHK-T7 cells at 90% confluency (3×10^6 cells) seeded in 60-mm dishes were co-transfected with plasmids representing the cloned reovirus genome using 3 μl of TransIT-LT1 transfection reagent (Mirus) per μg of plasmid DNA (29). Following 1–5 days of incubation, recombinant virus was isolated from transfected cells by plaque purification using monolayers of L929 cells. To confirm sequences of the mutant viruses, viral RNA was extracted from purified virions, subjected to Onestep RT-PCR (Qiagen) using gene-specific primers (sequences available upon request), and sequenced. Recombinant viruses were plaque purified, amplified using L929 cells, purified using CsCl-gradient centrifugation (54), and stored as diluted aliquots at -80°C.

Plasmids. The plasmids pNF-κB and pRenilla-luc were previously reported (22). The plasmid pISRE-luc (Stratagene) encodes five tandem copies of the ISG54 interferon-stimulated response element (ISRE) 5’ to a gene encoding firefly luciferase. The plasmid pIFN-β-luc was provided by John Hiscott (McGill University, Montreal, Canada). To generate pcDNA3-FLAG-μ2, the T3D M1 gene was subcloned into the *Eco*RI and *Not*I restrictions sites of pcDNA3 (Invitrogen), and a C-terminal FLAG epitope tag was inserted using the *Not*I and *Xba*I restriction sites. To generate pcDNA3-FLAG-μ2-YYFF, both tyrosine residues in the ITAM were substituted with phenylalanine using the QuikChange Site-Directed Mutagenesis Kit.

Quantification of viral replication. L929 cells or primary cardiac myocyte cultures were plated in 96-well clusters. For single-cycle assays, cells were infected at a multiplicity of infection (MOI) of 3 plaque-forming units (PFU) per cell. For multi-cycle assays, cells were infected at an MOI of 0.1 PFU per cell. After 1 h incubation at 37°C, additional medium was added to each well, and cells were incubated for various intervals before freezing at -80°C. Cells were subjected to two additional freeze-thaw cycles and subsequently lysed in 0.5% NP-40. Viral titers were determined by plaque assay using L929 cells (50). For each experiment, triplicate wells were individually assessed in duplicate plaque-assay wells, and averages and standard deviations were determined.

Assessment of cytopathic effect. L929 cells or primary cardiac myocyte cultures were plated in 96-well clusters. L929 cells were infected at an MOI of 10 PFU per cell (single-cycle assay) or 0.1 PFU per cell (multi-cycle assay) in four replicate wells. Primary cardiac myocyte cultures were infected at an MOI of 1 PFU per cell in five replicate wells. After 1 h incubation at 37°C, additional medium was added to each well. At 24 h, 5 days, or 7 days post-infection, cell viability was quantified using an MTT assay (53). An automated microplate reader (TECAN Sunrise Microplate Reader) was used to determine the optical density (OD) at 570 nm and 650 nm. The absorbance was determined by subtracting OD at 650 nm from OD at 570 nm, and replicate wells were averaged and standard errors of the mean were determined.

Transfections. AD-293 cells were plated in 96-well clusters (four replicate wells per sample), and HEK-293 cells were plated in 96-well clusters (four or five replicate wells) or in 6-well clusters (two replicate wells). Cells were transfected using 5 µl (96-well clusters) or 100 µl (6-well clusters) of a 100 µl reaction. For AD-293 cell transfections, each 100 µl reaction contained 3 µl of FuGENE 6 (Roche, no. 11814443001), 0.1 µg of pRenilla-luc, and 1 µg of pNF-κB-luc reporter plasmid. At 24 h post-transfection, AD-293 cells were washed twice with fresh medium and infected at an MOI of 10 PFU per cell. After 1 h incubation at 37°C, additional medium was added to each well, and cells were incubated for 12 or 24 h.

For HEK-293 cell transfections, each 100 µl reaction contained 6 µl FuGENE 6, 0.1 µg of pRenilla-luc, 1 µg of either pNF-κB-luc, pIFN-β-luc, or pISRE-luc reporter plasmids, and 1 μg, 0.1 μg, or 0.05 μg of either pcDNA3-FLAG, pcDNA3-FLAG-μ2, or pcDNA3-FLAG-μ2-YYFF effector plasmids. Cells were incubated for 24 h.

Luciferase assay. Transfected cells in 96-well clusters were lysed, and luciferase activity was determined using a dual luciferase reporter assay system (Promega, no. E1960) according to the manufacturer's instructions. Luciferase activity for each sample was normalized to the internal *Renilla* luciferase control, and replicate wells were averaged and standard errors of the mean were determined.

SDS-PAGE and immunoblotting. Transfected cells in 6-well clusters were lysed to generate total cellular protein extracts using RIPA lysis buffer (50 mM Tris HCl [pH 7.4], 1% NP-40, 0.25% sodium deoxycholate, 150 mM NaCl, 1 mM EDTA) supplemented to contain 1% sodium dodecylsulfate (SDS) and a cocktail of protease and phosphatase inhibitors (Sigma-Aldrich, no. P8340 and P2850, respectively). Cells were rocked on ice for 15 min and centrifuged at 10,000 x *g* for 10 min at 4°C to remove cellular debris. Protein concentrations were determined using a bicinchoninic acid protein assay (Thermo Fisher Scientific, no. 23227), and 20 μg of protein from each lysate was boiled for 5 min in 1x Laemmli sample buffer and resolved using 10% SDS-polyacrylamide gel electrophoresis (SDS-PAGE). After protein transfer onto nitrocellulose, membranes were blocked for 1 h in Tris-buffered saline (20 mM Tris [pH7.6], 137 mM NaCl) containing 0.1% Tween 20 (TBS-T) and 3% milk for probing with anti-FLAG or 5% milk for probing with anti-GAPDH. Membranes were incubated overnight at 4°C with a mouse anti-FLAG monoclonal (primary) antibody (1:2,500; Sigma-Aldrich, no. F3165) or a goat anti-GAPDH HRP-conjugated polyclonal antibody (1:160;

Santa Cruz Biotechnology, no. sc-20357-HRP). Membranes were washed three times for 5 min each in TBS-T. For detection of the FLAG epitope, blots were incubated for 1 h at room temperature with a goat anti-mouse HRP-conjugated polyclonal (secondary) antibody (1:2,000; Millipore, no. 12-349). Membranes were washed, and proteins were visualized using enhanced chemiluminescence (ECL) or ECL Plus kits (GE Healthcare, no. RPN2108 and RPN2132) according to the manufacturer's instructions. Membranes were exposed to film and converted to digital format using an HP Scanjet G4050; quantification of the digitized bands was determined using UN-SCAN-IT software (Silk Scientific).

Quantitative (real-time) reverse transcription-PCR (qRT-PCR). Cells were plated in triplicate in 24-well (L929 cells) or 48-well (primary cardiac myocyte cultures) clusters and infected at an MOI of 25 PFU per cell (L929 cells) or 10 PFU per cell (primary cardiac myocyte cultures). After 1 h incubation at 37°C, additional medium was added to each well, and cells were incubated for 8 or 12 h, respectively. Cells were lysed, and total RNA was harvested using an RNeasy kit (Qiagen). RNA was treated with RNase-free DNase I (Qiagen). One-third of the RNA from each well was used to generate cDNA by reverse transcription in 100 µl containing 5 µM oligo(dT) (Invitrogen), 1X Taq buffer (Promega), 7.5 mM $MgCl_2$ (Promega), 1 mM dithiothreitol (Promega), 1 mM each deoxynucleoside triphosphate (Roche), 0.67 U/µl RNasin (Promega), and 0.20 U/µl AMV reverse transcriptase (Promega). Five percent of the resultant cDNA was amplified using an iCycler iQ Real-Time PCR Detection System (Bio-Rad Laboratories) in 96-well plates. Each duplicate 25 µl reaction contained 1X Quantitech SYBR Green master mix (Qiagen), 10 mM fluorescein, and 0.3 µM of each forward and reverse primer. Primer sequences were as previously published (55). Relative abundance of IFN-β and GAPDH mRNA was determined by comparison to a standard curve generated from serial dilutions of a DNA standard, and IFN-β expression was normalized to GAPDH expression.

Statistical analysis. A Student's two-sample *t* test (pooled variance) was applied using Systat 9.0 software. Results were considered significant if the *P* value was < 0.05.

RESULTS

Three reovirus proteins each contain an ITAM. The protein sequences encoded by each of the 10 reovirus gene segments were searched for potential ITAMs using the consensus motif YxxI/Lx$_{(6-12)}$YxxI/L (56). Remarkably, ITAMs were identified in three reovirus proteins: σ2 (amino acids [aa] 130-147), μ2 (aa 118-134), and λ2 (aa 671-684) encoded by the S2, M1, and L2 gene segments, respectively (Fig 1A). ITAMs were not identified in a search of the related *Reoviridae* virus, rotavirus. ITAMs in the reovirus σ2, μ2, and λ2 proteins were identical among prototype strains type 1 Lang (T1L), type 2 Jones (T2J), and T3D. However, variability was evident in the T2J sequences immediately adjacent to the ITAMs. A clustal alignment of the μ2 ITAM with corresponding motifs from DAP12, FcRγ, and CD3ζ family members indicated conservation of the ITAM as well as acidic residues in μ2 that are found in many cellular ITAMs (Fig. 1B). Conservation of the critical residues in the motif across reovirus serotypes suggests a role for ITAMs in viral replication and pathogenesis.

The μ2 ITAM impairs reovirus replication in cardiac myocytes but not in L929 cells. To determine whether ITAMs function in reovirus replication, plasmid-based reverse genetics was employed to engineer wild-type (WT) reovirus strain T3D and mutant viruses in which the two canonical ITAM tyrosine residues in σ2, μ2, or λ2 were exchanged with phenylalanine residues (YYFF). Tyrosine-to-phenylalanine substitutions were chosen to prevent the phosphorylation required for ITAM function and to minimally alter protein structure given the similarity of the tyrosine and phenylalanine side chains. Mutant viruses with altered ITAMs in the λ2 protein could not be recovered despite three independent rescue attempts. However, viruses with altered σ2 (σ2-YYFF) or μ2 (μ2-YYFF) ITAMs were readily isolated and formed plaques similar in size to WT virus (data not shown).

To determine whether the σ2 or μ2 ITAMs are required for reovirus replication in cell culture, titers of WT and mutant viruses were determined at multiple intervals during a single cycle of replication in L929 cells and primary cardiac myocyte cultures. While WT T3D achieved significantly higher titers than μ2-YYFF or σ2-YYFF at early times post-infection in both L929 cells and primary cardiac myocyte cultures ($P < 0.05$, Fig. 2), μ2-YYFF and σ2-YYFF achieved titers equivalent to WT T3D in L929 cells at late times post-infection (Fig. 2A). Thus, the μ2-YYFF and σ2-YYFF viruses are not globally defective in replication. In contrast, μ2-YYFF achieved higher titers than WT T3D or σ2-YYFF viruses in primary cardiac myocyte cultures at 18 h post-infection (*P* < 0.05, Fig. 2B). Therefore, the µ2 ITAM in WT virus is disadvantageous for viral replication in cardiac myocytes.

The µ2 ITAM regulates activation of NF-κB. Cellular ITAMs can signal via transcription factor NF-κB (20). Reovirus activates NF-κB during infection, mediating apoptosis in the brain and an antiviral IFN response in the heart (43). To determine whether the σ2 or µ2 ITAMs influence the activation of NF-κB by reovirus, NF-κB-stimulated luciferase reporter gene expression was quantified using cells that are both transfected and infected at high efficiency (293 cells; Fig. 3). At 12 h post-infection, WT T3D and σ2-YYFF viruses activated NF-κB, but µ2-YYFF did not (Fig. 3A, left panel). While µ2-YYFF achieved titers intermediate to those of WT T3D and σ2-YYFF viruses at 12 h post-infection (Figs. 2A and 2B), it remained possible that differences in NF-κB activation might reflect differences in replication. However, even at 24 h post-infection when µ2-YYFF achieved titers greater than or equal to those of WT T3D and σ2-YYFF viruses (Figs. 2A and 2B), µ2-YYFF failed to activate NF-κB as efficiently as WT T3D and σ2-YYFF viruses (Fig. 3A, right panel). Therefore, failure of µ2-YYFF to activate NF-κB does not reflect diminished viral replication.

To determine whether NF-κB is activated by ectopically expressed µ2 protein in the absence of viral infection and, if so, whether such activation requires the µ2 ITAM, HEK-293 cells were transfected with plasmids expressing recombinant FLAG-tagged µ2 or FLAG-tagged µ2-YYFF. Over-expressed FLAG-µ2 protein alone activated NF-κB, providing the first evidence that a reovirus protein can activate NF-κB in the absence of viral infection. In sharp contrast, FLAG-µ2-YYFF protein activation of NF-κB was minimal or undetectable (Fig. 3B), providing a direct biochemical link between the μ2 ITAM and NF-κB activation. As a control, μ2 expression levels in cell lysates generated from replicate cultures were quantified (Fig. 3C). Even when levels of FLAG-μ2-YYFF protein were greater than five-fold higher than those of FLAG-μ2 protein, FLAG-μ2-YYFF activation of NF-κB was undetectable or significantly less than that for FLAG-μ2 (compare 1 μg μ2-YYFF to 0.1 μg μ2, Figs. 3B and 3C). Finally, neither FLAG-μ2 nor FLAG-μ2-YYFF protein induced IFN-β or the IFN-stimulated pathway (as monitored by an ISRE reporter; Fig. 3B), consistent with a requirement for viral activation of IRF3 for IFN induction and indicating the specificity of μ2 and μ2 ITAM effects on NF-κB. Therefore, the μ2 ITAM regulates activation of NF-κB and can do so even in the absence of viral infection.

The σ2 and μ2 ITAMs do not influence cytopathic effect in L929 cells after a single cycle of replication. Reovirus activation of NF-κB can lead to apoptosis in some cell types, including L929 cells (10, 11). To determine whether the μ2 ITAM contributes to reovirus-induced cytopathic effect after a single cycle of replication, L929 cells were infected with WT T3D, σ2-YYFF, and μ2-YYFF viruses at an MOI of 10 PFU per cell, and cell viability was quantified at 24 and 48 h post-infection using an MTT assay. The three viruses were equally cytopathic (Fig. 4), indicating that μ2 ITAM-mediated activation of NF-κB is not required for reovirus-induced cytopathic effect after a single cycle of replication in L929 cells.

The μ2 ITAM regulates induction of IFN-β. Viral activation of NF-κB is also required for maximum induction of IFN-β (16). To determine whether the μ2 ITAM contributes to reovirus induction of IFN-β, L929 cells or primary cardiac myocyte cultures were infected with WT T3D and mutant reoviruses, and the induction of IFN-β mRNA was examined at 8 or 10 h post-infection, respectively (Fig. 5). In L929 cells, μ2-YYFF induced significantly less IFN-β than did either WT T3D or σ2-YYFF viruses (Fig. 5A), despite replicating to higher titers than σ2-YYFF early in infection (Fig. 2A). In primary cardiac myocyte cultures, μ2-YYFF again induced significantly less IFN-β than either virus, despite reaching equivalent or higher titers at that time point (Fig. 2B). Thus, the μ2 ITAM regulates the induction of IFN-β.

The μ2 ITAM effect on viral spread is cell type-specific. Viral spread is determined by viral replication, virus-induced cytopathicity for virus release, and the effect of virus-induced anti-viral cytokines such as IFN-β. To determine the effect of the μ2 ITAM on viral spread, cell cultures were infected at a low MOI and incubated for 5 to 7 days to allow multiple cycles of viral replication. In L929 cells, μ2-YYFF was significantly less cytopathic than either WT T3D or σ2-YYFF viruses at both 5 and 7 days post-infection (Fig. 6, left and middle panels). In contrast, viral titer, which is assessed after artificially lysing cells, was equivalent for the three viruses after multiple cycles of replication (Fig. 7, left panel). Together, these data suggest that in L929 cells, while an effect of the μ2 ITAM on viral replication (Fig. 2A) or viral cytopathic effect (Fig. 4) is not detectable after a single cycle of replication, a benefit of the μ2 ITAM to viral spread is apparent following multiple cycles of viral growth. In direct contrast to L929 cells, μ2-YYFF was significantly more cytopathic than either WT T3D or σ2-YYFF viruses in primary cardiac myocyte cultures (Fig. 6, right panel). Moreover, μ2-YYFF achieved a significantly higher titer than that of either WT T3D or σ2-YYFF viruses after multiple cycles of replication in primary cardiac myocyte cultures (Fig. 7, right panel). Therefore, in cardiac myocytes, where the IFN response is critical to limit viral damage (21, 43, 53) and where NF-κB is not required for apoptosis (9, 43), the μ2 ITAM diminishes viral replication (Fig. 2B) and spread (Figs. 6 and 7). Thus, the effect of the μ2 ITAM on reovirus replication and cytopathology is cell type-specific.

DISCUSSION

Viral infections evoke a variety of cellular responses that can either enhance or inhibit viral replication. We report here that reoviruses contain three ITAMs, that the ITAM in the M1 gene-encoded μ2 protein regulates activation of NF-κB and induction of IFN-β, and that the benefit of the ITAM to the virus is cell type-specific.

The PRRs RIG-I and MDA5 detect viral RNA (36) and signal via the adaptor protein IPS-1, also known as MAVS, VISA, or Cardif (26, 39, 49, 58), for induction of type I IFN. Investigations to determine whether RIG-I, MDA5, or both receptors recognize reovirus RNA have generated conflicting results (22, 24, 35), suggesting that PRR use may be context- (17) or cell type-specific. Diminished expression of IPS-1 by RNA interference inhibits reovirus-induced activation and translocation of IRF3 and also inhibits IRF3-dependent IFN-stimulated gene expression (22, 35). However, diminished expression of IPS-1 does not affect reovirus activation of NF-κB (22), indicating that reovirus activation of NF-κB, unlike activation of IRF3, is regulated independently of IPS-1. Here, we found that the reovirus μ2 protein activates NF-κB and can do so in the absence of viral infection (Fig. 3B). Importantly, alteration of μ2 to prevent the possibility of ITAM phosphorylation in the context of either recombinant virus or ectopically expressed FLAG-tagged μ2 renders the protein essentially incapable of NF-κB activation (Fig. 3). While it is likely that other events during reovirus infection contribute to the activation of NF-κB, as suggested by the detectable activation of NF-κB by the μ2-YYFF virus at 24 h post-infection, results here demonstrate a requirement of the μ2 ITAM for maximal activation. Ectopically expressed μ2 does not activate IFN-β or ISRE luciferase reporters (Fig. 3B, right panel), consistent with the expected requirement for additional transcription factors such as IRF3 and confirming the specificity of the μ2 effect on NF-κB. While previously reported ITAMs can signal through NF-κB (20), none are reported to function through RIG-I, MDA5, or IPS-1. Collectively the data indicate that reovirus activation of NF-κB can be mediated by the μ2 ITAM and that this activation is likely independent of PRRs and IPS-1.

The μ2 ITAM is required for the induction of IFN-β in both L929 cells and primary cardiac myocyte cultures (Fig. 5), consistent with a requirement for NF-κB activation for induction of this cytokine (16). Importantly, IFN-β is critical for protection against reovirus replication and cytopathic effect in cardiac myocytes (21, 53). NF-κB also participates in reovirus-induced apoptosis in many cell types (11, 43), but it is not required for apoptosis in cardiac myocytes (9, 43). Reovirus expressing a μ2 protein altered to prevent the possibility of ITAM phosphorylation, μ2-YYFF, produced higher titers (Figs. 2B and 7) and was more cytopathic (Fig. 6) than WT T3D virus in cardiac myocytes but less cytopathic than WT T3D virus in L929 cells (Fig. 6). Thus, the effect of the μ2 ITAM on reovirus replication and cell damage is cell type-specific. Together, these data suggest that the μ2 ITAM is beneficial to the virus in some cell types but detrimental to the virus in others, perhaps especially in those in which the IFN response is essential for protection and NF-κB is not required for apoptosis.

Some Src family kinases and Syk family kinases are expressed in only certain cell types (5), providing an alternative but not mutually exclusive explanation for the cell type-specificity of the reovirus μ2 ITAM. Moreover, multiple enveloped viruses contain ITAMs, and these viral ITAMs can display cell type-specific kinase associations. The simian immunodeficiency virus (SIV) Nef protein ITAM associates with Src in 3T3 cells (15) yet requires Lck binding in Jurkat cells (37). The Epstein-Barr virus (EBV) LMP2A ITAM is phosphorylated by Csk in epithelial cells (48) but can associate with Lyn, Lck, and Fyn in BJAB cells, a B cell line (8). Most viruses with known ITAMs target specific cells or tissues. Reovirus infects a wide variety of tissues *in vivo*, including the brain, heart, liver, intestine, and spleen (47). Possible associations of the Src and Syk family kinases with the μ2 ITAM could vary between cell types to influence the capacity of the μ2 ITAM to modulate cell signaling, a topic that will require further investigation.

Viral ITAMs can modulate a variety of host cell functions (32). The hantavirus ITAM is found in the cytoplasmic tail of the envelope G1 glycoprotein (19). Studies using endothelial and immune cells suggest that the G1 ITAM likely disrupts normal cell responses through G1 protein association with kinases that regulate functions of endothelial and immune cells

(19). Interestingly, the ITAM is highly conserved in hantavirus strains causing hantavirus pulmonary syndrome but absent in those causing hemorrhagic fever with renal syndrome or nonpathogenic strains (19), suggesting that this viral ITAM is a determinant of disease pathogenesis. SIV strains that contain ITAMs in the Nef protein are generally more virulent in macaques than SIV strains that lack ITAMs, most likely due to perturbation of cell signaling pathways (13). EBV LMP2A-mediated alteration of B-cell signaling requires LMP2A ITAM association with Syk. Kaposi sarcoma-associated herpesvirus (KSHV) contains an ITAM in the K1 transmembrane protein (34) that activates NFAT in B cells (33). KSHV ITAM activation may modulate KSHV lytic replication in B cells (30) as well as development of tumors. Activation of NFAT by another herpesvirus, rhesus monkey rhadinovirus (RRV), also is mediated by an ITAM, in this case, in viral protein R1 (12). Finally, two oncogenic retroviruses contain ITAMs. An ITAM in the mouse mammary tumor virus envelope protein is required for maximal expression of transformation markers in mammary cells (25, 45). Two ITAMS in the bovine leukemia virus gp30 protein (3) may be critical for infection and persistence (57). Thus, viral ITAMs play important and diverse roles in virus-cell interactions and viral pathogenesis.

The hantavirus G1 protein ITAM is required for ubiquitylation and degradation of this protein (18). The reovirus ITAM-containing μ2 protein also can be ubiquitylated and degraded, and this fate is virus strain-specific. However, μ2 ubiquitylation and degradation are not directed by the ITAM but rather by amino acid 208: a serine at μ2 residue 208 is associated with μ2 ubiquitylation and degradation, while a proline at this residue inhibits these processes (40). Ubiquitylation and degradation regulate levels of certain cellular proteins to prevent constitutive signaling. Interestingly, the protein Casitas B-lineage lymphoma (also called Cbl) is associated with ubiquitylation and degradation of Syk family kinases (41). Therefore, it is possible that μ2 is also ubiquitylated and degraded to prevent over-stimulation of ITAM pathways.

The μ2 protein of reovirus does not span membranes, suggesting that it functions in a manner that differs from other viral or cellular ITAM-containing proteins. Reovirus μ2 is found in low copy number in the viral core but abundantly in infected cells (44). It has both NTPase (27) and RNA-binding (6, 27, 42) activities and most likely associates with the reovirus polymerase to form the viral RNA synthesis complex (47). In infected cells, the μ2 protein forms viral inclusion bodies that serve as sites for viral replication and assembly (38, 44). The μ2 protein also functions as a strain-specific repressor of IFN signaling (61). There is no known cellular ligand for the reovirus μ2 protein, although it is known to bind microtubules. Thus, it is unclear how the μ2 ITAM would be phosphorylated by Src family kinases upon ligand-receptor binding or upon ligand-receptor-adaptor binding. However, activation of the EBV ITAM-containing protein, LMP2A, does not result from ligand binding but rather depends on cell adhesion (48). Moreover, the ITAM in the KSHV K1 protein is constitutively activated by the extracellular domain of the protein (31). Future studies will determine whether the reovirus μ2 ITAM is activated by an analogous non-ligand-dependent mechanism to mediate its functions in reovirus replication and pathogenesis.

ACKNOWLEDGEMENTS

We thank Ralph Baric, Lianna Li, Ray Pickles, Frank Scholle, and Jennifer Zurney for helpful discussions and Lance Johnson for excellent technical assistance. This research was supported by Public Health Service awards T32 CA09385 (K.W.B.), F32 AI075776 (K.W.B.), R37 AI38296 (T.S.D.), R01 AI50080 (T.S.D.), and R01 A1083333 (B.S.) and the Elizabeth B. Lamb Center for Pediatric Research. Additional support was provided by Public Health Service awards CA68485 for the Vanderbilt-Ingram Cancer Center and DK20593 for the Vanderbilt Diabetes Research and Training Center.

REFERENCES

1. **Barrow, A. D., and J. Trowsdale.** 2006. You say ITAM and I say ITIM, let's call the whole thing off: the ambiguity of immunoreceptor signalling. Eur J Immunol **36:**1646-1653.

2. **Baty, C. J., and B. Sherry.** 1993. Cytopathogenic effect in cardiac myocytes but not in cardiac fibroblasts is correlated with reovirus-induced acute myocarditis. J Virol **67:**6295-6298.

3. **Beaufils, P., D. Choquet, R. Z. Mamoun, and B. Malissen.** 1993. The (YXXL/I)2 signalling motif found in the cytoplasmic segments of the bovine leukaemia virus envelope protein and Epstein-Barr virus latent membrane protein 2A can elicit early and late lymphocyte activation events. EMBO J **12:**5105-5112.

4. **Berton, G., A. Mócsai, and C. A. Lowell.** 2005. Src and Syk kinases: key regulators of phagocytic cell activation. Trends Immunol **26:**208-214.

5. **Bradshaw, J. M.** 2010. The Src, Syk, and Tec family kinases: distinct types of molecular switches. Cell Signal **22:**1175-1184.

6. **Brentano, L., D. L. Noah, E. G. Brown, and B. Sherry.** 1998. The reovirus protein mu2, encoded by the M1 gene, is an RNA-binding protein. J Virol **72:**8354-8357.

7. **Breun, L. A., T. J. Broering, A. M. McCutcheon, S. J. Harrison, C. L. Luongo, and M. L. Nibert.** 2001. Mammalian reovirus L2 gene and lambda2 core spike protein sequences and whole-genome comparisons of reoviruses type 1 Lang, type 2 Jones, and type 3 Dearing. Virology **287:**333-348.

8. **Burkhardt, A. L., J. B. Bolen, E. Kieff, and R. Longnecker.** 1992. An Epstein-Barr virus transformation-associated membrane protein interacts with src family tyrosine kinases. J Virol **66:**5161-5167.

9. **Clarke, P., R. L. Debiasi, S. M. Meintzer, B. A. Robinson, and K. L. Tyler.** 2005. Inhibition of NF-kappa B activity and cFLIP expression contribute to viral-induced apoptosis. Apoptosis **10:**513-524.

10. **Clarke, P., S. M. Meintzer, L. A. Moffitt, and K. L. Tyler.** 2003. Two distinct phases of virus-induced nuclear factor kappa B regulation enhance tumor necrosis factor-related apoptosis-inducing ligand-mediated apoptosis in virus-infected cells. J Biol Chem **278:**18092-18100.

11. **Connolly, J. L., S. E. Rodgers, P. Clarke, D. W. Ballard, L. D. Kerr, K. L. Tyler, and T. S. Dermody.** 2000. Reovirus-induced apoptosis requires activation of transcription factor NF-kappaB. J Virol **74:**2981-2989.

12. **Damania, B., M. DeMaria, J. U. Jung, and R. C. Desrosiers.** 2000. Activation of lymphocyte signaling by the R1 protein of rhesus monkey rhadinovirus. J Virol **74:**2721-2730.

13. **Dehghani, H., C. R. Brown, R. Plishka, A. Buckler-White, and V. M. Hirsch.** 2002. The ITAM in Nef influences acute pathogenesis of AIDS-inducing simian immunodeficiency viruses SIVsm and SIVagm without altering kinetics or extent of viremia. J Virol **76:**4379-4389.

14. **Dermody, T. S., L. A. Schiff, M. L. Nibert, K. M. Coombs, and B. N. Fields.** 1991. The S2 gene nucleotide sequences of prototype strains of the three reovirus serotypes: characterization of reovirus core protein sigma 2. J Virol **65:**5721-5731.

15. **Du, Z., S. M. Lang, V. G. Sasseville, A. A. Lackner, P. O. Ilyinskii, M. D. Daniel, J. U. Jung, and R. C. Desrosiers.** 1995. Identification of a nef allele that causes lymphocyte activation and acute disease in macaque monkeys. Cell **82:**665-674.

16. **Fensterl, V., and G. C. Sen.** 2009. Interferons and viral infections. Biofactors **35:**14-20.

17. **Fredericksen, B. L., B. C. Keller, J. Fornek, M. G. Katze, and M. Gale.** 2008. Establishment and maintenance of the innate antiviral response to West Nile Virus involves both RIG-I and MDA5 signaling through IPS-1. J Virol **82:**609-616.

18. **Geimonen, E., I. Fernandez, I. N. Gavrilovskaya, and E. R. Mackow.** 2003. Tyrosine residues direct the ubiquitination and degradation of the NY-1 hantavirus G1 cytoplasmic tail. J Virol **77:**10760-10868.

19. **Geimonen, E., R. LaMonica, K. Springer, Y. Farooqui, I. N. Gavrilovskaya, and E. R. Mackow.** 2003. Hantavirus pulmonary syndrome-associated hantaviruses contain conserved and functional ITAM signaling elements. J Virol **77:**1638-1643.

20. **Hara, H., C. Ishihara, A. Takeuchi, L. Xue, S. W. Morris, J. M. Penninger, H. Yoshida, and T. Saito.** 2008. Cell type-specific regulation of ITAM-mediated NF-kappaB activation by the adaptors, CARMA1 and CARD9. J Immunol **181:**918-930.

21. **Holm, G. H., A. J. Pruijssers, L. Li, P. Danthi, B. Sherry, and T. S. Dermody.** 2010. Interferon regulatory factor 3 attenuates reovirus myocarditis and contributes to viral clearance. J Virol **84:**6900-6908.

22. **Holm, G. H., J. Zurney, V. Tumilasci, S. Leveille, P. Danthi, J. Hiscott, B. Sherry, and T. S. Dermody.** 2007. Retinoic acid-inducible gene-I and interferon-beta promoter stimulator-1 augment proapoptotic responses following mammalian reovirus infection via interferon regulatory factor-3. J Biol Chem **282:**21953-21961.

23. **Humphrey, M. B., L. L. Lanier, and M. C. Nakamura.** 2005. Role of ITAM-containing adapter proteins and their receptors in the immune system and bone. Immunol Rev **208:**50-65.

24. **Kato, H., O. Takeuchi, E. Mikamo-Satoh, R. Hirai, T. Kawai, K. Matsushita, A. Hiiragi, T. S. Dermody, T. Fujita, and S. Akira.** 2008. Length-dependent recognition of double-stranded ribonucleic acids by retinoic acid-inducible gene-I and melanoma differentiation-associated gene 5. J Exp Med **205:**1601-1610.

25. **Katz, E., M. H. Lareef, J. C. Rassa, S. M. Grande, L. B. King, J. Russo, S. R. Ross, and J. G. Monroe.** 2005. MMTV Env encodes an ITAM responsible for transformation of mammary epithelial cells in three-dimensional culture. J Exp Med **201:**431-439.

26. **Kawai, T., K. Takahashi, S. Sato, C. Coban, H. Kumar, H. Kato, K. J. Ishii, O. Takeuchi, and S. Akira.** 2005. IPS-1, an adaptor triggering RIG-I- and Mda5-mediated type I interferon induction. Nat Immunol **6:**981-988.

27. **Kim, J., J. S. Parker, K. E. Murray, and M. L. Nibert.** 2004. Nucleoside and RNA triphosphatase activities of orthoreovirus transcriptase cofactor mu2. J Biol Chem **279:**4394-4403.

28. **Kobayashi, T., A. A. Antar, K. W. Boehme, P. Danthi, E. A. Eby, K. M. Guglielmi, G. H. Holm, E. M. Johnson, M. S. Maginnis, S. Naik, W. B. Skelton, J. D. Wetzel, G. J. Wilson, J. D. Chappell, and T. S. Dermody.** 2007. A plasmid-based reverse genetics system for animal double-stranded RNA viruses. Cell Host Microbe **1:**147-157.

29. **Kobayashi, T., L. S. Ooms, M. Ikizler, J. D. Chappell, and T. S. Dermody.** 2010. An improved reverse genetics system for mammalian orthoreoviruses. Virology **398:**194-200.

30. **Lagunoff, M., D. M. Lukac, and D. Ganem.** 2001. Immunoreceptor tyrosine-based activation motif-dependent signaling by Kaposi's sarcoma-associated herpesvirus K1 protein: effects on lytic viral replication. J Virol **75:**5891-5898.

31. **Lagunoff, M., R. Majeti, A. Weiss, and D. Ganem.** 1999. Deregulated signal transduction by the K1 gene product of Kaposi's sarcoma-associated herpesvirus. Proc Natl Acad Sci U S A **96:**5704-5709.

32. **Lanier, L. L.** 2006. Viral immunoreceptor tyrosine-based activation motif (ITAM)-mediated signaling in cell transformation and cancer. Trends Cell Biol **16:**388-390.

33. **Lee, B. S., S. H. Lee, P. Feng, H. Chang, N. H. Cho, and J. U. Jung.** 2005. Characterization of the Kaposi's sarcoma-associated herpesvirus K1 signalosome. J Virol **79:**12173-12184.

34. **Lee, H., J. Guo, M. Li, J. K. Choi, M. DeMaria, M. Rosenzweig, and J. U. Jung.** 1998. Identification of an immunoreceptor tyrosine-based activation motif of K1 transforming protein of Kaposi's sarcoma-associated herpesvirus. Mol Cell Biol **18:**5219-5228.

35. **Loo, Y. M., J. Fornek, N. Crochet, G. Bajwa, O. Perwitasari, L. Martinez-Sobrido, S. Akira, M. A. Gill, A. García-Sastre, M. G. Katze, and M. Gale.** 2008. Distinct RIG-I and MDA5 signaling by RNA viruses in innate immunity. J Virol **82:**335-345.

36. **Loo, Y. M., and M. Gale.** 2011. Immune Signaling by RIG-I-like Receptors. Immunity **34:**680-692.

37. **Luo, W., and B. M. Peterlin.** 1997. Activation of the T-cell receptor signaling pathway by Nef from an aggressive strain of simian immunodeficiency virus. J Virol **71:**9531-9537.

38. **Mbisa, J. L., M. M. Becker, S. Zou, T. S. Dermody, and E. G. Brown.** 2000. Reovirus mu2 protein determines strain-specific differences in the rate of viral inclusion formation in L929 cells. Virology **272:**16-26.

39. **Meylan, E., J. Curran, K. Hofmann, D. Moradpour, M. Binder, R. Bartenschlager, and J. Tschopp.** 2005. Cardif is an adaptor protein in the RIG-I antiviral pathway and is targeted by hepatitis C virus. Nature **437:**1167-1172.

40. **Miller, C. L., J. S. Parker, J. B. Dinoso, C. D. Piggott, M. J. Perron, and M. L. Nibert.** 2004. Increased ubiquitination and other covariant phenotypes attributed to a strain- and temperature-dependent defect of reovirus core protein mu2. J Virol **78:**10291-10302.

41. **Mócsai, A., J. Ruland, and V. L. Tybulewicz.** 2010. The SYK tyrosine kinase: a crucial player in diverse biological functions. Nat Rev Immunol **10:**387-402.

42. **Noble, S., and M. L. Nibert.** 1997. Core protein mu2 is a second determinant of nucleoside triphosphatase activities by reovirus cores. J Virol **71:**7728-7735.

43. **O'Donnell, S. M., M. W. Hansberger, J. L. Connolly, J. D. Chappell, M. J. Watson, J. M. Pierce, J. D. Wetzel, W. Han, E. S. Barton, J. C. Forrest, T. Valyi-Nagy, F. E. Yull, T. S. Blackwell, J. N. Rottman, B. Sherry, and T. S. Dermody.** 2005. Organ-specific roles for transcription factor NF-kappaB in reovirus-induced apoptosis and disease. J Clin Invest **115:**2341-2350.

44. **Parker, J. S., T. J. Broering, J. Kim, D. E. Higgins, and M. L. Nibert.** 2002. Reovirus core protein mu2 determines the filamentous morphology of viral inclusion bodies by interacting with and stabilizing microtubules. J Virol **76:**4483-4496.

45. **Ross, S. R., J. W. Schmidt, E. Katz, L. Cappelli, S. Hultine, P. Gimotty, and J. G. Monroe.** 2006. An immunoreceptor tyrosine activation motif in the mouse mammary tumor virus envelope protein plays a role in virus-induced mammary tumors. J Virol **80:**9000-9008.

46. **Sada, K., T. Takano, S. Yanagi, and H. Yamamura.** 2001. Structure and function of Syk protein-tyrosine kinase. J Biochem **130:**177-186.

47. **Schiff, L. A., M. L. Nibert, and K. L. Tyler.** 2007. Orthoreoviruses and Their Replication, p. 1854-1915. *In* D. M. Knipe and P. M. Howley (ed.), Fields' virology, 5th ed, vol. 2. Wolters Kluwer Health/Lippincott Williams & Wilkins, Philadelphia.

48. **Scholle, F., R. Longnecker, and N. Raab-Traub.** 1999. Epithelial cell adhesion to extracellular matrix proteins induces tyrosine phosphorylation of the Epstein-Barr virus latent membrane protein 2: a role for C-terminal Src kinase. J Virol **73:**4767-4775.

49. **Seth, R. B., L. Sun, C. K. Ea, and Z. J. Chen.** 2005. Identification and characterization of MAVS, a mitochondrial antiviral signaling protein that activates NF-kappaB and IRF 3. Cell **122:**669-682.

50. **Sherry, B., C. J. Baty, and M. A. Blum.** 1996. Reovirus-induced acute myocarditis in mice correlates with viral RNA synthesis rather than generation of infectious virus in cardiac myocytes. J Virol **70:**6709-6715.

51. **Sherry, B., and M. A. Blum.** 1994. Multiple viral core proteins are determinants of reovirus-induced acute myocarditis. J Virol **68:**8461-8465.

52. **Sherry, B., F. J. Schoen, E. Wenske, and B. N. Fields.** 1989. Derivation and characterization of an efficiently myocarditic reovirus variant. J Virol **63:**4840-4849.

53. **Sherry, B., J. Torres, and M. A. Blum.** 1998. Reovirus induction of and sensitivity to beta interferon in cardiac myocyte cultures correlate with induction of myocarditis and are determined by viral core proteins. J Virol **72:**1314-1323.

54. **Smith, R. E., H. J. Zweerink, and W. K. Joklik.** 1969. Polypeptide components of virions, top component and cores of reovirus type 3. Virology **39:**791-810.

55. **Stewart, M. J., K. Smoak, M. A. Blum, and B. Sherry.** 2005. Basal and reovirus-induced beta interferon (IFN-beta) and IFN-beta-stimulated gene expression are cell type specific in the cardiac protective response. J Virol **79:**2979-2987.

56. **Underhill, D. M., and H. S. Goodridge.** 2007. The many faces of ITAMs. Trends Immunol **28:**66-73.

57. **Willems, L., J. S. Gatot, M. Mammerickx, D. Portetelle, A. Burny, P. Kerkhofs, and R. Kettmann.** 1995. The YXXL signalling motifs of the bovine leukemia virus transmembrane protein are required for in vivo infection and maintenance of high viral loads. J Virol **69:**4137-4141.

58. **Xu, L. G., Y. Y. Wang, K. J. Han, L. Y. Li, Z. Zhai, and H. B. Shu.** 2005. VISA is an adapter protein required for virus-triggered IFN-beta signaling. Mol Cell **19:**727-740.

59. **Yin, P., N. D. Keirstead, T. J. Broering, M. M. Arnold, J. S. Parker, M. L. Nibert, and K. M. Coombs.** 2004. Comparisons of the M1 genome segments and encoded mu2 proteins of different reovirus isolates. Virol J **1:**6.

60. **Zurney, J., K. E. Howard, and B. Sherry.** 2007. Basal expression levels of IFNAR and Jak-STAT components are determinants of cell-type-specific differences in cardiac antiviral responses. J Virol **81:**13668-13680.

61. **Zurney, J., T. Kobayashi, G. H. Holm, T. S. Dermody, and B. Sherry.** 2009. Reovirus mu2 protein inhibits interferon signaling through a novel mechanism involving nuclear accumulation of interferon regulatory factor 9. J Virol **83:**2178-2187.

A

Protein	Strain	Sequence
σ2	T3D	C D D Y P F L A R D P R F K H R – V Y Q Q L S A V T
	T2J	. . . . – . . . . I .
	T1L	. . . . – . . . .
μ2	T3D	D D E Y N Q L A R – – A F K I S D V Y A P L I S S T
	T2J	. . . . V . – – . . . L . . . . T . . V . . S
	T1L	. . . . – – . . . .
λ2	T3D	S G V Y F F L V D – – H F – Y R – – Y E T L S T I S
	T2J	. . . . – – . . – . . – – . . . . . A . .
	T1L	. . . . – – . . – . . – – . . . .

B

Species	Protein	Sequence
T3D	μ2	D D E Y N Q L A R A F K I S D V Y A P L I S S T
T2J	μ2	D D E Y N Q L V R A F K L S D V Y T P L V S S S
T1L	μ2	D D E Y N Q L A R A F K I S D V Y A P L I S S T
Hs	DAP12	E S P Y Q E L Q - G - Q R S D V Y S D L N T Q R
Mm	Dap12	E S P Y Q E L Q - G - Q R P E V Y S D L N T Q R
Dr	Dap12	E S P Y Q E L Y - G - V Q S D I Y S D L Q Q Y R
Dr	CD3ζL 2	E T H Y Q E L R - A - H A S D E Y Q Q I G T K G
Hs	FcRγ	D G V Y T G L S - T - R N Q E T Y E T L K H E K
Mm	FcRγ	D A V Y T G L N - T - R S Q E T Y E T L K H E K
Xl	FcRγ	E G E Y T G L E - S - V D K G T Y E T I K G E S
Dr	FcRγ	E G V Y E G L K - P - H E T D T Y E T I K M K S
Hs	CD3ζ 3	D G L Y Q G L S - T - A T K D T Y D A L H M Q A
Mm	CD3ζ 3	D G L Y Q G L S - T - A T K D T Y D A L H M Q T
Dr	CD3ζ 3	D Q L Y Q G L S - S - V T K D T Y D S L Q M Q Q
Xl	CD3ζ 3	D P V Y Q G L H - S - G S R D T Y D A L H M Q P
Gg	CD3ζ 3	D A V Y Q G L S - A - A T R D T Y D A L H M Q P
Dr	FcRγL	G D L Y Q D L G - R - R D A D T Y D T L H G M K
Dr	CD3ζ 2	D E T Y T P L T - R - K G D D T Y R E L E T K G
Hs	CD3ζ 1	N Q L Y N E L N - L - G R R E E Y D V L D K R R
Mm	CD3ζ 1	N Q L Y N E L N - L - G R R E E Y D V L E K K R
Gg	CD3ζ 1	D D V Y N K L S - R - G H R D E Y D V L G T R R
Xl	CD3ζ 1	D N N Y D E L N - P - S G Q S K Y D A L N V R R
Hs	CD3ζ 2	E G L Y N E L Q - K D K M A E A Y S E I G M K G
Mm	CD3ζ 2	E G V Y N A L Q - K D K M A E A Y S E I G T K G
Gg	CD3ζ 2	D T V Y S S L Q - K D K M G E A Y S E I G K K G
Xl	CD3ζ 2	D S T Y T G L Q - R D K M S D P Y S D I R P K Q
Dr	CD3ζ 1	E S H Y Q A I D - K - L G K S E Y A T A N R T Q
Dr	CD3ζL 1	E P V Y T D L D - L P Q V G S D Y Q Q L D R P I

Figure 3.1. Reovirus proteins contain ITAMs. (A) ITAMs in the reovirus σ2, μ2, and λ2 proteins. ITAMs of prototype reovirus strains T3D, T2J, and T1L are shown. Sequences are from previous publications (25, 57, 206). (B) Reovirus μ2 ITAMs aligned with cellular ITAMs. Black indicates conserved ITAM residues. Grey indicates additional residues common to many ITAMs. Hs = *Homo sapiens* (human); Mm = *Mus musculus* (mouse); Dr = *Danio rerio* (zebrafish); Xl = *Xenopus laevis*; Gg = *Gallus gallus* (chicken). The numerals 1, 2, and 3 distinguish between the three ITAMs in each of the indicated proteins.

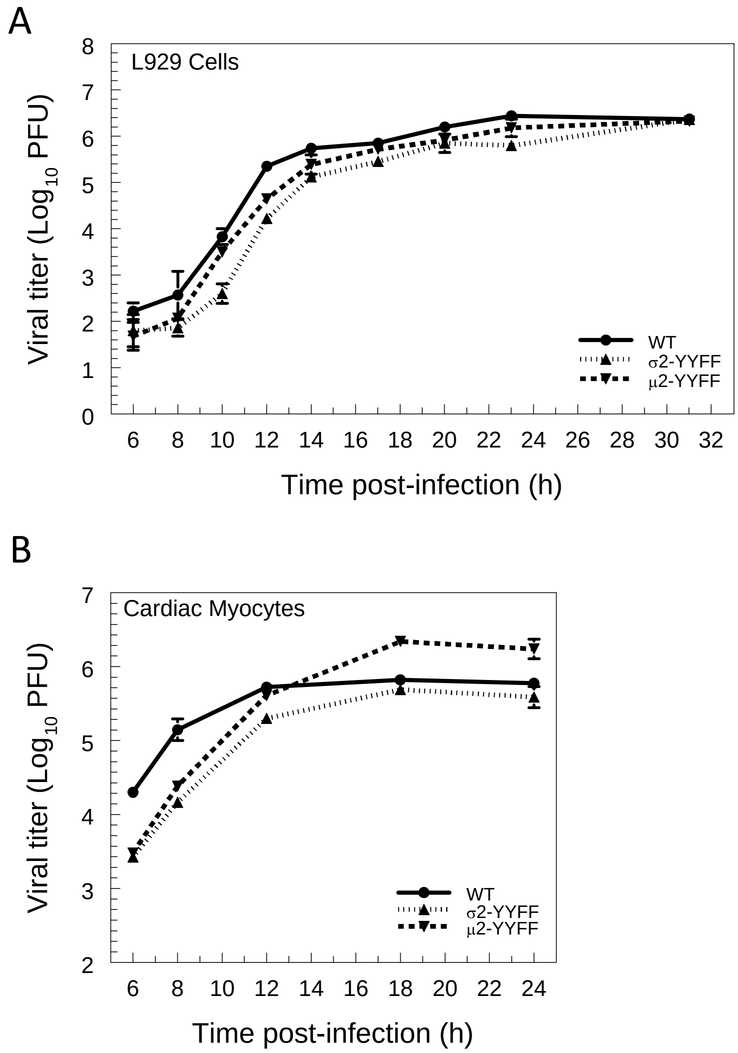

Figure 3.2. The μ2 ITAM impairs replication in cardiac myocytes but not in L929 cells. L929 cells (A) or primary cardiac myocyte cultures (B) were infected with WT T3D, σ2-YYFF, or μ2-YYFF viruses at an MOI of 3 PFU per cell for the times shown, and viral titers were determined by plaque assay. Results are expressed as the mean of triplicate samples ± standard deviation for two independent experiments in L929 cells and a representative of two experiments in primary cardiac myocytes.

Figure 3.3. The μ2 ITAM regulates activation of NF-κB. (A) AD-293 cells were transfected with an NF-κB-luciferase reporter plasmid and a constitutively-expressing Renilla-luciferase plasmid as an internal standard. At 24 h post-transfection, cells were infected with WT T3D, σ2-YYFF, or μ2-YYFF viruses at an MOI of 10 PFU per cell. At 12 and 24 h post-infection, luciferase activity was quantified. *, significantly different from WT T3D and σ2-YFF ($P < 0.05$); **, not significantly different from mock ($P < 0.05$). (B) HEK-293 cells were transfected with the indicated FLAG-tagged plasmid, the constitutively-expressing Renilla-luciferase plasmid as an internal standard and luciferase reporter plasmids regulated by NF-κB (as in A), IFN-β, or ISRE promoters. At 24 h post-transfection, luciferase activity was quantified. Results are expressed as the mean ± standard error of the mean normalized to *Renilla* expression (A and B). (C) Whole-cell lysates corresponding to (B) were resolved by SDS-PAGE, transferred to a nitrocellulose membrane, and immunoblotted using mouse anti-FLAG or anti-GAPDH antibodies. Gels were scanned, and band intensity was quantified as indicated. Each panel includes a representative of at least two independent experiments.

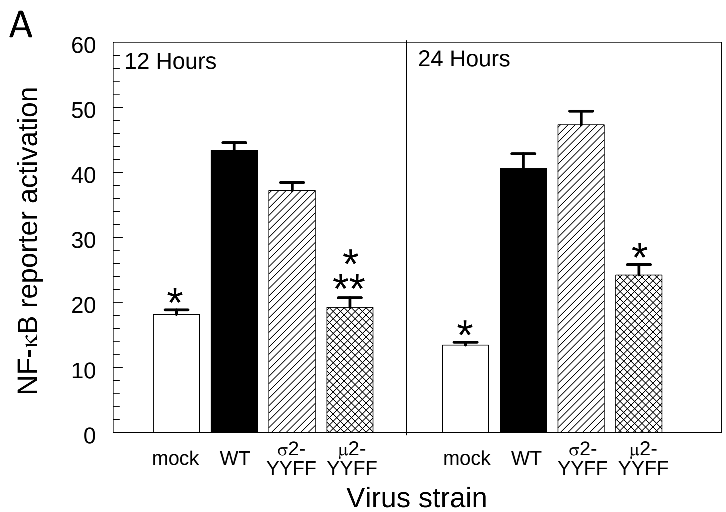

A
12 Hours
24 Hours
NF-κB reporter activation
60
50
40
30
20
10
0
mock
WT
σ2-YYFF
μ2-YYFF
Virus strain

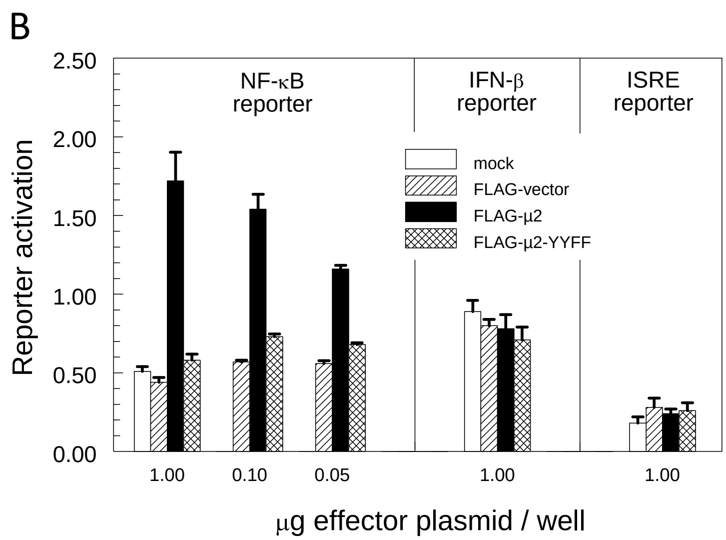

B
NF-κB reporter
IFN-β reporter
ISRE reporter
mock
FLAG-vector
FLAG-μ2
FLAG-μ2-YYFF
Reporter activation
2.50
2.00
1.50
1.00
0.50
0.00
1.00
0.10
0.05
μg effector plasmid / well

C

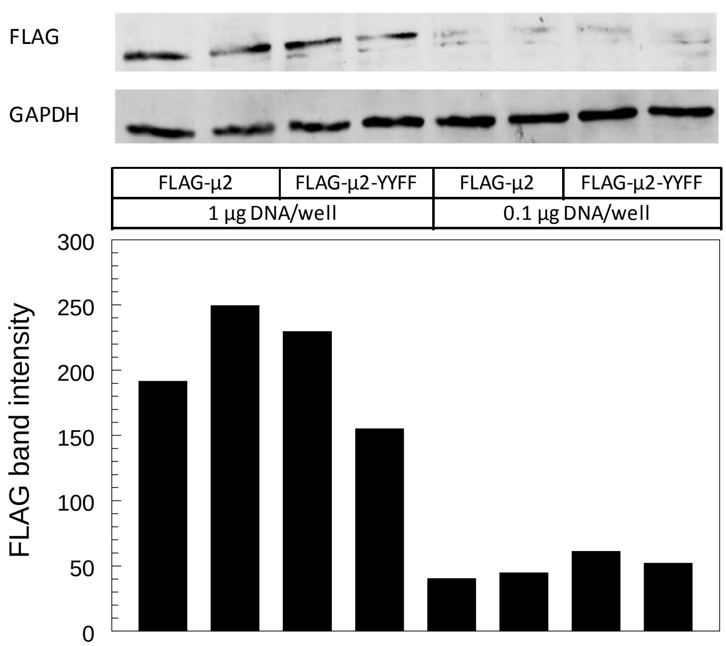
FLAG
GAPDH
FLAG-μ2
FLAG-μ2-YYFF
FLAG-μ2
FLAG-μ2-YYFF
1 μg DNA/well
0.1 μg DNA/well
FLAG band intensity
300
250
200
150
100
50
0

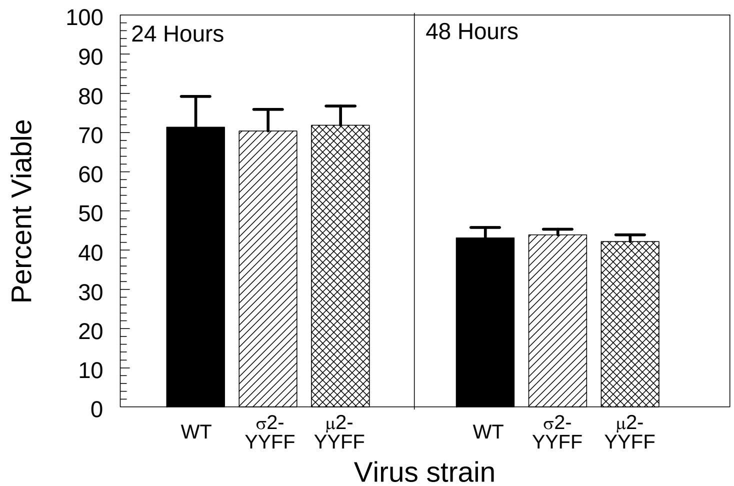

Figure 3.4. The σ2 and μ2 ITAMs do not influence cytopathic effect in L929 cells after a single cycle of replication. L929 cells were infected with WT T3D, σ2-YYFF, or μ2-YYFF viruses at an MOI of 10 PFU per cell. At 24 and 48 h post-infection, cell viability was quantified by MTT assay. Results are expressed as the mean ± standard deviation relative to mock-infected cultures and are representative of at least four independent experiments. Student's *t* test did not identify any significant differences between these virus strains at any time point ($P < 0.05$).

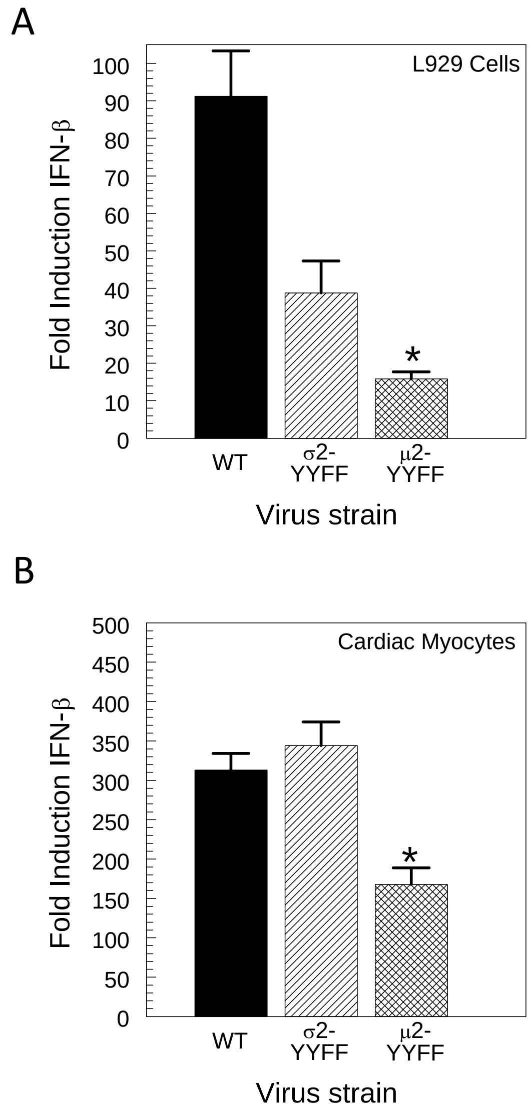

Figure 3.5. The μ2 ITAM regulates induction of IFN-β. WT T3D, σ2-YYFF, or μ2-YYFF viruses were added to L929 cells at an MOI of 25 PFU per cell (A) or primary cardiac myocyte cultures at an MOI of 10 PFU per cell (B). At 8 (A) or 10 (B) h post-infection, RNA was quantified by reverse transcription and quantitative RealTime PCR, and copy number was normalized to GAPDH. Fold induction of IFN-β is expressed relative to uninfected cultures. Results are expressed as the mean ± standard error of the mean for a representative of three independent experiments. Asterisks indicate significant differences between infection with μ2-YYFF and WT T3D or σ2-YYFF viruses (Student's *t* test, $P < 0.05$).

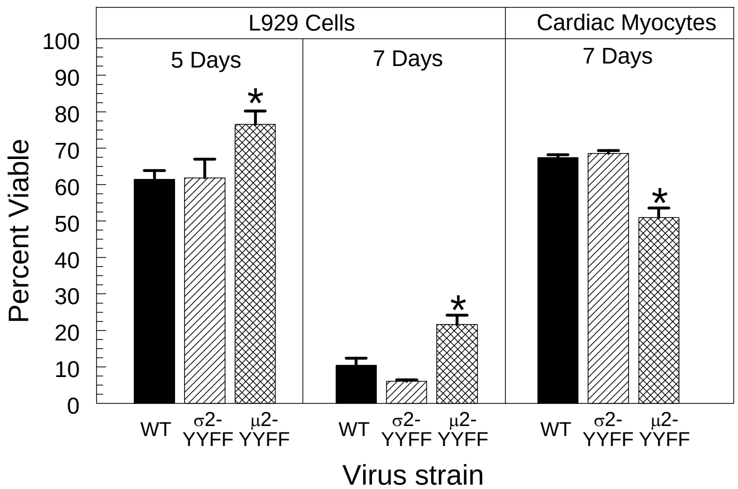

Figure 3.6. The μ2 ITAM effect on cytopathic effect after multiple cycles of replication is cell type-specific. WT T3D, σ2-YYFF, or μ2-YYFF viruses were added to L929 cells at an MOI of 0.1 PFU per cell or primary cardiac myocyte cultures at an MOI of 1 PFU per cell (cytopathic effect was undetectable when 0.1 PFU per cell was used; data not shown). At 5 and 7 days post-infection, cell viability was quantified by MTT assay. Results are expressed as the mean ± standard error of the mean relative to mock-infected cultures for a representative of at least two independent experiments. Asterisks indicate significant differences between infection with μ2-YYFF and infection with WT T3D or σ2-YYFF viruses (Student's t test, $P < 0.05$).

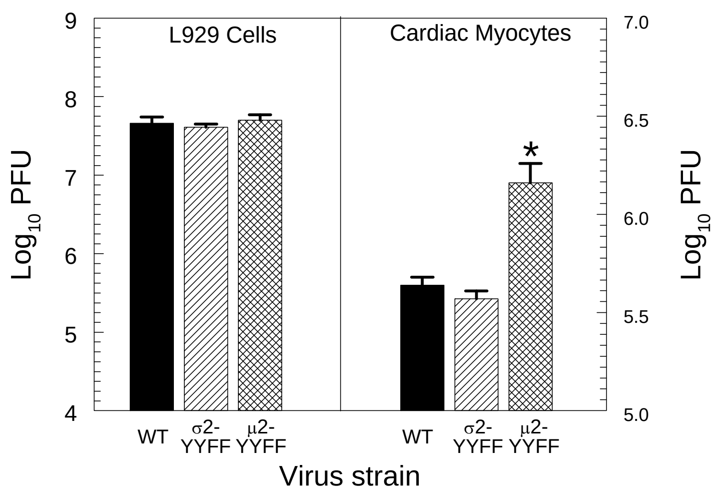

Figure 3.7. The µ2 ITAM effect on viral titer after multiple cycles of replication is cell type-specific. L929 cells and primary cardiac myocyte cultures were infected with WT T3D, σ2-YYFF, or µ2-YYFF viruses at an MOI of 0.1 PFU per cell. At 5 days post-infection, viral titers were determined by plaque assay. Results are expressed as the mean ± standard deviation for a representative of at least two independent experiments. Asterisk indicates a significant difference between infection with µ2-YYFF and infection with WT T3D or σ2-YYFF viruses (Student's *t* test, $P < 0.05$).

SUMMARY

Previously, we determined that the reovirus M1 gene encode μ2 protein is a strain-specific repressor of interferon (IFN) (6). Reovirus strain type 1 Lang (T1L), as well as recombinant and reassortant viruses containing a T1L M1 gene, repress IFN signaling. In direct contrast, strain type 3 Dearing (T3D), as well as recombinant and reassortant viruses containing a T3D M1 gene, do not repress IFN signaling. Interestingly, the T1L M1 gene is associated with an unusual nuclear accumulation of interferon regulatory factor 9 (IRF9). In Chapter 2, we demonstrate that specifically amino acid 208 of the μ2 protein determines the strain-specific repression of IFN signaling. Furthermore, in primary cardiac myocyte cultures where the IFN response is critical for protection, μ2 amino acid 208 modulates reovirus induction of IFN, determines reovirus replication, and influences cytopathic effect after multiple cycles of replication. In contrast, in primary cardiac fibroblast cultures, where reovirus induces less IFN than it does in cardiac myocytes, μ2 amino acid 208 only influences reovirus replication. Finally, in a mouse model, we determined that μ2 amino acid 208 modulates myocarditis, likely through repression of IFN signaling.

In previous studies in vitro, we found a greater nuclear concentration of HA-tagged T1L μ2 when overexpressed in vitro as compared to HA-tagged T3D μ2 (B. Sherry, unpublished data). Overexpression of proteins can induce artifacts. Also, the effect of μ2 amino acid 208 was not previously investigated. Therefore, it would be interesting to determine the state of nuclear accumulation of the μ2 protein during virus infection using T1L, T3D, and the series of recombinant viruses utilized in Chapter 2.

Previously, we also found that recombinant viruses containing a proline at μ2 amino acid 208 induce nuclear accumulation of IRF9 similar to T1L. Nuclear import and export of the ISGF3 complex, which contains IRF9, as well as IRF9 alone or in complex with STAT2, utilize karyopherins-1, -4-, -6, and Crm1. It remains to be determined if T1L μ2 can participate in protein-protein interactions with karyopherins or Crm1 as a mechanism for disrupting IRF9 export. Multiple virus proteins are reported to bind karyopherins (2). The ebola virus protein VP24 (3, 4) and severe acute respiratory syndrome protein ORF6 (1) both bind karyopherins to inhibit normal ISGF3 complex nuclear trafficking which results in inhibition of IFN signaling. If interactions between μ2 and karyopherins are not detected by co-immunoprecipitation and Western Blot, mass spectrometry could reveal novel μ2 binding partners at a time during infection when nuclear accumulation of IRF9 occurs.

Since μ2 amino acid 208 is also a determinant of viral inclusion body (VIB) morphology, further studies are needed to determine the relationship between repression of IFN signaling and VIBs. Furthermore, since VIBs are perinuclear in distribution (5), it would be interesting to determine if ISGF3 components, specifically IRF9, colocalize with VIBs. Colocalization of VIBs and ISGF3 components could be examined by immunofluorescence microscopy, using rabbit anti-μ2 antibody and commercial antibodies directed against ISGF3 components.

Immunoreceptor tyrosine-based activation motifs (ITAMs) are well known for their function in the T cell receptor, the B cell receptor, and in adaptor proteins such as DAP12. More recently, ITAMs were discovered in multiple enveloped viruses where they contribute to viral pathogenesis or viral oncogenesis. Here, we report an ITAM in three reovirus proteins: the S2 gene-encoded σ2 protein, the M1 gene-encoded μ2 protein, and the L2 gene-encoded λ2 protein (Chapter 3). This is the first report of ITAMs in a non-enveloped virus.

In general, ITAMs are found in the cytoplasmic tail of transmembrane proteins.An ITAM is activated by a ligand-receptor binding event. Once activated, an ITAM is phosphorylated by Src family kinases which then recruit Syk family kinases to the ITAM. Syk family kinases (Syk or Zap70) then auto-phosphorylate and stimulate downstream signaling which can result in an array of responses ranging from cellular proliferation to cytokine release. We determined the μ2 ITAM regulates reovirus activation of the transcription factor NF-κB, induction of the cytokine interferon (IFN), and viral spread. Whether the μ2 ITAM is beneficial or disadvantageous is cell type-specific and likely reflects the cell type-specific roles of both NF-κB and IFN-β. Additional studies are needed to determine when the μ2 ITAM is phosphorylated during reovirus replication. This may prove especially difficult because the timing for ITAM phosphorylation and Src kinase interactions is unclear. That is, μ2 is not a transmembrane protein in contrast to all known ITAM-containing receptors, μ2 is not known to interact with cellular transmembrane proteins like cellular ITAM-containing adaptors, and there is no known ligand-receptor interaction between μ2 and another protein. Furthermore, if the μ2 ITAM signals similarly to previously described ITAMs, there should be a detectable protein-protein interaction between the μ2 ITAM and Src family kinases as well as between the μ2 ITAM and Syk family kinases. Protein-protein interactions could be detected by co-immunoprecipitation and Western Blot. An alternative approach that would expand the search for possible μ2 binding partners beyond these kinases could utilize co-immunoprecipitation of μ2 followed by mass spectrometry. Again, these interactions may be difficult to detect because of unknown timing. Further investigation is needed to identify possible functions of the σ2 and λ2 ITAMs. Studies of the σ2 ITAM did not reveal a function, but this ITAM may function in pathways not examined or it may serve as a decoy for cellular ITAMs by sequestering ITAM-pathway members such as Src and Syk family kinases. Though a λ2-ITAM mutated virus was not viable upon rescue, overexpression of the WT λ2 and ITAM-mutant λ2 proteins could reveal functions of the λ2 ITAM.

REFERENCES

1. **Frieman, M., B. Yount, M. Heise, S. A. Kopecky-Bromberg, P. Palese, and R. S. Baric.** 2007. Severe acute respiratory syndrome coronavirus ORF6 antagonizes STAT1 function by sequestering nuclear import factors on the rough endoplasmic reticulum/Golgi membrane. J Virol **81:**9812-9824.

2. **Gustin, K. E.** 2003. Inhibition of nucleo-cytoplasmic trafficking by RNA viruses: targeting the nuclear pore complex. Virus Res **95:**35-44.

3. **Reid, S. P., L. W. Leung, A. L. Hartman, O. Martinez, M. L. Shaw, C. Carbonnelle, V. E. Volchkov, S. T. Nichol, and C. F. Basler.** 2006. Ebola virus VP24 binds karyopherin alpha1 and blocks STAT1 nuclear accumulation. J Virol **80:**5156-5167.

4. **Reid, S. P., C. Valmas, O. Martinez, F. M. Sanchez, and C. F. Basler.** 2007. Ebola virus VP24 proteins inhibit the interaction of NPI-1 subfamily karyopherin alpha proteins with activated STAT1. J Virol **81:**13469-13477.

5. **Schiff, L. A., M. L. Nibert, and K. L. Tyler.** 2007. Orthoreoviruses and Their Replication, p. 1854-1915. *In* D. M. Knipe and P. M. Howley (ed.), Fields' virology, 5th ed, vol. 2. Wolters Kluwer Health/Lippincott Williams & Wilkins, Philadelphia.

6. **Zurney, J., T. Kobayashi, G. H. Holm, T. S. Dermody, and B. Sherry.** 2009. Reovirus mu2 protein inhibits interferon signaling through a novel mechanism involving nuclear accumulation of interferon regulatory factor 9. J Virol **83:**2178-2187.